CHAPTER I

INTRODUCTION

Bcl-2 and its homologue Bcl-x_L, have roles in both cell survival and cell cycle. This dissertation explores the role of the anti-apoptotic molecules Bcl-2 and Bcl-x_L in regulating mammalian cell cycle and G_0 arrest. The goal of this dissertation is to determine the relationship between the cell survival and the cell cycle functions of Bcl-2/Bcl-x_L, and to determine the mechanism of Bcl-2/Bcl-x_L cell cycle function. The introduction will focus on the Bcl-2 family, the role of Bcl-2 family members and mitochondria in cell death, and the regulation of cell cycle from arrest to DNA synthesis. This dissertation examines the mechanism of cell cycle entry delay and whether the anti-apoptotic and the cell cycle functions of Bcl-2/Bcl-x_L can be genetically distinguished from each other (Chapter III). Chapter IV discusses the possible role of Bcl-2 in the Myc pathway. Chapter V elucidates the relationship between the cell death and cell cycle functions of Bcl-2/Bcl-x_L. Finally, Chapter VI presents possible models of Bcl-2/Bcl-x_L function and future directions.

Bcl-2 Family of Proteins

The proper development and functioning of an organism depends on the coordination of processes that determine the cell contents of that organism, such as the rates of proliferation, differentiation, and death. Apoptosis is essential for the development and function of multi-cellular organisms, and occurs extensively during

tissue remodeling, resolution of inflammation, and T cell selection. Apoptosis is characterized by a series of morphological and biochemical changes, such as cell shrinkage, internucleosomal fragmentation of genomic DNA, caspase activation, formation of apoptotic bodies, and corpse clearance (Saraste, 2000). Interruption of the apoptotic program may lead to inability to clear unwanted cells. Persistence of these cells in an organism leads to potentially cancerous growth. The Bcl-2 family of proteins controls the life and death decisions of a cell.

The Bcl-2 family of proteins is a key regulator of programmed cell death and can be separated into its anti-apoptotic members, including Bcl-x_L (Boise et al., 1993), Bcl-W (Gibson et al., 1996), Mcl-1 (Kozopas et al., 1993), A1 (Lin et al., 1993) and Boo (Song et al., 1999), and the pro-apoptotic members, including Bax (Oltvai et al., 1993), Bak (Chittenden et al., 1995; Kiefer et al., 1995), Bad (Yang et al., 1995), Bid (Wang et al., 1996), Bim (Puthalakath et al., 1999), Bcl-x_S (Boise et al., 1993) and Bik. The interaction between the pro- and anti-apoptotic members of the family and ratio of pro-apoptotic proteins to anti-apoptotic proteins, in part, determine the decision of a cell to enter apoptosis. The anti-apoptotic proteins such as Bcl-2 and its close homologue Bcl-x_L are localized to the outer mitochondrial membrane, endoplasmic reticlulum and peri-nuclear membrane. The pro-apoptotic molecule Bak is localized mostly at the outer mitochondrial membrane of healthy cells. However, its close homologue Bax inserts into the outer mitochondrial membrane following death signaling. Bad is also normally cytosolic; however, it inserts into the outer mitochondrial membrane upon a death signal. Sequence analysis of the Bcl-2 family has shown that the members share one to four BH domains (Bcl-2 homology) (Figure 1). The subtle differences in the primary structure

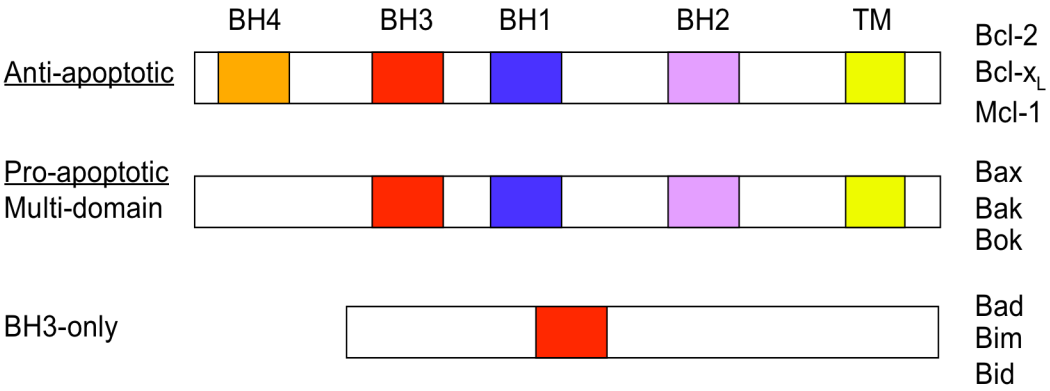

Figure 1: Diagram of representative members of the Bcl-2 family. The anti-apoptotic members such as Bcl-2, Bcl-x_L, or Mcl-1 contain all four of the BH domains. The pro-apoptotic members are divided into two subfamilies, the multi-domain (Bax, Bak, and Bok), and the BH-3-only (Bad, Bim, and Bid).

and arrangement of these alpha-helical domains may determine the pro- or anti-apoptotic function of the members of the Bcl-2 family (Gross, 1999). Bcl-2 was cloned as the deregulated oncogene at the translocation breakpoint of t(14;18) in follicular lymphomas. It was found to enhance tumorigenesis by prolonging cellular survival. However, it has also been shown that the anti-proliferative function of Bcl-2 inhibits tumor progression in animal models and human cancers. Contrary to previous reports, where it was shown that Bcl-2 cooperates with Myc in development of lymphoma (Strasser et al., 1990) and breast cancer (Jager et al., 1997) by protecting cells from Myc-induced cell death, in liver models, Bcl-2 was shown to delay the growth of early proliferative foci in both Myc- and TGFα-induced tumorigenesis (de la Coste et al., 1999; Pierce et al., 2002). In mammary tumor models, Bcl-2 inhibits mitotic activity during the initial proliferative stage; this inhibition is lost as the tumors progress to hyperplasia and adenocarcinoma (Furth et al., 1999; Murphy et al., 1999). These data show that Bcl-2 can both promote and suppress oncogenesis, depending on the tissue of origin. The ability to control the anti-apoptotic and anti-proliferative functions of Bcl-2 independently can lead to generation of Bcl-2 molecules that are either oncogenes or tumor suppressors. For example, a Bcl-2 molecule that does not affect cell death but restrains cell cycle would be a tumor suppressor.

Bcl-2 and Bcl-x_L

Eighty-five percent of follicular lymphomas are characterized by a t(14;18) chromosomal translocation (Yunis et al., 1982). The analysis of chromosomal rearrangements, which occur frequently in human hematologic malignancies, has been an

excellent approach in studying the molecular mechanisms that drive malignant cell growth. Examination of the t(14;18) translocation led to the identification of the Bcl-2 gene (Tsujimoto et al., 1984). This breakpoint joins the Bcl-2 gene at 18q21 with the J_H region of the immunoglobulin (Ig) heavy chain locus at 14q32 and results in the transcriptional activation of the Bcl-2 gene (Bakhshi et al., 1985; Chen-Levy et al., 1989). Bcl-2 was shown to promote the survival of cytokine-dependent hematopoietic cells in the absence of cytokines (Vaux et al., 1988). The Bcl-2 transgenic mice containing a Bcl-2-Ig minigene exhibited increased numbers of mature B-cells in lymphoid follicles of the spleen due to prolonged survival (McDonnell et al., 1989). These observations first established Bcl-2 as an effecter of cellular survival. Further studies extended the role of Bcl-2 as a survival factor in multiple cell types, including fibroblasts and neurons. Bcl-2 suppresses cell death in response to a variety of death stimuli, including growth factor withdrawal, serum deprivation, viral infection, chemotherapeutic drugs, oxidative stress, and DNA damage [reviewed in (Yang and Korsmeyer, 1996)]. Mature Bcl-2-Ig transgenic mice displayed prolonged survival of mature B cells, which eventually resulted in follicular hyperplasia and high-grade lymphoma in some mice (McDonnell et al., 1990). In a different transgenic mouse model using the *lck* proximal promoter that overexpressed Bcl-2 in T cells, thirty percent of the mice developed peripheral T-cell lymphomas (Linettte, et al., 1994). Deregulation of the c-Myc oncogene was found to be prevalent in the tumors of the Bcl-2-Ig mice (McDonnell and Korsmeyer, 1991). Deregulation of Myc is also common in lymphoma, and its translocation from chromosome 8 to the Ig locus, t(8;14) is responsible for Burkitt's lymphoma. Double transgenic mice expressing Eμ-Myc and Bcl-2-Ig developed a rapid onset of lymphoma

and all mice died by 2 months of age (Marin et al., 1995). In comparison, mice expressing only Eμ-Myc had fifty percent survival by 4 months of age; thirty percent of the Bcl-2-Ig mice developed tumors by 24 months of age (Marin et al., 1995). Myc induces cell death as well as cell proliferation. However, Bcl-2 inhibits Myc-induced cell death, while not altering Myc's proliferative ability (Vaux et al., 1988), suggesting that Bcl-2 cooperates with Myc to enhance oncogenesis. The experiments in Bcl-2 transgenic mice established Bcl-2 as an oncogene.

Bcl-x_L was cloned using a Bcl-2 cDNA probe (Boise et al., 1993), and shares forty-four percent sequence homology with Bcl-2. Bcl-2 and Bcl-x_L are considered to be functionally equivalent, however Bcl-2 and Bcl-x_L display differences in expression patterns. For example, Bcl-x_L is more prevalent than Bcl-2 in the brain, central nervous system and adult thymus, while Bcl-2 is expressed in the kidney. Bcl-x_L protein is important for survival of immature thymocytes, while Bcl-2 protein is important for the survival of mature thymocytes (Ma et al., 1995, Ranger et al., 2001, Yang and Korsmeyer, 1996). Bcl-x_L knockout mice die at E13 due to massive apoptosis in the brain, and hematopoietic tissues (Motoyama et al., 1995). Bcl-2 deficient mice die within weeks of birth from polycystic kidney disease (Veis et al., 1993). Bcl-2 knockout mice develop failure of their immune function due to loss of T and B cell through apoptosis (Nakayama et al., 1993). The different phenotypes of the Bcl-2 and Bcl-x_L knockout mice suggest that the proteins perform overlapping, but not identical functions. Bcl-2 and Bcl-x_L are guardians of the mitochondria, where they counteract the activity of pro-apoptotic members of the Bcl-2 family, and of many other death proteins. Based on the Bcl-x_L crystal structure and on data from reconstituted mitochondrial liposomes, Bcl-

2 and Bcl-x_L are believed to form pores in the outer mitochondrial membrane, similar to those pores formed by bacterial diptheria toxins, and serve as selective ion channels (Minn et al., 1997; Muchmore et al., 1996). Bcl-2 and Bcl-x_L co-immunoprecipitate with Voltage Dependent Anion Channels (VDACs) (see Mitochondria). VDACs regulate the transport of molecules between the intermembrane space and the outer mitochondrial membrane. Mutational data indicate that Bcl-x_L can maintain cell survival through its heterodimerization function alone or through its ion channel function alone, but the activity of one of these properties is required for enhancement of cell survival by Bcl-x_L (Minn, et al., 1999). The ability of Bcl-2 and Bcl-x_L to form and regulate channels is important for their survival functions (Reed, 1997, Vander Heiden et al., 1999).

Bad

Bad is pro-apoptotic member of the Bcl-2 family containing only a BH-3 domain. Bad is normally cytosolic; however, upon death stimuli Bad translocates to the outer mitochondrial membrane and binds Bcl-x_L (Yang et al., 1995; Zha et al., 1996). Under normal conditions Bad is bound by 14-3-3, which protects three phosphorylation sites on Bad. Upon a death stimulus, 14-3-3 dissociates from Bad, and Bad is subsequently dephosphorylated by protein phosphatase 2A (Chiang et al., 2001), protein phosphatase 1α (Ayllon et al., 2000) or protein phosphatase 2B (Wang et al., 1999). Bad is believed to sensitize cells to death by binding up Bcl-2 or Bcl-x_L so that the protective Bax/Bcl-2 or Bax/Bcl-x_L dimers cannot occur. Overexpression of Bad in hematopoietic cells overexpressing Bcl-x_L abolishes the protective effects of Bcl-x_L. However, when Bad possessing a mutation in the BH3 domain eliminating its ability to bind Bcl-x_L is used,

the protective effects of Bcl-x_L are restored (Kelekar et al., 1997; Zha et al., 1997). Binding of Bcl-2/Bcl-x_L by Bad allows Bak/Bax to homodimerize and initiate the mitochondrial death cascade (Letai et al., 2002).

Bak/Bax

Bak and Bax are multi-domain pro-apoptotic members of the Bcl-2 family. Bax was first identified as a dimerization partner of Bcl-2 (Oltvai et al., 1993), and can homodimerize or heterodimerize with Bcl-2 or Bcl-x_L. The BH3 domain of Bax converts Bcl-2 into a pro-apoptotic protein despite the presence of BH4 domain (Hunter and Parslow, 1996). Bak is localized to the outer mitochondrial membrane in healthy cells. Bax is normally cytosolic. Its C-terminal tail is protected inside a hydrophobic pocket, preventing the binding of Bax to membranes (Suzuki et al., 2000; Nechushtan et al., 1999). Upon homodimerization, Bax and Bak fully insert into mitochondrial membrane resulting in changes in mitochondrial membrane potential and promoting the release of cytochrome c (Wang et al., 1998). *Bak*$^{-/-}$ mice are developmentally normal. Bax knockout mice are viable; however, they exhibit defects in hematopoietic and neuronal development, and male *Bax*$^{-/-}$ mice are sterile due to defects in spermatogenesis. *Bak*$^{-/-}$/*Bax*$^{-/-}$ fibroblasts fail to release cytochrome c and are resistant to most apoptotic stimuli (Reed and Green, 2002).

Apoptosis

Apoptotic signaling occurs through two pathways, receptor-mediated (extrinsic) and mitochondria-mediated (Figure 2). The mitochondria-mediated pathway for

induction of apoptosis involves the release of cytochrome c from the mitochondria, as stimulated by genotoxic damage, cytotoxic stress, or growth factor deprivation among others. Translocation of cytochrome c from the mitochondria to the cytosol is a crucial step in the apoptotic pathway. In the cytosol, cytochrome c binds Apaf-1 (apoptotic protease activating factor) and caspase 9, forming a heptomeric complex called the apoptosome. In the presence of ATP, the apoptosome initiates the caspase cascade, which results in the hallmark features of apoptosis such as chromatin condensation and nuclear DNA fragmentation (Mignotte, 1998).

The extrinsic pathway for apoptosis signaling involves the activation of death receptors through trimerization leading to caspase activation. One example of such a pathway is Fas receptor signaling. Binding of Fas ligand induces the trimerization of Fas receptor. Fas recruits and binds FADD (Fas associating protein with death domain) through the interaction of their death domains. The N-terminal DED (death effector domain) of FADD recruits procaspase 8, resulting in activation of the caspase. Active caspase 8 can directly activate the cell death machinery through caspase cascade activation, or indirectly, by cleaving Bid. Truncated Bid translocates to the mitochondria where it mediates cytochrome c release.

Mitochondria

The mitochondrion is well known as the powerhouse of the cells- the site of cellular energy production. In the last decade, the mitochondria have been established as crucial players in the regulation of programmed cell death. The mitochondrion is enveloped by two membranes. The inner membrane surrounds the mitochondrial matrix

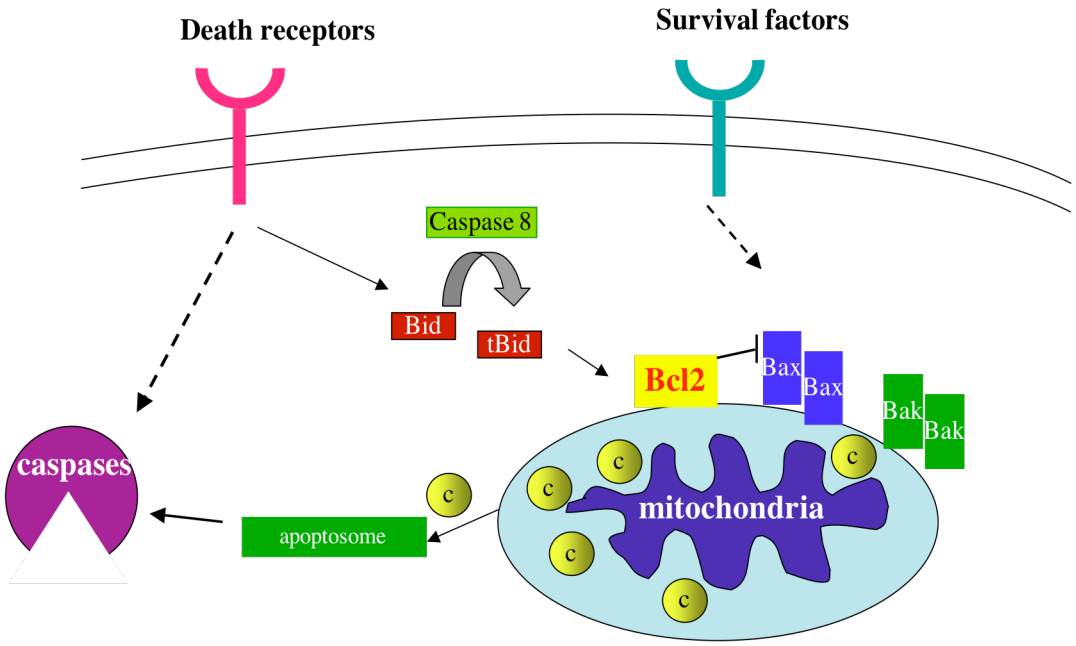

Figure 2: Bcl-2 family members in receptor-mediated and mitochondria-mediated apoptosis. Genotoxic damage, cytotoxic stress, or growth factor deprivation among others stimulate activation of Bax/Bax and Bak/Bak dimmers, which results in increased mitochondrial membrane permeability. In the cytosol, cytochrome c binds Apaf-1 (apoptotic protease activating factor) and caspase 9, forming a heptomeric complex called the apoptosome. In the presence of ATP, the apoptosome initiates the caspase cascade. Bcl-2 blocks the action of Bax/Bax and Bak/Bak dimmers through heterodimerization with Bax and Bak.

and is folded into cristae. The inner mitochondrial membrane houses the molecular complexes of the electron transport chain, which generates the H^+ ion gradient necessary for ATP production. The inner membrane also contains the adenine nucleotide translocator (ANT), which exchanges ADP for ATP between the mitochondrial matrix and the intermembrane space. The outer mitochondrial membrane (OMM) surrounds the inner mitochondrial membrane, creating an intermembrane space. In the intermembrane space, mitochondria sequester apoptosis promoting proteins such as cytochrome c, apoptosis inducing factor (AIF), Smac/Diablo, and Omi/Htr2. The impermeability of the OMM is very important to the regulation of apoptosis. If cytochrome c is released, it can form the apoptosome and initiate the caspase cascade. However, the OMM must also remain permeable to metabolic anions to sustain cell survival. The exchange of ATP/ADP between the mitochondria and cytosol is a regulated event critical for cell survival (Vander Heiden et al., 1999). Lack of ADP in the mitochondrial matrix prevents the F_1F_0 ATP synthase from being able to use the H^+ ion gradient created by electron transport. This causes hyperpolarization of mitochondrial membrane and matrix swelling leading to loss of OMM integrity and cytochrome c release. This is achieved through the VDAC (voltage dependent anion channel). VDAC mediates the permeability of the OMM and is the most ubiquitous protein in the outer mitochondrial membrane.

Bcl-2 localizes to the OMM and regulates apoptosis, possibly through the regulation of OMM integrity and function. The biochemical mechanism by which Bcl-2 regulates apoptosis is unclear; however, there are several models (Harris, 2000). One possible mechanism of apoptosis inhibition by Bcl-2 is through the regulation of VDAC. Bcl-2 and Bcl-x_L have been shown to prevent the disruption of ATP/ADP exchange that

occurs following nutrient or growth factor withdrawal (Vander Heiden et al., 2000). The defect has been identified as disrupted ADP uptake into the mitochondria of cells that have been deprived of growth factors, and this defect is prevented by Bcl-x_L expression (Vander Heiden et al., 1999). In addition, Bcl-x_L has been shown to increase VDAC opening in planar phospholipid membranes when the physiologic voltage of -25mV and +25mV is applied (Vander Heiden et al., 2001). Maintenance of ATP/ADP exchange by Bcl-x_L expression enhances cell survival by allowing mitochondria to remain coupled at a lower level of cellular metabolism. Another model for Bcl-x_L action holds that Bcl-x_L inhibits cell death by preventing the release of cytochrome c from the mitochondria. Evidence led to the model that Bcl-x_L binding to VDAC closes the channel, preventing the release of cytochrome c into the cytosol thus preventing cell death (Shimizu et al., 1999). When VDAC was reconstituted in liposomes that were loaded with cytochrome c and with addition of recombinant Bcl-x_L it was found that Bcl-x_L inhibited VDAC-dependent cytochrome c release (Shi et al., 2003).

Reactive oxygen species (ROS) are generated in all aerobic cells as byproducts of certain metabolic reactions. The mitochondria are the major site of ROS generation due to electron transfer to oxygen in the respiratory chain. An excess of ROS in the mitochondria results in oxidative stress, which causes intramolecular crosslinking, and release of calcium from mitochondria. Evidence supports that Bcl-2 may act as an antioxidant to block a putative ROS-mediated step in the apoptotic pathway. Following glucose deprivation and H_2O_2 treatment, Bcl-2 prevents accumulation of ROS and the subsequent steps in the apoptosis pathway (Ouyang et al., 2002). Bcl-2 or Bcl-x_L expression can protect cells from ROS-induced apoptosis (Harris, 2000); however, it is

unclear whether Bcl-2/Bcl-x_L acts as a scavenger or regulates the production of ROS. This model relates to the regulation of mitochondrial membrane permeability by Bcl-2. ADP is the substrate for the F_1F_0 ATPase. As ADP becomes limiting to the mitochondria in starvation conditions due to a change in OMM permeability, a backup in the electron transport chain results in mitochondrial hyperpolarization. By restoring OMM permeability (Vander Heiden et al., 2001), Bcl-2 relieves the block in the electron transport chain and prevents ROS production and hyperpolarization.

Caspases

Caspases are cysteinyl aspartate-specific proteinases that mediate the specific cleavage events, which result in the manifestation of the apoptotic phenotype. Caspases are evolutionarily conserved proteases that can be found in worms to humans. In humans, caspases are ubiquitously expressed in the cytosol as latent zymogens. Caspases are regulated by the conversion of zymogens into active forms by inflammatory or apoptotic stimuli, and by IAP's (inhibitors of apoptosis proteins)- a family of natural regulators of caspase activation. Mammalian caspases are divided into two major groups: cytokine activators and apoptotic caspases. Members of the cytokine activators group, such as caspase 1, 11, and 12, participate in the processing of pro-inflammatory cytokines, while the apoptotic caspases, such as caspases 3, 6, 7, 8, and 9, sense and execute the apoptotic response. Activation of caspases is central to the execution of apoptosis and results in the hallmark morphological changes observed during apoptosis.

Emerging evidence suggest that caspases may regulate cell cycle in addition to apoptosis. Caspase 3 has been implicated as a negative regulator of B cell cycling (Woo

et al., 2003). Splenic B cells from *casp3*$^{-/-}$ mice exhibit normal apoptosis, but increased proliferation due to increased numbers of p21 molecules associated with PCNA. Olson et. al. showed that dense human B cells treated with proliferative stimuli selectively upregulated caspase 6 and caspase 8 activity, while caspase 3 activity and apoptosis were reduced. The activities of caspases 6 and 8 were shown to be upregulated following B cell activation, but caspase 3 activity and apoptosis were decreased (Olson et al., 2003). Interestingly, pretreatment of B cells with the caspase 6 inhibitor VEID-fmk, blocked induction of RNA synthesis, increase in cell size, as well as induction of cyclins D2 and D3, and CDK4, while increasing the level of p27 in response to a proliferation stimulus (Olson et al., 2003). Additional evidence for the role of caspases in cell cycle is provided by patients with a genetic deficiency in caspase 8, who exhibit defects in apoptosis as well as activation of T, B, and NK cells (Chun et al., 2002).

Bcl-2 and the Cell Cycle

In addition to its apoptosis-inhibitory function, Bcl-2 also affects cell cycle control. The anti-proliferative effect of Bcl-2 was initially documented in T cells stimulated to enter cell cycle by activation and on quiescent fibroblasts stimulated to enter cycle by serum induction (Linette et al., 1996; O'Reilly et al., 1996). Overexpression of Bcl-2 in T cells resulted in a marked decrease of cells in S phase as compared to wild type T cells (Linette et al., 1996; Mazel et al., 1996). The effect on cell cycle progression appears to be dose-dependent on Bcl-2, as *bcl-2*$^{+/-}$ and *bcl-2*$^{-/-}$ T cells exhibit accelerated activation-induced cell cycle entry (Linette et al., 1996). It has been shown in HL60 cells that Bcl-2 speeds up the entry of cells into G_0 upon induction of

differentiation by DMSO (Vairo et al., 1996). Bax transgenic mice have greatly reduced numbers of mature thymocytes and enter S phase faster than controls upon IL-2 stimulation (Brady et al., 1996).

The cell cycle delay phenotype of Bcl-x_L and Bcl-2 initially observed in quiescent T cells and fibroblasts has been confirmed and extended in our lab. Our experiments showed that Bcl-x_L caused a delay in S phase entry by approximately 4 hours in serum-stimulated fibroblasts (Greider et al., 2002). To temporally place the activity of Bcl-x_L and Bcl-2 within the cell cycle, the ability of Bcl-x_L and Bcl-2 to delay S phase entry in response to specific events between G_0/G_1 and G_1/S was examined. Raf, Myc and E2F-1 are members of interconnected pathways that control the balance between cellular proliferation and apoptosis (Grandori, 2000; Sears, 1999). It has been shown that Ras, through the Raf/MEK/ERK pathway, increases the stability of the Myc protein (Sears, 1999). Myc is an early G_1 event and has been shown to directly contribute to the activation of E2F's (Sears, 2002). The E2F transcription factors are considered a late G_1 event and are responsible for activation of a large number of genes essential for proliferations phase entry (Santoni-Rugiu, 2000). The activation of Raf, or Myc, or E2F-1 in the absence of serum is able to cause entry of cells into S phase. Expression of Bcl-2 or Bcl-x_L delayed serum-stimulated, Myc-ER and Raf-ER-induced S phase entry in NIH 3T3 cell by 2 hours, 6 hours and 3 hours, respectively (Figure 3). Neither Bcl-2 nor Bcl-x_L was able to delay the S phase entry in response to E2F-1 induction (Greider et al., 2002). These data temporally placed the activity of Bcl-2/Bcl-x_L between activities of Myc and E2F.

Binding of the cdk inhibitor p27 regulates the activity of cyclin/cdk complexes.

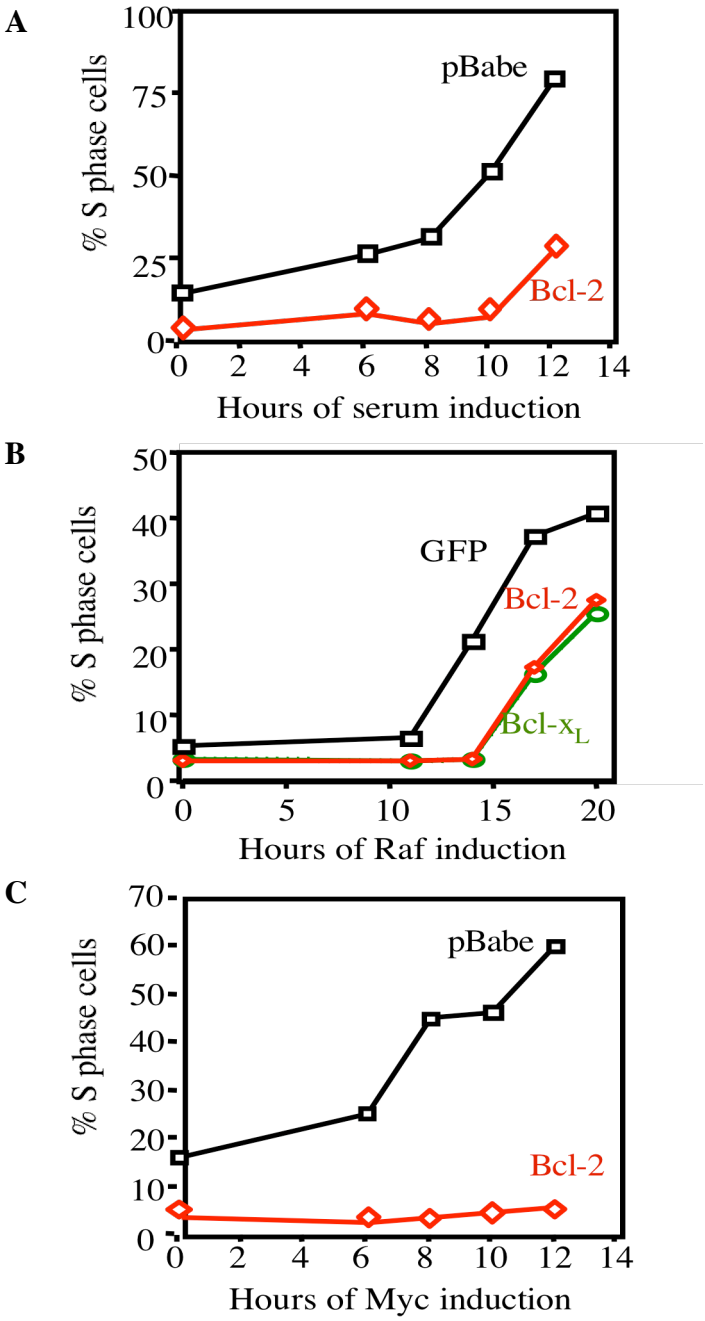

Figure 3: Bcl-2 and Bcl-x_L delay serum stimulated, Raf-induced, and Myc-induced cell cycle entry in fibroblasts. Graphs of S phase cell percentage versus hours after cell cycle stimulation by either serum addition (**A**), induction of Raf by 4-hydroxytamoxifen (4-OHT) addition (**B**), or Myc by 4-OHT addition (**C**). Percentages of S phase cells were obtained by PI staining and FACS analysis. One representative experiment of at least three is shown.

Protein levels of p27 are high during cell cycle arrest and are rapidly decreased during cell cycle entry. Bcl-x_L and Bcl-2 expressing cells consistently exhibit higher p27 levels than controls at the end of serum starvation and at all time points following stimulation (Greider et al., 2002). However, there was no difference in levels of p27 protein in vector alone and Bcl-2/Bcl-x_L during asynchronous growth (Greider et al., 2002), indicating that Bcl-2/Bcl-x_L affected p27 specifically during cell cycle exit or quiescence. The data suggest that upregulation of p27 may be causal to the cell cycle delay effect of Bcl-2/Bcl-x_L. This was confirmed by the inability of Bcl-x_L or Bcl-2 to delay serum-induced cell cycle entry in $p27^{-/-}$ MEFs (Greider et al., 2002). The upregulation of p27 in Bcl-2/Bcl-x_L cells indicated that these molecules exerted a significant effect in G_0 arrest. In Myc induction and serum stimulation models, our lab has reported significant delays in the activation of cyclin D/cdk4 and cyclin E/cdk2 in Bcl-2/Bcl-x_L cells (Greider et al., 2002). Inhibition of G_1 cyclin/cdk's is consistent with Bcl-2/Bcl-x_L also interfering with G_1progression.

Cell Cycle and Quiescence

The mammalian cell cycle is a highly regulated series of events (Figure 4) (Ho, 2002; Malumbres, 2001). The cell division cycle is subdivided into four phases: Gap 1 (G_1), Synthesis (S), Gap 2 (G_2), and Mitosis (M). Most of the cells in the body are non-dividing and this state is referred to as G_0 or quiescence. In G_0, cells are small and generally have depressed RNA, protein, and ATP synthesis compared to growing cells. The levels of the cyclin-dependent kinase inhibitor p27 are high and early response genes such as Myc and cyclin D are low in G_0. Appropriate stimuli, such as growth factors, can

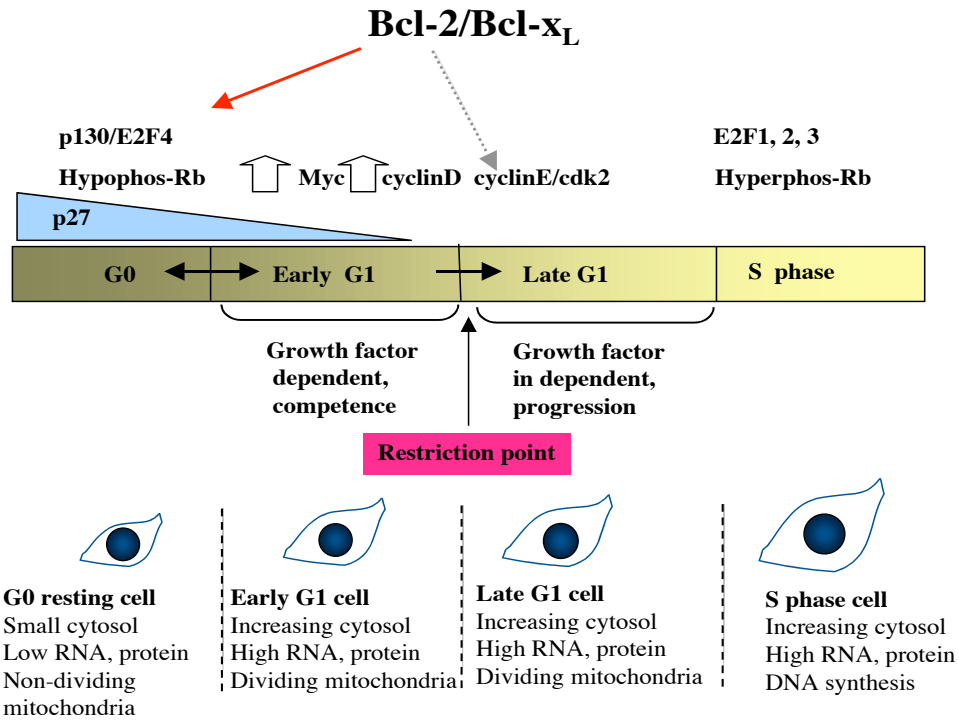

Figure 4: Molecular events and phases of cell cycle progression. In G_0 or quiescence cells are generally small in size due to low levels of macromolecular synthesis. Cells contain high levels of CDKI p27, and pRb is hypophosphorylated. In early G_1 cells increase their size and initiate RNA and protein synthesis. Upon cell cycle entry, cyclins complexed with cyclin-dependent kinases phosphorylate pRb, resulting in translation of genes necessary for S phase entry.

cause G_0 cells to enter G_1. At this time, immediate early genes such as Myc, Jun and Fos are activated, and are thought to transcribe genes involved in cell cycle progression. Myc transcribes a multitude of genes that affect cell growth, proliferation and apoptosis (Bello-Fernandez, 1993; Leone, 2001). G_1 phase is divided into early and late G_1. Early G_1 is a growth factor dependent phase: cell size is increased, rRNA synthesis is initiated, mitochondria multiply and cells gain competence to complete G_1. In late G_1, a growth factor-independent phase, cells continue to increase in size. Not only does mitochondrial mass increase from G_0 to G_1, but mitochondrial morphology also changes from reticular to fragmented during cell cycle progression (Marginteantu et al., 2002). The restriction point, usually defined by the activation of cyclin/cdk complexes, marks the transition from early to late G_1. While early G_1 cells can re-enter G_0 if correct signaling is absent, late G_1 cells are committed to progress into S phase. The increase in ribosomal RNA synthesis and ribosomal biogenesis that occur during G_1 is necessary to support macromolecular synthesis. Therefore, cell cycle progression must be synchronized with cell growth. In early G_1 cyclin D and cyclin E are induced. Association of the cyclins with their cdk partners activates cdks to phosphorylate pRB, resulting in disruption of pRB binding to E2F. The activation of free E2Fs as transcription factors is considered the beginning of S phase.

Although "quiescence" has been used to imply G_0, cells can be arrested in G_0 or G_1. However, these two states are physiologically distinct. Low RNA content and lack of Myc and cyclin D expression have been used to characterize cells in G_0, while early G_1 cells have more rRNA and express Myc and cyclin D. Recruitment of cells from G_0-G_1 only routinely occurs at sites in the hematopoietic system, the skin, and the

gastrointestinal tract. When cells lose their ability to enter quiescence, pathological states such as cancer can occur. Previous work has indicated that Bcl-x_L and Bcl-2 delay the onset of DNA synthesis compared to controls during entry into cell cycle from an arrested state. This finding does not distinguish whether Bcl-2/Bcl-x_L acts in G_0-G_1 transition or G_1. Data from our laboratory were consistent with Bcl-2/Bcl-x_L acting in both G_0 arrest and G_1 progression. Further experiments, reported below, suggested that a major function of Bcl-2/Bcl-x_L is in enhanced G_0 arrest, which can be manifested as a delay in progression to S phase, possibly through an effect on cell growth.

Myc

The Myc family, comprised of c-Myc, N-Myc, and L-Myc, regulates cell growth, proliferation, and apoptosis. Myc heterodimerizes with Max through their C-terminal basic helix-loop-helix zipper domains. The Myc-Max heterodimer recognizes the canonical E-box sequence CACGTG. Although the list of Myc target genes is growing and changing at a fast pace, it is clear that overexpression or downregulation of Myc in cells has significant effects on cell growth and cell cycle. Myc null mice are embryonic lethal; however, conditional knockout animals have been made (Moreno de Aborani et al., 2001). MEF's deficient in c-Myc exhibit prolonged doubling time due to overexpression of p27 (de Alboran et al., 2001), and B lymphocytes null for c-Myc show impaired mitogenic response and accumulation in G_0/G_1 (de Alboran et al., 2001). While our data showed that Bcl-2/Bcl-x_L does not directly interfere with Myc's ability to trans-activate or trans-repress, it is still possible that Bcl-2/Bcl-x_L regulates cell growth downstream of Myc. Cell growth must occur prior to cell proliferation. Protein

accumulation is used as a marker for cell growth because about 70% of a cell's dry mass is protein (Grummt, 2003; White, 2005). Protein synthesis is performed by ribosomes, which consist of protein and RNA subunits. RNA polymerases I, II, and III are responsible for synthesis of the ribosomal subunits. Proteomic comparisons of cells with inducible Myc and cells lacking Myc, showed that the largest class of genes induced by c-Myc were Pol II target genes encoding ribosomal and nucleolar proteins (Schlosser et al., 2003). Myc has been shown to directly activate RNA pol III, which is responsible for transcribing rRNAs (Gomez-Roman et al., 2003). Recent evidence showed that Myc controls ribosomal RNA synthesis in mammalian as well as Drosophila cells (Arabi et al., 2005; Grewal et al., 2005; Grandori et al., 2005). In addition to direct transcriptional targets, Myc may also regulate cell growth through protein-protein interactions. Myc was shown to bind pRB *in vitro* and alter transcription of target genes such as pol I (Schmidt, 1999). Myc has been shown to regulate all three of the RNA polymerases, making Myc one of the major regulators of cell growth (Arabi et al., 2005; Grandori et al., 2005; Grewal et al., 2005; Schlosser et al., 2003; White, 2005).

Cyclin-dependent kinase inhibitor p27

p27 was the first identified cyclin-dependent kinase inhibitor. It functions in G_0, by binding to cyclin E/cdk 2 complexes to prevent the progression of cells into cycle. Protein levels of p27 are high in G_0 and decrease as cells enter the cell cycle. The amount of p27 within cells is controlled by multiple mechanisms. At the transcriptional level, p27 is repressed by Myc (Yang et al., 2001) or can be upregulated by FoxO1 (Machida et al., 2003). However, the ubiquitination pathway is the major regulator of p27 abundance

in cells (Philipp-Staheli et al., 2001). Phosphorylation of p27 at Thr187 by cyclinE/cdk2 targets p27 for ubiquitination and degradation (Tsvetkov et. al., 1999; Ungermannova et al., 2005). Data from $p27^{-/-}$ mice showed that p27 is a very important regulator of cell proliferation, as these mice exhibit larger size due to increased cell numbers (Nakayama et al., 1996; Fero et al., 1996). p27 regulates cell proliferation in a multitude of tissues as is evident from the increase in overall animal size (Nakayama et al., 1996; Fero et al., 1996).

Akt/PKB

Akt/PKB is a serine/threonine kinase involved in cell survival and cell growth signaling in a PI(3)kinase-dependent manner. There are three Akt isoforms that have been identified in mice and humans to date. Although different genes encode the Akt proteins, the differences in amino acid composition and protein domain structure are subtle. The Akt signaling pathway can be activated by a number of growth factors, cytokines, hormones, and neurotransmitters (such as IL3, insulin, TCR, CD28 et al.). Upon ligation of a receptor tyrosine kinase, PI(3)K generates the membrane phospholipids phosphotydylinositol (3,4,5) trisphosphate (PIP3). PIP3 recruits Akt to the plasma membrane where Akt is activated through phosphorylation at Thr308 and Ser473 by PDK1 (Song et al., 2005). Akt is a critical effecter of cell survival, and enhances cell survival through direct and indirect means. For example, Akt phosphorylates the pro-apoptotic protein Bad (del Peso et al., 1997). Wild type Akt or myristoylated Akt, but not a kinase dead mutant, were shown to phosphorylate Bad at the same residues as is induced by IL-3 (del Peso et al., 1997). The phosphorylated form of Bad is bound to 14-

3-3, which sequesters Bad in the cytosol preventing cell death. Akt has also been shown to phosphorylate several members of the FoxO transcription factor family (Fabre et al., 2005; Skurk et al., 2005). The FoxO proteins affect survival through the regulation of transcription of their target genes such as Fas ligand, TRAIL (TNF related apoptosis inducing ligand), TRADD (TNF receptor type 1 associated death domain), and Bim. However, the major physiologic function of Akt is the regulation of cell metabolism. Overexpression of Akt in *Drosophila* increases cell size without stimulating cell proliferation (Verdu et al., 1999). Studies in mammalian cells showed that Akt maintains cell survival and cell metabolism in the absence of growth factor (Rathmell et al., 2000). Mice expressing a myristoylated Akt transgene in T cells develop both tumors and autoimmunity (Rathmell et al., 2003). Active Akt resulted in T cell size enlargement, increased basal glycolytic rate, while remaining in a non-proliferative state (Rathmell, et al., 2003). The cell survival and cell metabolism functions of Akt are at least in part coupled. Akt increases the association and activity of mitochondrial hexokinase (mHK) at the mitochondria (Majewski et al., 2004b), and Akt also requires glucose and active mHK to inhibit apoptosis (Majewski et al., 2004a). mHK acts at the first step of glucose metabolism by converting glucose to glucose-6-phosphate. mHK also regulates apoptosis by binding to VDAC, preventing the access of Bax/Bak to the VDAC/ANT complex.

Summary

Compounding evidence links cell proliferation and cell death (Olson et al., 2003; Woo et al., 2003; Linette et al., 1996); however, the relationship between the two

processes remains unclear. Bcl-2 family members are able to regulate both cell cycle and apoptosis (Chattopadhyay et al., 2001; Janumyan et al., 2003). The goal of this dissertation is to elucidate the relationship between the cell cycle and cell death functions of Bcl-2, as well as to determine the mechanism of Bcl-2 cell cycle delay.

CHAPTER II

MATERIALS AND METHODS

Cell Culture

Fibroblasts were maintained in Dulbecco's Modified Eagle Medium (DMEM) supplemented with 10% fetal calf serum (FCS) or calf serum (CS), 2mM L-glutamine and 100 U penicillin/streptomycin per mL (BioWhittaker). In Rat1 MycER cells (gift of Gerard Evan), Myc expression was induced by the addition of 4-hydroxytamoxifen (4-OHT) to the media at 1uM. In Rat1RafER cells (gift of Dr. McMahon), Raf expression was induced by the addition of 4-OHT to the media at 200 nM. *TSC1* $^{+/+}$ and *TSC!* $^{-/-}$ mouse embryonic fibroblasts were kindly provided by Dr. David Kwiatkowski. FL5.12 cells were maintained in IMDM supplemented with 5% fetal calf serum, 2mM L-glutamine, 100 U penicillin/streptomycin per ml and IL-3. 143B rho 0 cells (a gift from Dr. James Sligh) were maintained in DMEM supplemented with 10% fetal calf serum, 2mM L-glutamine, 100 U penicillin/streptomycin, 5 ug/ml uridine and 100 mM pyruvate.

Murine T cell Isolation

For cell cycle experiments of T cells, single cell suspensions were prepared from the spleens of 10-12 week old lck^{pr}-Bcl2 or Eμ-Bcl-x_L mice, and wildtype littermate controls. After hypotonic lysis of red blood cells, T cells were isolated by negative selection using an indirect magnetic labeling system. B cells, NK cells, dendritic cells, macrophages, granulocytes and erythroid cells were selected out of spleen cell

suspensions with a cocktail of biotin-conjugated antibodies against CD45R (B220), DX5, CD11b (Mac-1), and Ter-119 (Miltenyi Biotec) (Linette et al., 1996). Magnetically labeled cells were depleted from the spleen cell suspension by passing the cell suspension through a magnetic column. Isolated T cells were plated in 24-well dishes coated with anti-CD3 mAb (3ug/ml) (Pharmingen) to stimulate cell cycle entry.

Retroviral Infection

Bcl-x_L and Bcl-2 and caspase 9 dominant negative were introduced into cells by retroviral infection. pBabe-puro or pWzl-neo constructs containing full length Bcl-2 (human) or Bcl-x_L (mouse) were transfected using calcium phosphate into BOSC cells. Briefly, 10μg of DNA was mixed with 1 ml of HBSP buffer [50mM HEPES pH 7.05, 10mM KCl, 12mM dextrose, 280mM NaCl, and 1.5 mM Na_2HPO_4] and 125mM $CaCl_2$ and added drop-wise to BOSC cells. After 8 hours, the fresh complete medium was added to the BOSC cells. Two days later, viral supernatant was collected, filtered, and used to infect the fibroblasts four times at 2-hour intervals. Cells were selected in media containing puromycin (4 ug/ml) or G418 (0.75mg/ml) 48 hours after infection.

Cell Cycle Analysis

Cells were plated in six-well dishes and allowed to incubate overnight. The next day, cells were washed three times with phosphate-buffered saline (PBS) and cultured in medium containing 0.05% fetal bovine serum (FBS) for Rat1MycER and Rat1RafER cells or 0.5% calf serum (CS) for NIH 3T3 cells. After 72 hrs, Rat1MycER cells were stimulated with either 4-OHT or 10% serum. At indicated times, cells were collected,

resuspended in Krishan's reagent (0.1 mg/ml propidium iodide, 0.02 mg/ml RNase A, 0.3% NP-40 and 0.1% Na Citrate) and analyzed on a FACSCalibur flow cytometer (Becton Dickinson). For contact inhibition, cells were plated at 5×10^6 cells per 10 cm plate and allowed to reach confluence for 4 days. For BrdU incorporation, cells were plated in 10 cm dishes. At indicated times, 10 uM BrdU was added to the cells for 30 min. Cells were then harvested, washed once with PBS, and fixed in ice-cold 70% ethanol, treated with 4 N HCl, neutralized by 0.1 M borax, washed with PBS containing 0.05% bovine serum albumin (BSA), and incubated sequentially with anti-BrdU antibody (Becton Dickinson) and FITC-conjugated anti-mouse secondary antibody (Sigma) in the presence of 0.5% BSA and 0.5% Tween-20. Cells were resuspended in PBS containing propidium iodide and RNase A, and analyzed by flow cytometry. Data were analyzed using Cell Quest and ModFit software.

Immunoblots

Cells were lysed by the addition of 1× SDS PAGE running buffer (Tris pH 6.8, 2% SDS, 10% glycerol, and Bromophenol Blue) with 0.5% DOC and 5% β-mercaptoethanol. Cell lysates were separated by electrophoresis on a 12.5% SDS-PAGE, and transferred to a polyvinylidene difluoride (PVDF) membrane. The membranes were immunoblotted with 2A1 for Bcl-x_L (gift from Dr. Lawrence Boise), polyclonal 10929 for Bad (gift from Dr. Stanley Korsmeyer), 6C8 for human Bcl-2 (PharMingen), p27 (Transduction Labs), caspase 9 (Cell Signaling), caspase 3 (Cell Signaling), Akt (Beckton-Dickenson), phospho-serine 473 Akt (Cell Signaling).

RNA/DNA Staining

Simultaneous Hoechst and pyronin Y staining was performed according to the protocol of Darzynkiewicz (1994). Cells were collected and resuspended in one part cold saline GM (1.1 g/l glucose, 8 g/l NaCl, 0.4 g/l KCl, 0.39 g/l Na2 HPO4, 0.15 g/l KH2 PO4, 0.5 mM EDTA) and three parts 100% cold ethanol. After fixation, cells were first resuspended in 0.25 ml saline GM containing 1 ug/ml Hoechst (Polysciences, Inc.), then 0.25 ml saline GM containing 2 ug/ml pyronin Y (Polysciences, Inc.) was added to make ~10^6 cells/ml. Samples were analyzed on a FACSTAR Plus flow sorter (Becton Dickinson). Hoechst was excited with the UV line and pyronin Y was excited with the 488 line of an Enterprise laser. Hoechst emission was detected with a 424/44 dichroic filter, and pyronin Y fluorescence was detected with a 575/26 dichroic filter. For 7-AAD and pyronin Y staining, 1.25 mg/ml of 7-AAD (BD-PharMingen) was added instead of Hoechst. Samples were analyzed on a FACSCalibur (Becton Dickinson). 7-AAD fluorescence was collected in FL3, and pyronin Y staining was collected in FL2.

ATP Measurement

An ATP Bioluminescence kit (Roche) was used to measure ATP content of cell lysates, where light emitted by the catalysis of luciferin is directly proportional to the amount of ATP in the cells. To elevate intracellular ATP levels, NIH3T3 cells were treated with 50 uM adenine during serum stimulation.

TMRE and MTG staining of mitochondria

Cells were incubated in medium containing 50 nM tetramethyl rodamine ester

(TMRE) or 500 nM MitoTracker Green (MTG) for 30 minutes at 37 C. Cells were removed from the wells, kept in the dye-containing medium, and analyzed by flow cytometry. TMRE fluorescence was detected in FL2 and MTG fluorescence was detected in FL1.

CHAPTER III

BCL-2 AND BCL-X_L DELAY CELL CYCLE ENTRY BY ENHANCING G_0 ARREST

Introduction

To date, the cell cycle function of Bcl-2/Bcl-x_L has been measured as prolonged time to enter S phase. However, it was not established whether the lengthened time to reach S phase was a result of prolonged G_1 phase or the inability to exit from G_0. Bcl-2 was shown to speed up the exit to G_0 in HL60 cells induced to differentiate with DMSO (Vairo et al., 1996); and Bcl-2 has been shown to prolong G_1 (Linette et al., 1996; Mazel et al., 1996). The CDKI p27 is upregulated in quiescent T cells and arrested fibroblasts overexpressing Bcl-2 or Bcl-x_L (Linette et al., 1996, Vairo et al., 2000), and ablation of p27 in fibroblasts results in the inability of Bcl-x_L to delay S phase entry (Greider et al., 2002). In addition to p27, Bcl-2 has also been shown to upregulate the pRB family member p130, which functions in G_0 to inhibit E2F-1 expression (Lind et al., 1999, Vairo et al., 2000). These data suggest that Bcl-2/Bcl-x_L functions in G_0 to exert its cell cycle effect. However, our lab has also shown that during serum-induced or Myc-induced cell cycle entry of fibroblasts, the activities of cyclin D/cdk4 and cyclin E/cdk2 are greatly diminished in cells overexpressing Bcl-2 or Bcl-x_L (Greider et al., 2002). These data indicate that Bcl-2/Bcl-x_L may function in G_1 to prevent the progression of cell cycle events. The following data distinguished whether the action of Bcl-2/Bcl-x_L occurs in G_0 or G_1. Knowledge of the biochemical step affected by Bcl-2/Bcl-x_L in cell cycle progression sheds light on the relationship between cell survival and cell cycle control.

Results

Y28Bcl-2 mutation does not separate the cell death and cell cycle functions of Bcl-2

Mutations of the Y28 residue in BH4 of Bcl-2 have been reported to abrogate the cell cycle delay function of Bcl-2 without affecting its anti-apoptosis activity. We tested the effects of this mutation (as well as 22 other mutants (Janumyan et al., 2003) work of Courtney Greider, Ph.D. in our lab) in Myc-induced and serum-induced cell cycle entry. Bcl-2 cDNAs encoding the wild type or the Y28F allele were retrovirally introduced into Rat1 cells harboring a 4-hydroxytamoxifen (4-OHT) sensitive Myc-ER fusion. Rat1MycER cells containing pBabe vector, wildtype Bcl-2 (wtBcl-2), or Y28F-Bcl-2 were serum starved for 3 days, then stimulated to re-enter cell cycle with the addition of 4-OHT or 10% FCS DMEM. Following induction of Myc-ER, control cells began to show a significant rise in S phase cells by 8 hours (Figure 5 A, B). Cells expressing wtBcl-2 remained in G_0/G_1 even after 12 hours following release, as previously reported (Greider et al., 2002). Surprisingly, cells expressing Y28F-Bcl-2 exhibited no increase in S phase cells up to 12 hours after MycER induction, exactly as wtBcl-2 cells. Similar results were observed in serum-induced cell cycle entry of Rat1MycER cells (Figure 6). Viability in 10% serum and in 0.1% serum plus 4-OHT showed that Y28F-Bcl-2 rescued Myc-induced apoptosis as efficiently as wtBcl-2, confirming that wtBcl-2 and Y28F-Bcl-2 proteins were functional in these cells (Figure 5 C). In experiments using several different lines constructed on separate occasions, we found that the Y28F mutation did not diminish the ability of Bcl-2 to delay Myc-induced or serum-induced S phase entry.

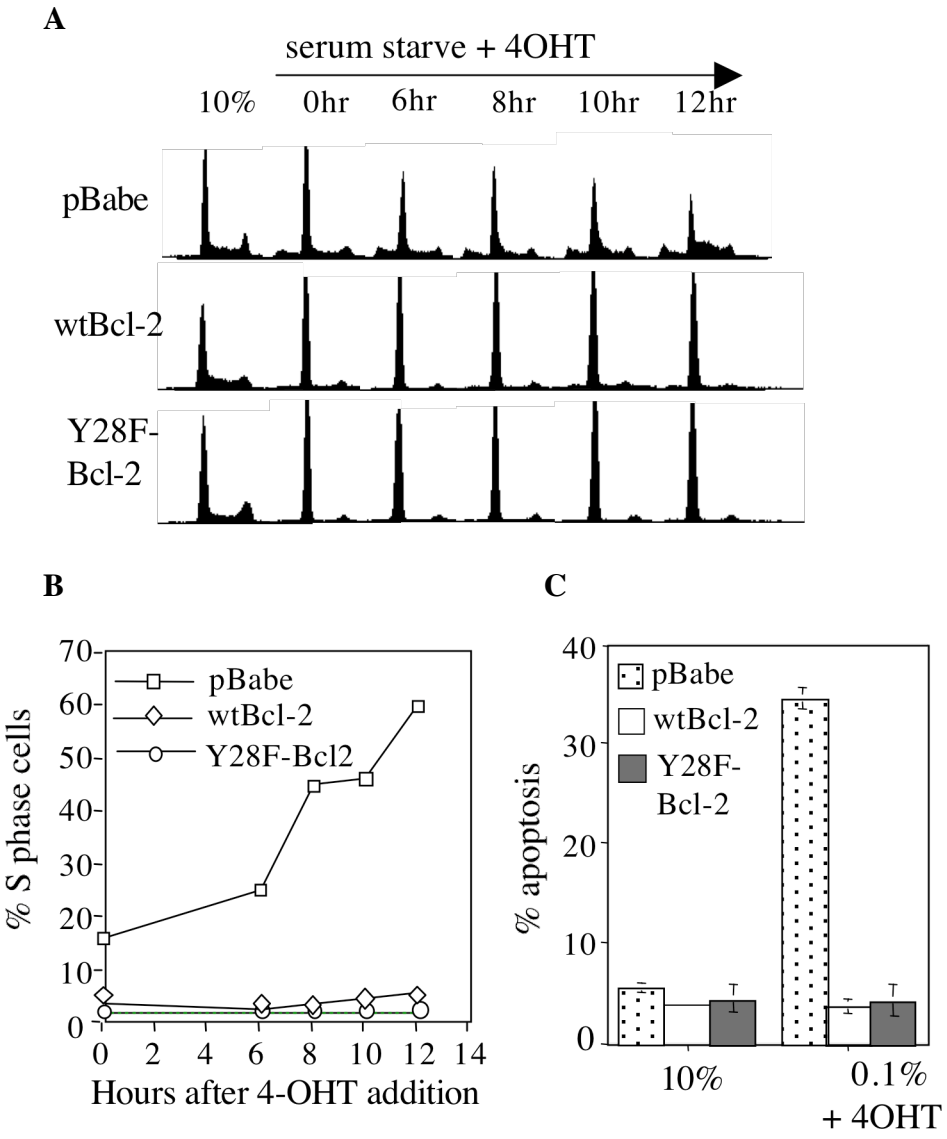

Figure 5: Y28F-Bcl-2 inhibits Myc-induced cell cycle entry and Myc-induced apoptosis. Rat1MycER cells expressing wtBcl-2, Y28F-Bcl-2, or pBabe vector were cultured in 0.05% FBS medium for 3 days, then 1mM 4-OHT was added. (**A**) Cells were collected before serum starvation (10%), after 3 days of serum starvation just prior to addition of 4-OHT (0 hr), and at the indicated times after MycER induction, and cell cycle profiles were obtained by PI /FACS analysis. (**B**) Graph of the percentages of cells in S phase obtained from Modfit analysis of data points in A. (**C**) Percentages of apoptotic cells as determined by PI exclusion assays are compared between asynchronously growing cells and cells which have been serum starved and treated with 4-OHT. One representative experiment of at least three is shown.

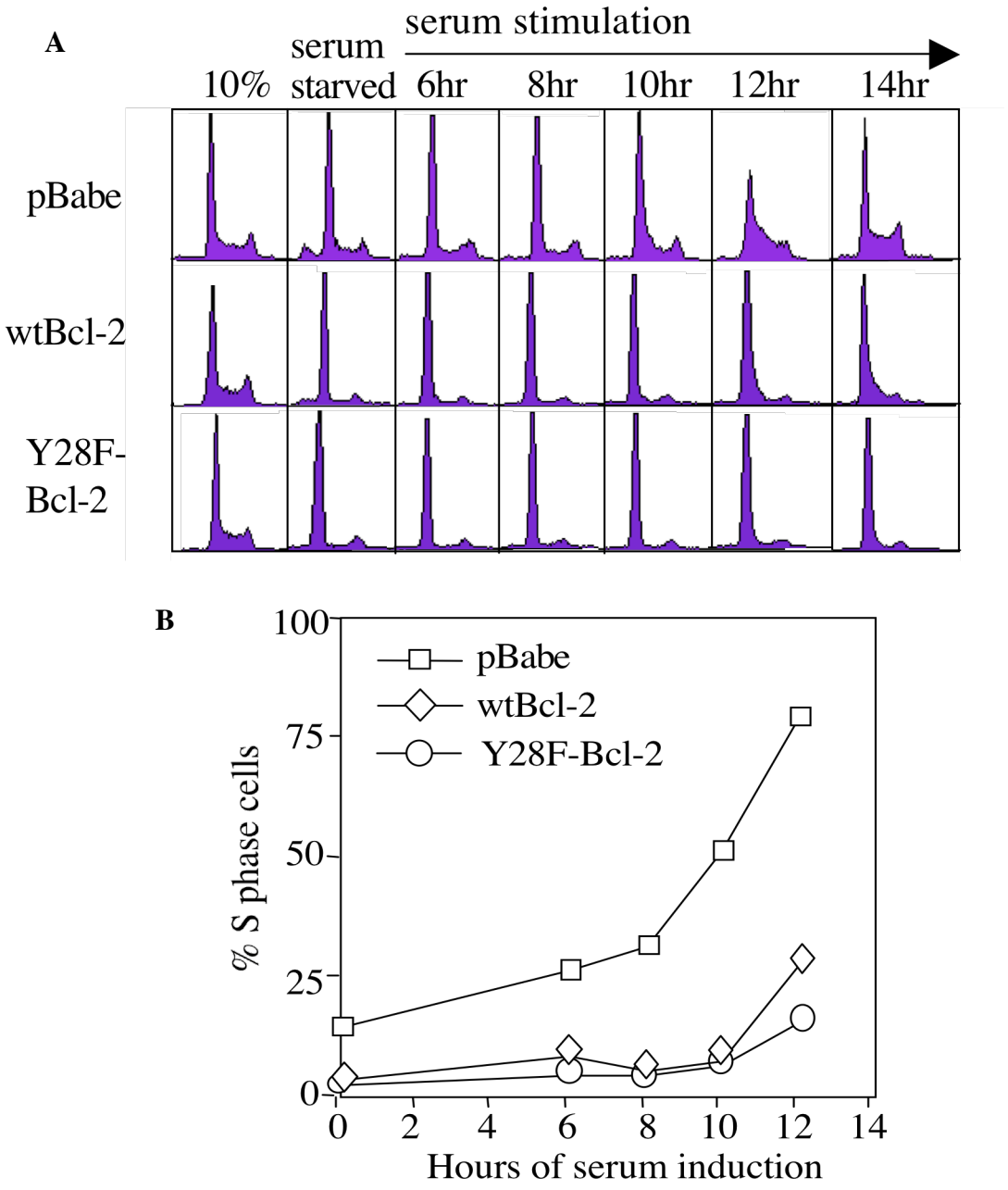

Figure 6: Y28F-Bcl-2 delays serum-induced cell cycle entry. Rat1MycER cells were serum starved as in Figure 6, but were induced to re-enter the cell cycle by the addition of 10% FBS medium. (**A**) PI/FACS cell cycle profiles before serum starvation (10%), after serum starvation (0 hr), and at the indicated times after addition of serum are shown. (**B**) Graph of percentages of S phase cells by Modfit analysis of data from A. One representative experiment of at least three is shown.

Since NIH3T3 was the cell line used in the original paper reporting the failure of Y28 mutations to delay cell cycle entry, in collaboration with M. Knudson's laboratory, we also expressed another allele of Y28, Y28A-Bcl-2, and wtBcl-2 cDNA in NIH3T3 cells by retroviral infection. Cells arrested by serum starvation and released by 10% serum were compared by BrdU incorporation. The ability of NIH3T3 cells expressing Y28A-Bcl-2 to incorporate BrdU at sequential time points following serum stimulation was very similar to cells expressing wtBcl-2 (Janumyan et al., 2003). In repeated experiments, we were unable to detect a difference in cell cycle kinetics between Bcl-2 mutated at Y28 and wtBcl-2. The data from other 22 Bcl-x_L mutants tested in Myc-induced and serum-induced cell cycle entry showed that the cell cycle delay phenotype co-segregated with the anti-apoptotic function (Janumyan et al., 2003).

Subcellular localization does not separate the cell death and cell cycle functions of Bcl-2

Bcl-2 protein is found in the mitochondrial outer membrane, endoplasmic reticulum (ER), and the nuclear membrane. Extensive studies focused on the anti-apoptosis function of Bcl-2 at the mitochondria. Survival function of Bcl-2 targeted only to the mitochondria outer membrane, by fusion with the targeting sequence from Listeria ActA protein (Bcl-2-acta), was not significantly affected (Zhu et al., 1996). However, when Bcl-2 was targeted only to the endoplasmic reticulum using the targeting sequence from cytochrome b5, selective protection against some apoptotic stimuli but not others was observed (Zhu et al., 1996; Lee et al., 1999). We tested ER- and mitochondrial-targeted Bcl-2 for cell cycle delay to ask whether this activity might be conferred by a particular subcellular localization of Bcl-2. Using Rat1MycER cell lines expressing

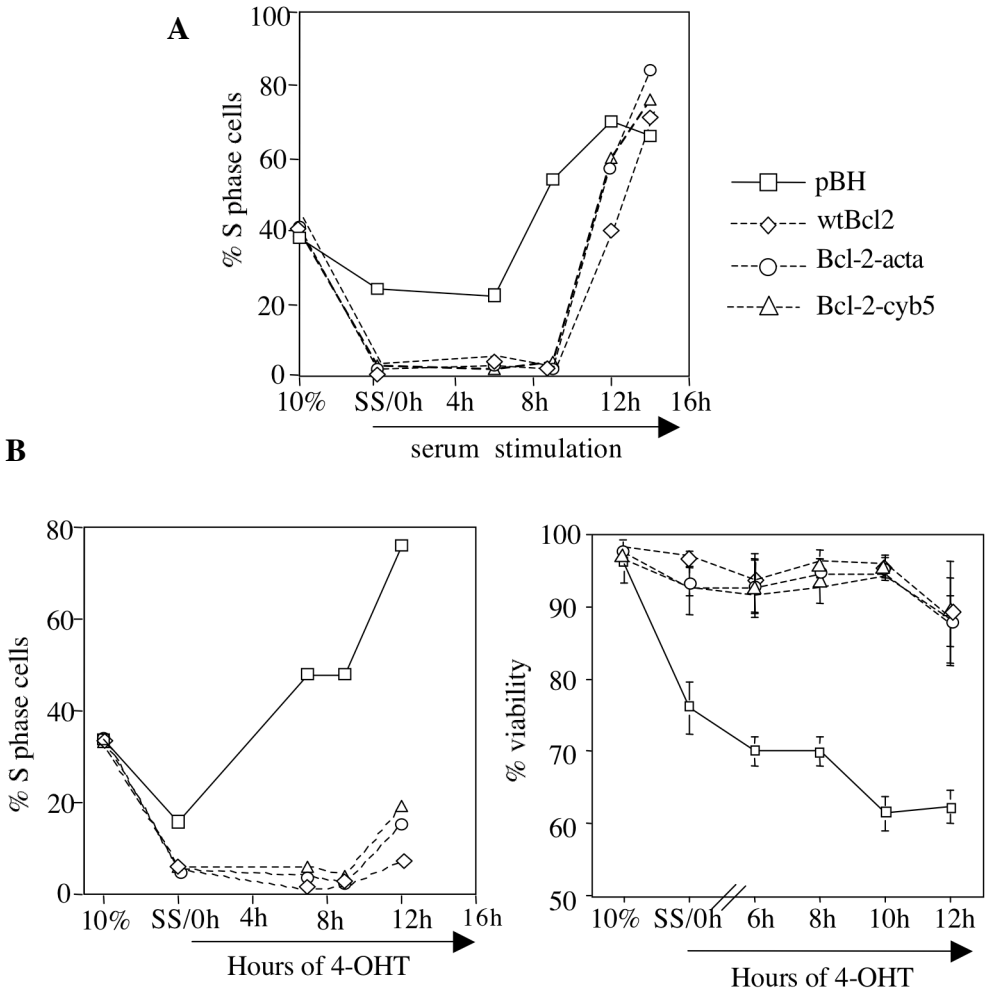

Figure 7: Bcl-2 targeted to the endoplasmic reticulum or the mitochondrial outer membrane retains cell cycle delay activity. Rat1MycER cells expressing wtBcl-2, Bcl-2 fused with the ActA mitochondria targeting sequence (Bcl-2-acta), Bcl-2 fused with the endoplasmic reticulum targeting sequence from cytochrome b5 (Bcl-2-cyb5), or pBH vector alone were cultured in 0.05% FBS for >48 hours, then stimulated with (**A**) addition of 10% serum or (**B**) treatment with 1mM 4-OHT. DNA content was measured by PI staining and FACS analysis. Percent S phase cells were obtained from Modfit program. Representative experiments of at least three are shown. Percent apoptosis was derived from PI exclusion assays. Standard deviations were obtained from 3 experiments. Similar results were obtained scoring Annexin V positivity and cells with subG1 DNA.

wtBcl-2, Bcl-2-cyb5 (ER), or Bcl-2-acta, we assayed the rate of serum-stimulated and Myc-induced S phase entry. In both cases, ER- and mitochondrial-targeted Bcl-2 delayed progression to S phase similar to wtBcl-2 (Figure 7 A, B). Cells expressing these constructs were also resistant to Myc-induced death (Figure 7 B), confirming that their anti-apoptosis activities were intact. Thus far, subcellular targeting did not differentially affect the cell cycle and cell survival activities of Bcl-2. These data led us to hypothesize that the activities of Bcl-2/Bcl-x_L on cell cycle and cell death are either interrelated or are two effects stemming from one function.

Activation of Myc and cyclin D proteins during cell cycle entry is unaffected by Bcl-x_L and Bcl-2, but cyclin/cdk activities are inhibited

To determine whether molecular events preceding S phase entry were also delayed in Bcl-2/Bcl-x_L cells, we compared the timing of activation of Myc and cyclin D1. NIH3T3 cells expressing pBabe puro or pBabe puro Bcl-x_L were cultured in 0.75% calf serum for three days. Cells were stimulated to enter cell cycle by re-addition of 10% calf serum. Cells were collected during arrest and at serial time points following serum stimulation of cell cycle entry. We had shown that cyclin Ds were induced on time (Greider et al., 2002), and then decided to examine the activation of Myc. Consistent with previous data in T cells (Linette et al., 1996), which show that during activation-induced cell cycle entry of T cells, RNA levels of c-Myc are unaffected by Bcl-2, we observed that NIH3T3 vector control and Bcl-x_L expressing cells show identical induction of Myc protein during serum stimulated cell cycle entry (Figure 8). As expected, c-Myc protein level is almost undetectable following serum starvation of control and Bcl-x_L cells. Two hours following serum stimulation of S phase entry, c-Myc

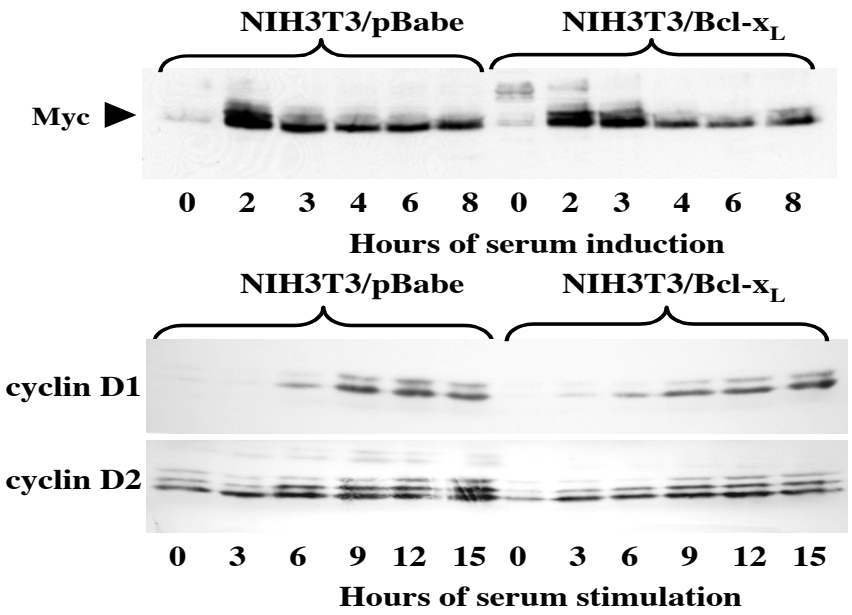

Figure 8: Induction of Myc and cyclin D is not affected by Bcl-x_L during cell cycle entry. NIH 3T3 cells were serum starved for three days in 0.75% CS medium, then released into cell cycle by serum re-addition. Equal amounts of protein were immunoblotted for Myc, cyclin D1, and cyclin D2 at indicated times following serum stimulation.

protein level increases in both control and Bcl-x_L cells. These data support the hypothesis that Bcl-2/Bcl-x_L acts downstream of Myc induction.

The induction of cyclin D is an early G_1 event. No difference was observed in the induction of cyclin D protein between vector alone and Bcl-x_L expressing cells during cell cycle entry (Greider et al., 2002). Cyclin D1 protein level was undetectable following serum starvation of NIH3T3 control and Bcl-x_L cells (Figure 8). Cyclin D1 induction occurs at 6 hours following serum stimulation in both control and Bcl-x_L cells, and levels of cyclin D1 remain high and similar between control and Bcl-x_L cells. Cyclin D2 levels are low following serum starvation and begin to increase at about 3 hours following serum stimulation of S phase entry comparably in control and Bcl-x_L cells. These data suggest that Bcl-x_L may act downstream of cyclin D.

Dr. C. Sansam in our lab examined the cell cycle effects of Bcl-x_L/2 by measuring the kinase activity of G_1 cyclin/cdk complexes. Consistent with G_0/G_1 arrest, kinase activity at the serum starvation time point was downregulated (Greider et al., 2002). After the induction of cell cycle entry by Myc activation or serum addition, cdk activity increased as cells progressed through cell cycle. Bcl-x_L expressing cells show delayed and reduced activity of the G_1 cyclin kinases. Bcl-x_L was more inhibitory to the cyclin kinase activity in Myc-induced cell cycle entry compared to serum-induced cell cycle entry. No detectable cdk activity was observed in Bcl-x_L expressing cells at 3, 6, and 9 hours after Myc induction as compared to control cells that showed cdk activity as soon as 3 hours after Myc induction (Greider et al., 2002).

Despite normal induction of early G_1 markers, Myc and cyclin D, activation of cyclin D/cdk 4 and cyclin E/cdk2 is delayed in Bcl-2/Bcl-x_L cells. These results indicate

that the signals for G_1 entry are activated normally in Bcl-2/Bcl-x_L cells, but progression to the restriction point is hindered.

Bcl-x_L does not affect the rate of exit to G_0 in NIH3T3 cells

It has been shown that in HL60 cells Bcl-2 accelerates the entry of cells into G_0 upon induction of differentiation by DMSO (Vairo et al., 1996). However, it has also been shown that Bcl-2 lengthens G_1 (Mazel et al., 1996). Thus, existing data do not clearly establish whether Bcl-2 effects G_0 or G_1. The levels of p27 are elevated in T cells and fibroblasts expressing Bcl-2, and Bcl-2/Bcl-x_L cannot delay S phase entry in the absence of p27 (Linette et al., 1996; Vairo et al., 2000; Greider et al., 2002). p130, which complexes with E2F-4 to inhibit E2F-1 expression, has also been shown to be upregulated by Bcl-2 (Lind et al, 1999; Vairo et al., 2000). These data suggest that Bcl-2 acts in G_0. The induction of cyclin D1 in Bcl-2/Bcl-x_L-expressing cells is normal; however, the activities of cyclin D/cdk 4 and cyclin E/cdk 2 are greatly diminished (Greider et al., 2002). These data suggest that Bcl-2 prevents progression of events in G_1. To determine whether Bcl-x_L hastened the exit of cells into G_0, we simultaneously stained vector control (pBabe puro) and Bcl-x_L cells for RNA and DNA during arrest. Transition to G_0 is accompanied by a significant decrease in ribosomal RNA, while DNA content remains the same (Polymenis and Schmidt, 1999; Stocker and Hafen, 2000). The fluorescent dye pyronin Y preferentially stains polyribosomal RNA, and an increase in pyronin Y fluorescence in cells with 2N DNA content indicates transition from G_0 to G_1 (Darzynkiewicz, 1994). NIH3T3 cells retrovirally infected with vector control or Bcl-x_L were either serum-starved in 0.75% calf serum medium or plated for contact inhibition.

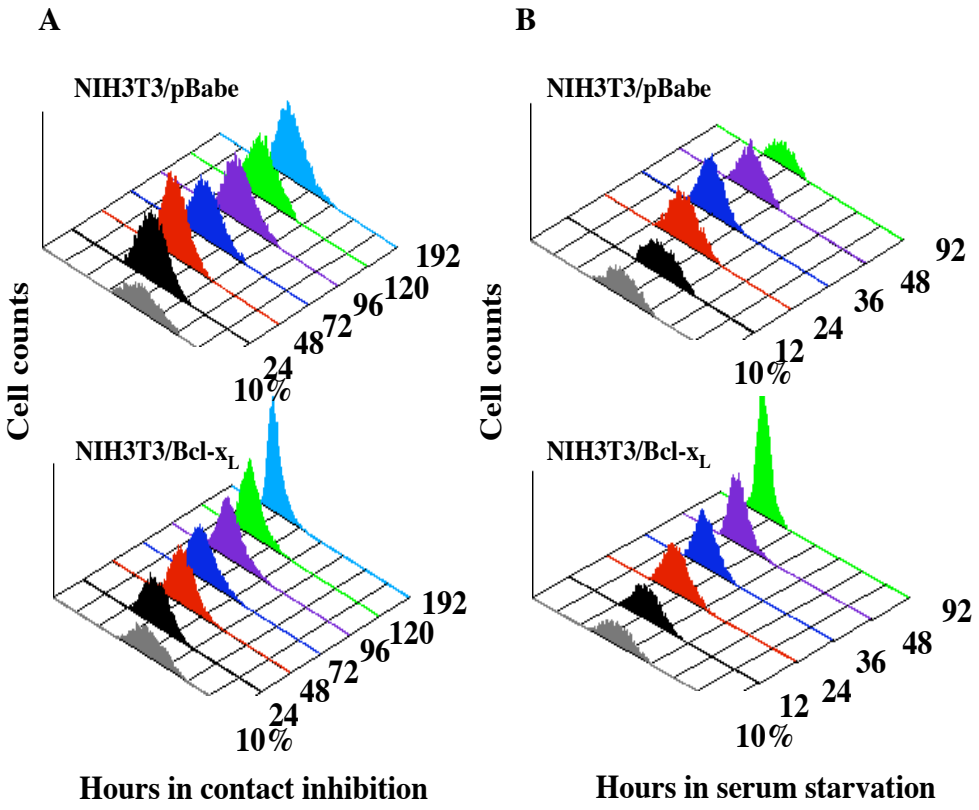

Figure 9: Bcl-x_L does not increase the rate of G_0 entry. NIH3T3 cells expressing pBabe empty vector or pBabeBcl-x_L were arrested by either contact inhibition (**A**) or serum starvation (**B**). Cells were collected at indicated time points and fixed in 70% ethanol. Cells were stained for DNA with 7-AAD and RNA with pyronin Y for FACS analysis. Histograms of pyronin Y fluorescence of asynchronously growing (10%) cells and during contact inhibition or serum starvation are shown. A representative experiment of three is shown.

Cells were collected every 12 hours during serum starvation and every 24 hours during contact inhibition and fixed with 70% ethanol. Samples were stained with Hoechst 33342 for DNA and pyronin Y for RNA content and analyzed by FACS. In both control cells and Bcl-x_L cells, RNA content starts to decrease by 24 hours following plating for contact inhibition, indicating that cells are beginning to enter G_0 (Figure 9). However, following 72 hours in contact inhibition, NIH3T3/pBabe cells stop reducing their RNA content, while NIH3T3/Bcl-x_L cells exhibit further reduction of RNA and the cell population is becoming more homogenous in terms of RNA content. Similar results were observed in serum-starved cells. Following 36 hours in starvation, NIH3T3/pBabe cells stop reducing their RNA content, while NIH3T3/Bcl-x_L cells exhibit further reduction of RNA. Following 92 hours in serum starvation pBabe puro cells exhibit diminished viability. The data suggest that Bcl-x_L does not affect the rate of G_0 entry rather Bcl-x_L allows cells to continue the G_0 path possibly by preventing cell death. However, cells arrested by contact inhibition remain in the presence of growth factors. Viability of contact inhibited pBabe puro cells is comparable to the viability of Bcl-x_L cells. Thus, Bcl-x_L cells are exhibiting the enhanced G_0 arrest phenotype in the absence of apoptotic stimulus, suggesting separation of cell cycle arrest and cell death functions of Bcl-x_L. The contact inhibition studies show that enhanced cell cycle arrest is not just a consequence of enhanced survival.

Bcl-x_L delays the increases in RNA accumulation and cell size during stimulation of cell cycle entry

To determine whether the delay in reaching S phase was caused by inability to exit G_0 or a prolongation of G_1, we simultaneously stained control and Bcl-2 cells for

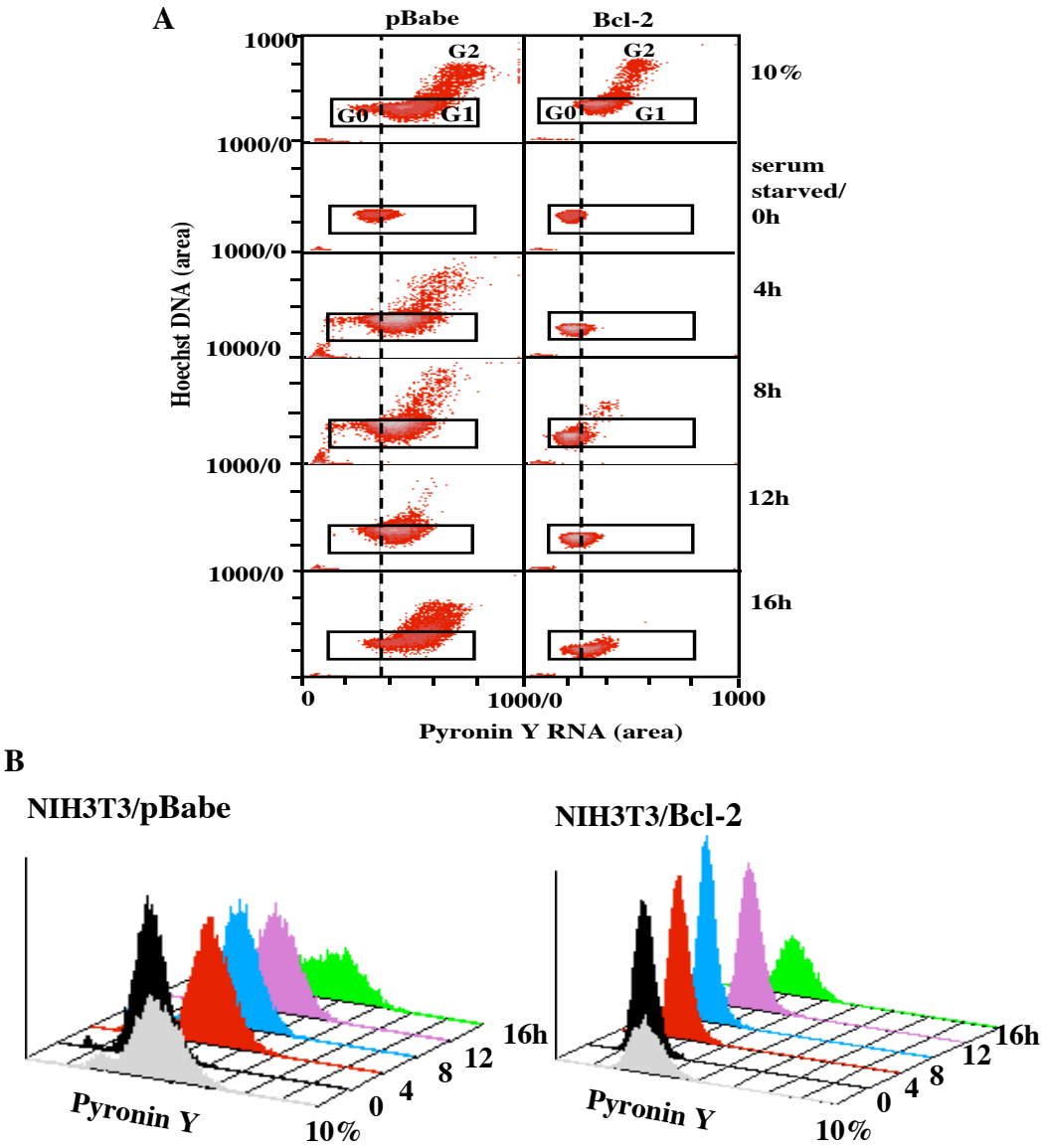

Figure 10: Bcl-2 expression retains cells in G_0 during serum-stimulated cell cycle entry following serum starvation. NIH3T3 cells retrovirally infected with pBabe or pBabeBcl-2 were arrested by culturing in 0.5% CS DMEM for 72 hours and stimulated to enter cell cycle by addition of 10% CS DMEM. Cells were collected at indicated times and stained with Hoechst 33342 and pyronin Y for FACS analysis. (**A**) Dot plot of Hoechst versus pyronin Y fluorescence for asynchronously growing cells (10%), following serum starvation (0 hrs), and at time points after serum stimulation. (**B**) Histograms of pyronin Y fluorescence of cells gated for 2N DNA content from (**A**). A representative experiment of three is shown.

RNA and DNA during arrest and release. Transition from G_0 to G_1 is accompanied by a significant increase in ribosomal RNA synthesis, while DNA content remains the same (Polymenis and Schmidt, 1999) (Stocker and Hafen, 2000). NIH3T3 cells retrovirally infected with vector (pBabe puro) or pBabe puro Bcl-2 were serum starved for 3 days, then stimulated to enter cell cycle with 10% serum. Cells were collected at 0, 4, 8, 12, and 16 hours after serum stimulation. Samples were stained with Hoechst for DNA content and with pyronin Y for RNA and analyzed by FACS (Figure 10 A, B). Mean Pyronin Y fluorescence of cells gated on 2N DNA content was compared between samples. In both control and Bcl-2 cells, pyronin Y staining decreased significantly after serum starvation, consistent with arrest in G_0. After serum stimulation, pyronin Y staining of control cells recovered by 4 hours to almost baseline level, indicating transition from G_0 to G_1 has occurred. In contrast, Bcl-2 cells continued to have low pyronin Y staining at 4 and 8 hours after serum addition, and only began to show a slight increase at 12 hours. Low pyronin Y fluorescence reflects lack of initiation of rRNA synthesis, consistent with prolonged G_0 phase in Bcl-2 cells. These results indicate that delayed S phase entry of Bcl-2 expressing cells during serum induction is associated with prolonged G_0.

To assess G_0 to G_1 transition in another model of cell cycle entry, Bcl-2, Bcl-x_L, and vector control cells were plated at high density (5×10^6 cells/10cm plate) and allowed to contact inhibit for 4 days, then re-plated at low density to stimulate cell cycle progression. Decreased pyronin Y fluorescence indicated that all cells reached G_0 after culturing in confluence for 3 days (Figure 11). Control cells regained RNA staining by 8 hours after re-plating. However, pyronin Y staining of Bcl-2 and Bcl-x_L cells remained

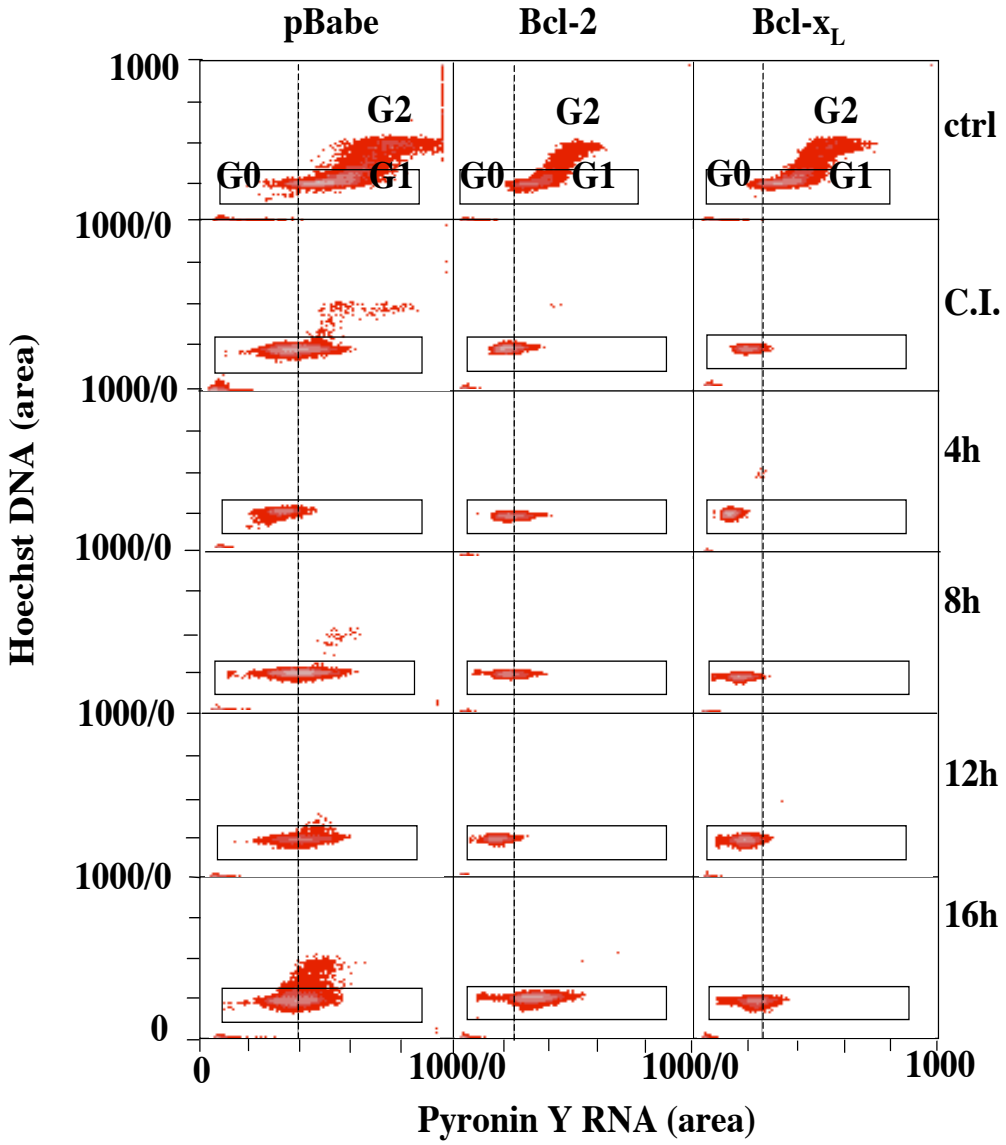

Figure 11: Bcl-2 expression retains cells in G_0 during serum-stimulated cell cycle entry following contact inhibition. NIH3T3 cells retrovirally infected with pBabe or pBabe Bcl-2 were arrested by culturing at high density ($5X10^6$ cells/10cm plate) for 4 days and stimulated to enter cell cycle by re-plating at low density. Cells were collected at indicated times and stained with Hoechst 33342 and pyronin Y for FACS analysis. Dot plot of Hoechst versus pyronin Y fluorescence for asynchronously growing cells (10%), following serum starvation (0 hrs), and at time points after serum stimulation. A representative experiment of three is shown.

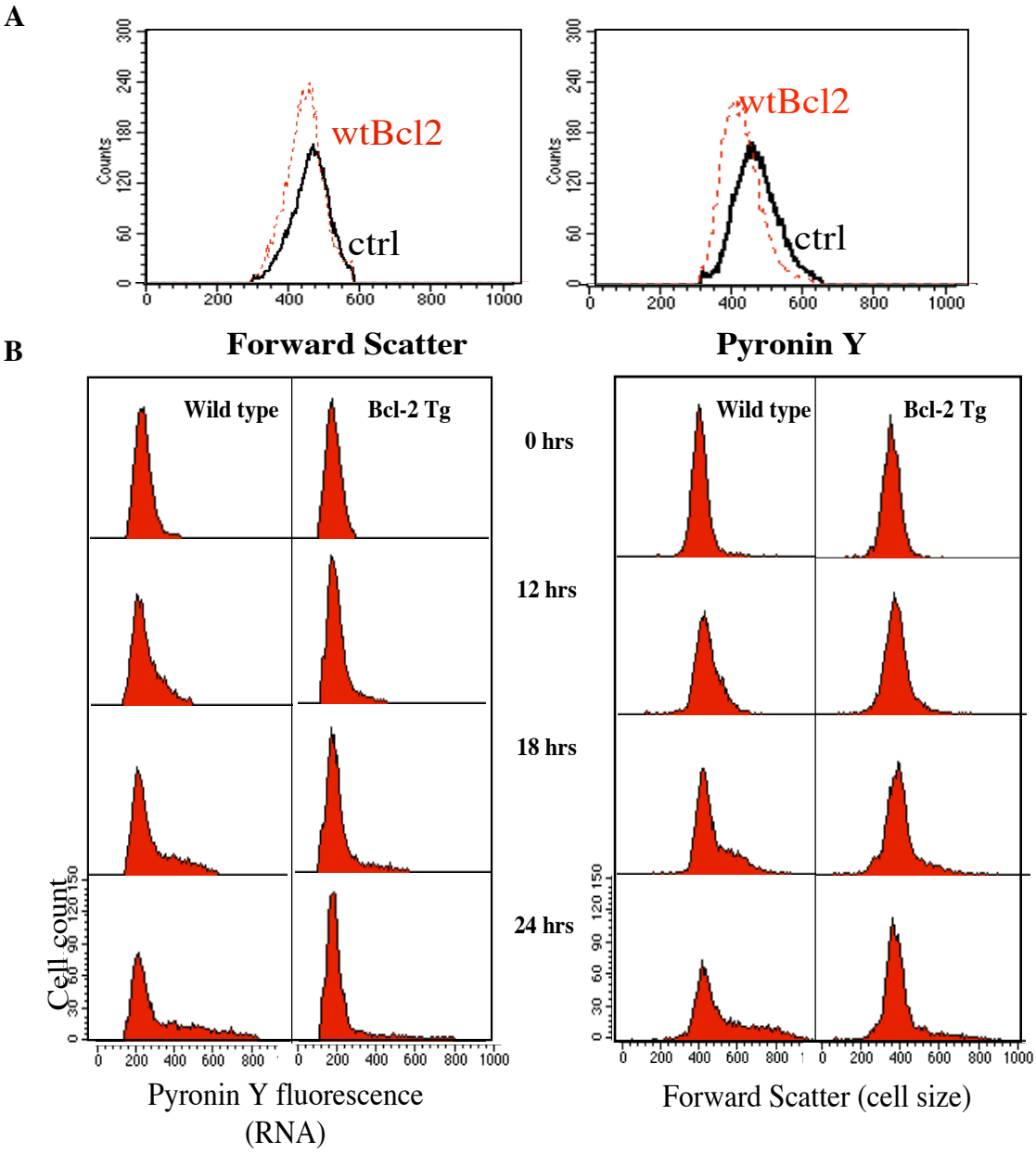

Figure 12: Bcl-2 transgenic murine T cells are smaller in size and contain less RNA than wild type T cells. (**A**) Forward scatter and pyronin Y histogram overlays of quiescent wild type and Bcl-2 transgenic T cells. (**B**) Pyronin Y and forward scatter histograms of wild type and Bcl-2 transgenic T cells during cell cycle entry. Primary murine T cells were isolated from spleens and plated in 12-well plates at $2X10^6$ per well. The wells were coated with α-CD3. The T cells were collected at indicated time points. A represetative experiment of three is shown.

low, and distinct shifts in the pyronin Y fluorescence peaks did not occur until 16 hours. The data indicate that following arrest by contact inhibition, Bcl-2 or Bcl-x_L expression delays G_1 entry by prolonging G_0.

Peripheral long-lived T cells are physiologically quiescent cells, which can be stimulated to divide upon activation by mitogens or T cell receptor signaling. T cells from lck^{pr}- Bcl-2 transgenic mice are smaller and exhibit delayed S phase entry as compared to littermate controls (Linette et al., 1996; Cheng et. al, 2004), while *bcl-2*$^{-/-}$ T cells exhibit accelerated progression to S phase (Linette et al., 1996). Consistent with our findings in fibroblasts, p27 was elevated in Bcl-2 transgenic T cells and induction of Myc was normal. Bcl-2 Tg quiescent T cells were smaller and had less total RNA than control cells (Figure 12 A). Increase in cells size and RNA content in Bcl-2 Tg cells lagged behind control cells during cell cycle entry (Figure 12 B). These results confirm that our cell culture system accurately reflects the effects of Bcl-2/Bcl-x_L expression *in vivo*. The data from primary cultures of T cells confirmed our published results from cell lines. These findings using RNA content as a marker for G_0 versus G_1 suggested that Bcl-2 and Bcl-x_L expression retains cells in G_0.

Bad expression reverses the effects of Bcl-x_L on cell size and RNA content

The pro-apoptotic member of the Bcl-2 family, Bad, heterodimerizes with Bcl-x_L and Bcl-2 through its BH3 domain and inactivates the pro-survival function of Bcl-2 and Bcl-x_L (Yang et al., 1995; Kelekar et al., 1997). To further assess the relationship between the effect of Bcl-x_L on G_0 to G_1 transition and its effect on cell death inhibition, we examined cell size and RNA content in cells expressing both Bcl-x_L and Bad. Bad

A

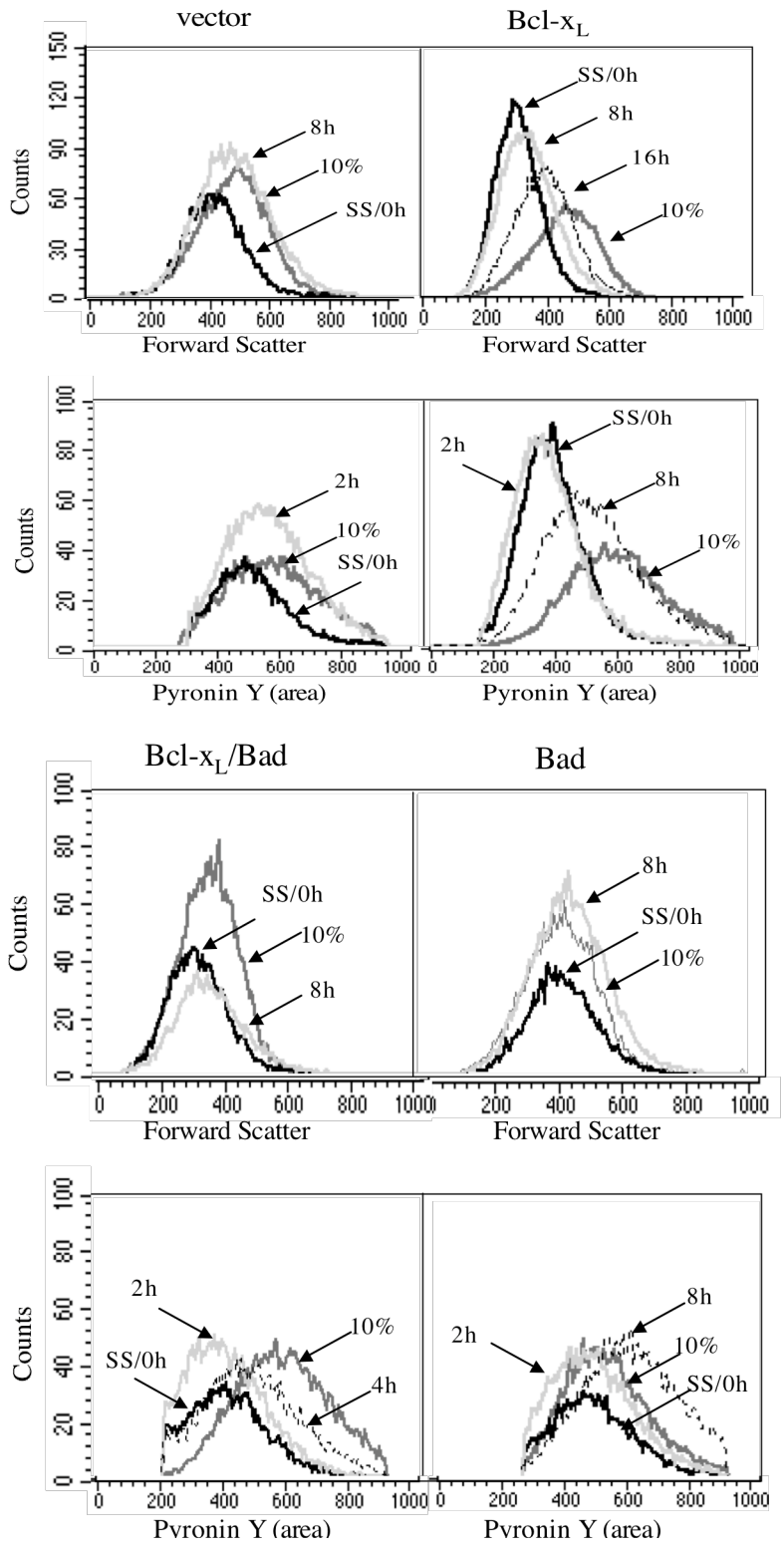
vector
Bcl-x_L
Counts
8h
10%
SS/0h
16h
Forward Scatter
2h
Pyronin Y (area)
Bcl-x_L/Bad
Bad
4h

B

Mean Forward Scatter

	Vector	Bcl-x_L	Bcl-x_L/Bad	Bad
10%	443	434	363	437
SS/0h	392	288	329	440
8h	452	320	368	462
16h	505	396	452	506

Mean Pyronin Y fluorescence

	Vector	Bcl-x_L	Bcl-x_L/Bad	Bad
10%	577	601	586	538
SS/0h	493	387	421	498
2h	552	377	415	476
4h	550	438	497	570
8h	546	526	518	613

C

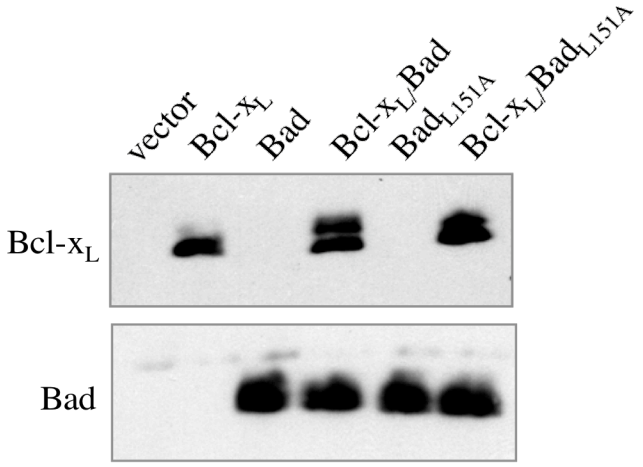

Figure 13: Bcl-x_L delays cell size and RNA increase following cell cycle stimulation, which is reversed by Bad expression. NIH3T3 cells expressing Bad. Bcl-x_L/Bad, Bcl-x_L or vector alone were arrested by serum starvation in 0.75% CS medium and released by serum stimulation. Cells were stained with Hoechst 33342 and pyronin Y and analyzed by flow cytometry. (**A**) Overlaid histograms of pyronin Y or forward scatter. (**B**) Mean forward scatter or mean pyronin Y fluorescence. A representative experiment of three is shown. (**C**) Expression of Bcl-x_L and Bad in NIH3T3 cells. Equal numbers of cells are loaded.

expression will antagonize the pro-survival function of Bcl-x_L, but how will it affect the cell cycle function of Bcl-x_L? Western analysis documented that expression of Bcl-x_L was not noticeably affected by the presence of Bad (Janumyan et al., 2003). In contrast to cells expressing Bcl-x_L only (434 to 288), serum starvation of cells expressing both Bcl-x_L and Bad resulted in a minimal decrease in FSC (363 to 329), which recovered completely by 8 hours (368). The FSC pattern in serum starvation and release of Bcl-x_L/Bad cells is identical to the pattern in control cells, indicating that the expression of Bad completely reversed the effect of Bcl-x_L on cell size (Figure 13). The pattern of pyronin Y staining in Bcl-x_L/Bad cells was intermediate between that of controls and Bcl-x_L cells. Pyronin Y fluorescence in Bcl-x_L/Bad cells decreased by 25% after serum starvation (586 to 421), compared to 15% in controls and 36% in Bcl-x_L cells. Bcl-x_L/Bad cells also had increased RNA content by 4 hours, which is sooner than Bcl-x_L cells, but not as fast as control cells. These experiments were repeated at least three times with similar results. These data indicate that in addition to reversing the effect of Bcl-x_L on cell size, Bad also negatively influences the ability of Bcl-x_L to inhibit initiation of RNA synthesis during G_0 to G_1 transition. Cell cycle profiles and BrdU incorporation (Janumyan et al., 2003) consistently showed that Bcl-x_L/Bad cells reach S phase at the same rate or faster than controls, indicating reversal of Bcl-x_L-mediated cell cycle delay by Bad. Moreover, expression of Bad_{L151A}, a mutation in the BH3 domain that disrupts binding to Bcl-x_L and Bcl-2, had no effect on the ability of Bcl-x_L to delay the onset of S phase as assessed by propidium iodide staining or BrdU analysis. This demonstrates that modulation of the cell cycle function of Bcl-x_L by Bad is dependent on binding to Bcl-x_L

No change in FSC (437 to 440) and minimal change (538 to 498) in pyronin Y

staining occurred in serum starved Bad expressing cells. This is consistent with our previous report that cells expressing Bad fail to arrest effectively in G_0/G_1 (Chattopadhyay et al., 2001). Pyronin Y fluorescence in Bad cells increased more quickly than control cells to a level higher than cultures grown in 10% serum, suggesting traverse to S phase was accelerated. This was confirmed by cell cycle profiles during serum induction showing that 67% of cells expressing Bad were in S phase by 12 hours while only 21% of pBabe control cells reached S phase at that time. The shortened interval to S phase in Bad expressing cells can be explained by bypass of G_0-G_1 transition or shortened G_1. This effect was absent in cells expressing the Bad_{L151A} mutant, consistent with our previous report that the cell cycle effect of Bad requires interaction with Bcl-x_L (Chattopadhyay et al., 2001). These experiments demonstrated that a molecule known to inhibit the anti-apoptotic function of Bcl-x_L also inhibited the cell cycle activities of Bcl-x_L, further supporting the hypothesis that the cell cycle effects are an intrinsic function of Bcl-x_L.

Bcl-x_L expression enhanced G_0 arrest

Cell size and RNA staining data showed that Bcl-2 or Bcl-x_L expression either caused more cells to arrest in G_0, or caused cells to arrest at a smaller size with less RNA. In order to compare cell cycle entry kinetics of cell populations that are comparable in states of arrest, we isolated contact inhibited control cells that were similar to Bcl-x_L cells in size and measured their rates of S phase entry (Figure 14). Control and Bcl-x_L cells were sorted by FSC into small and large populations (Figure 14 A, a). Re-analysis of the sorted cells by FSC (Figure 14 A, b) and Pyronin Y staining (Figure 14 A, e), as well as

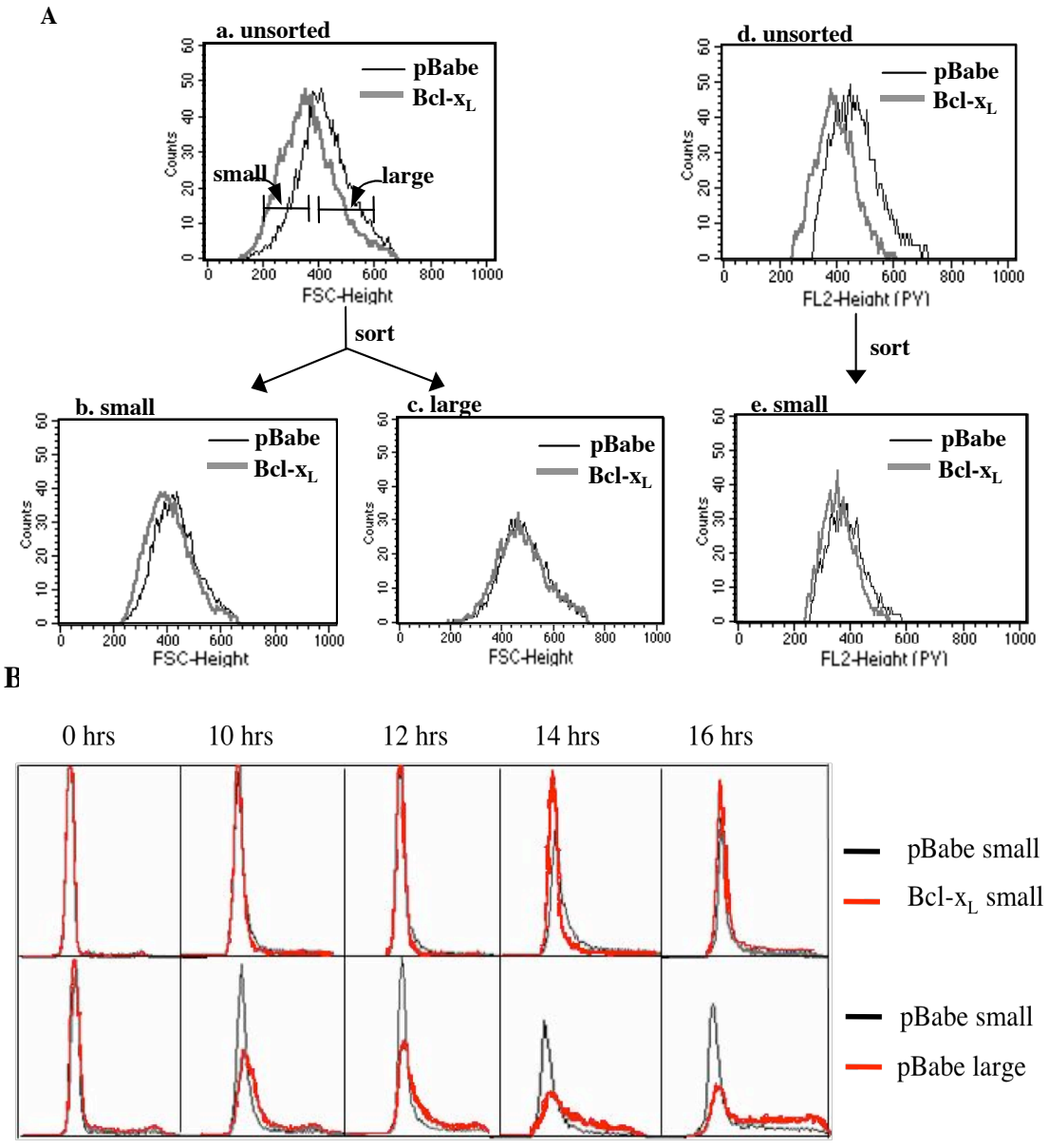

Figure 14: Enhanced G_0 arrest contributes significantly to the cell cycle delay function of Bcl-x_L. (**A**) FSC profiles of arrested NIH3T3 cells expressing pBabe or pBabeBcl-x_L were compared (a) and cells were sorted by FSC into (b) 'small' and (c) 'large' populations. Markers indicate the windows used for sorting. The sorting results were checked by re-analyzing FSC and pyronin Y (e) staining of sorted cells. (**B**) Sorted small and large cells were re-plated at low density, collected at the indicated times, and analyzed by PI/FACS. A representative experiment of three is shown.

PI staining (Figure 14 B, 0 hrs), confirmed that the sorting procedure successfully isolated small pBabe cells very similar to small Bcl-x_L cells. They were not identical because the sorted small Bcl-x_L population was skewed toward lower FSC and the sorted small pBabe population was skewed toward higher FSC. Sorted pBabe and Bcl-x_L cells were released from cell cycle arrest and followed for entry into S phase. Overlays of the DNA profiles, as well as comparisons of the percent of S+G_2/M cells, of small pBabe and small Bcl-x_L cells showed similar progression to S phase (Figure 14 B, top panel). However, there was a significant difference between small and large pBabe cells (Figure 14 B, lower panel). Sorted small Bcl-x_L cells represented the majority of the Bcl-x_L culture, but sorted small pBabe cells were only a minority of the total population with the majority of the cells being "less arrested." The small control cells entered cell cycle slowly, more similar to Bcl-x_L cells than large control cells. Furthermore, the delay in the total Bcl-x_L population was recapitulated in the overlays of the DNA profiles of small and large control cells, illustrating that the time to S phase correlated with the state of G_0 of the starting population. A small but distinct difference in S phase entry was repeatedly observed between small pBabe and small Bcl-x_L populations (Figure 14 B, top), suggesting that, in addition to more effective G_0 arrest, inhibition of G_1 progression may also be a component of the cell cycle function of Bcl-x_L. These experiments indicate that the ability of Bcl-2 and Bcl-x_L to accentuate cell cycle exit constitutes a significant mechanism of cell cycle delay by Bcl-2 and Bcl-x_L.

Summary

Experiments in NIH3T3 and Rat1 fibroblasts showed that Bcl-2 and Bcl-x_L

delayed serum-induced, Raf-induced, and Myc-induced but not E2F-induced cell cycle entry, placing the action of Bcl-2/Bcl-x_L between Myc and E2F. We showed that Bcl-x_L/Bcl-2 expression did not affect induction of early G_1 molecules Myc or cyclin D but inhibited the activity of G_1 cyclins/cdks, indicating that Bcl-2/Bcl-x_L blocks progression to the restriction point without affecting early G_1 signaling events. We consistently observed elevation of p27 during cell cycle arrest of Bcl-2/Bcl-x_L cells. Based on the mutational analysis and subcellularly targeted Bcl-2 mutants, we concluded that the cell cycle delay function was not separable from the cell survival function. However, cell cycle delay is not an inevitable consequence of enhanced survival, because contact-inhibited Bcl-2 or Bcl-x_L cells exhibited cell cycle entry delay and enhanced G_0 as measured by RNA content and cell size. We found that Bcl-x_L expression significantly enhanced G_0 arrest as measured by RNA content, cell size, and p27. The profound effect of Bcl-2/Bcl-x_L on cell cycle arrest is a major reason for the delay in cell cycle progression. These data led to the hypothesis that enhanced G_0 arrest is an intrinsic function of Bcl-2/Bcl-x_L, and that Bcl-2/Bcl-x_L enhances G_0 arrest by regulating the same mitochondrial functions as in cell survival. We hypothesize that Bcl-2/Bcl-x_L also has a distinct cell cycle function, which is the delay of G_0-G_1 transition through the regulation of cell growth. The model for the cell cycle action of Bcl-2/Bcl-x_L is that the ability of Bcl-2/Bcl-x_L to inhibit cell death during nutrient limited conditions allows these cells to enter a more enhanced state of G_0 (Figure 15). Due to this enhanced G_0, Bcl-2/Bcl-x_L cells take longer to reach the critical mass necessary for cell cycle entry, which results in delayed cell cycle entry. If there are mechanisms other than cell death inhibition by which Bcl-2/Bcl-x_L enhances cell cycle arrest, they could involve the regulation of

ATP/ADP exchange, mitochondrial bioenergetics, mitochondrial biogenesis, or cell growth.

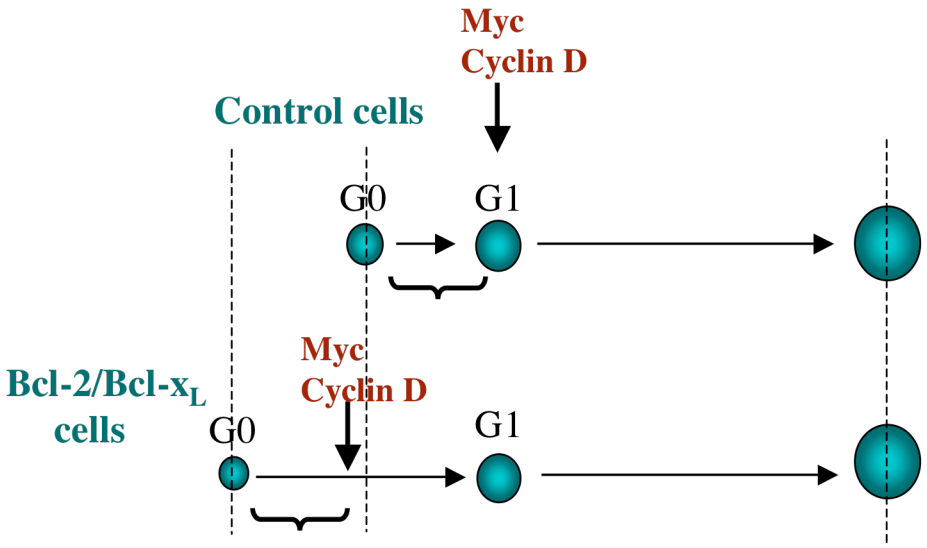

Figure 15: Enhanced cell cycle arrest is the major mechanism of Bcl-2/Bcl-x_L-mediated cell cycle entry delay. Bcl-2/Bcl-x_L expressing cells are more arrested following serum starvation or contact inhibition than control cells as measured by RNA content and cell size. The length of time from G_0 to G_1 (as indicated by the bracket) is prolonged in Bcl-2/Bcl-x_L cells due to a different starting point. However, Myc and cyclin D activation, which normally signal G_1 entry, occurs at the same time in control and Bcl-2/Bcl-x_L cells, suggesting separation of early molecular cell cycle events and cell growth.

CHAPTER IV

BCL-2/BCL-X_L MAY ACT ON THE MYC PATHWAY TO DELAY CELL CYCLE ENTRY

Introduction

We previously observed that Bcl-2/Bcl-x_L delays Myc-induced cell cycle entry much more efficiently than serum-induced cell cycle entry (see Chapter III and Greider et al., 2002). During serum stimulated cell cycle entry, cells receive signals from a multitude of growth factors leading to the activation of many signaling pathways resulting in cell growth and proliferation. However, in the case of Myc-induced cell cycle entry, Myc target genes are the only ones responsible for stimulation of cell cycle entry. Thus, we hypothesized that Bcl-2/Bcl-x_L may act on the Myc pathway to delay cell cycle entry. We tested that ability of Bcl-x_L to delay cell cycle entry and upregulate p27 in cells lacking Myc. We determined whether Bcl-2/Bcl-x_L is able to directly interfere with the transcriptional function of Myc.

Results

Bcl-x_L and Bcl-2 expression does not delay S phase entry in $myc^{-/-}$ cells

If the hypothesis that Bcl-2/Bcl-x_L has specific effects on the Myc pathway of cell cycle progression were true, then Bcl-2/Bcl-x_L would not be expected to delay cell cycle entry in cells lacking Myc. We compared the ability of Bcl-x_L to delay cell cycle entry in the somatic *myc*$^{-/-}$ cells (HO15) to the parental cell line TGR (rat fibroblasts) and the *myc*$^{-}$

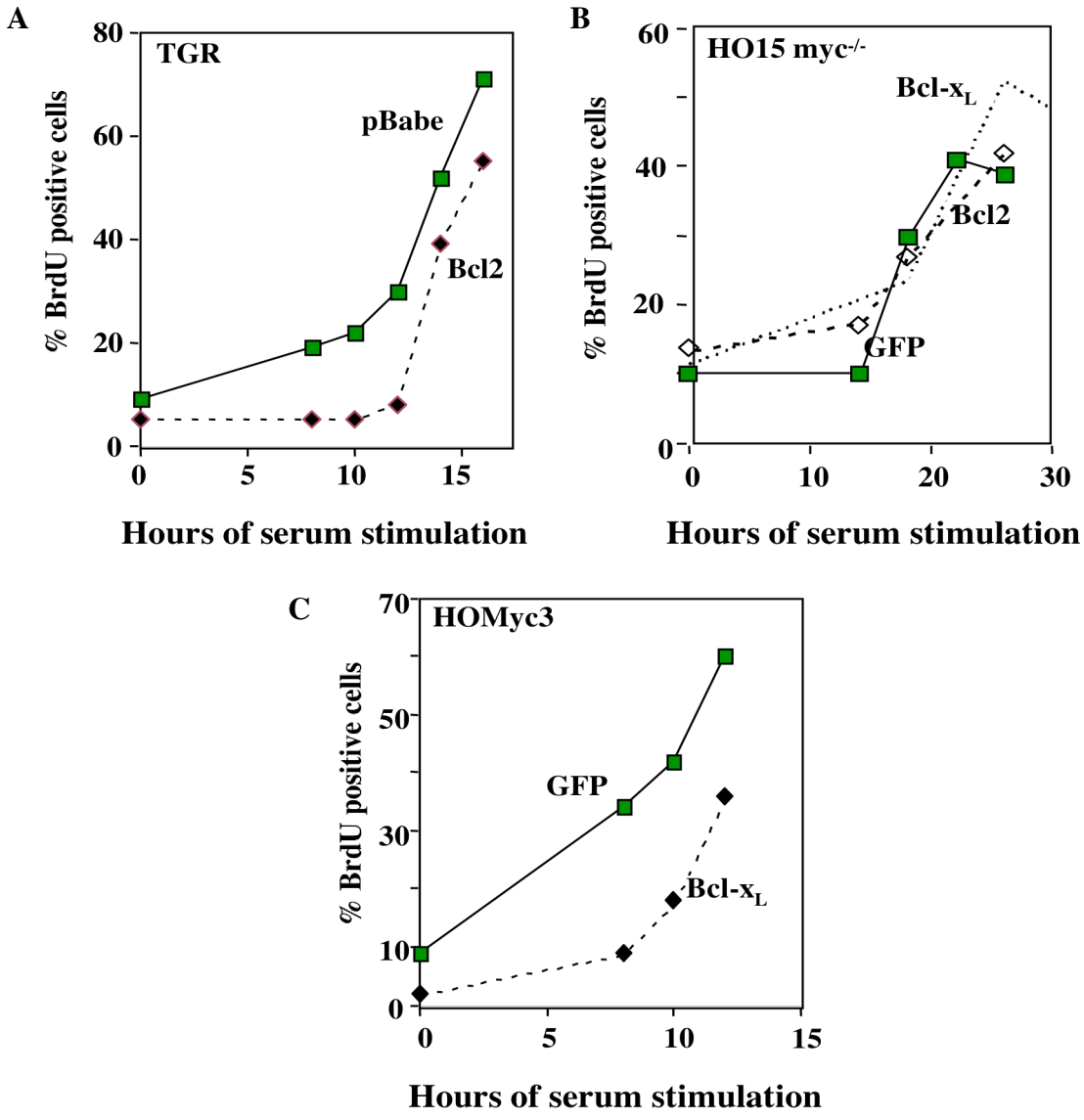

Figure 16: Bcl-2/Bcl-x_L expression does not delay S phase entry in $myc^{-/-}$ cells. Graphs of the percentage of BrdU incorporating cells versus hours following serum stimulated cell cycle entry in parental TGR cells (**A**), HO15*myc*$^{-/-}$ cells (**B**), *myc*$^{-/-}$ with re-introduced c-Myc HOMyc3 (**C**). TGR cells and HOMyc3 cells were serum starved in 0.2% FBS medium for 3 days. HO15 ($myc^{-/-}$) cells were serum starved in 0.2% FBS medium for 4 days due to their elongated cell cycle time. While the parental TGR cells exhibited cell cycle entry delay with Bcl-2 expression, the HO15 ($myc^{-/-}$) cells showed no difference in the kinetics of cell cycle entry with either Bcl-2 or Bcl-x_L expression. The cell cycle delay phenotype of Bcl-x_L was restored in HOMyc3 cells. Representative experiments of at least three are shown.

$^{-/-}$ with re-introduced Myc (HOMyc3). Cells were cultured in 0.2% serum for 4 days for *myc*$^{-/-}$ cells (cell cycle time for HO15 cells is 54 hours) and 3 days for TGR and HOMyc3 cells to induce G_0/G_1 arrest, then stimulated cell cycle entry with 10% serum and assayed S phase by BrdU incorporation (Figure 16). We observed no difference in S phase entry in the *myc*$^{-/-}$ cells expressing vector control or Bcl-x_L. The parental TGR cells expressing Bcl-x_L showed delay in S phase entry as compared to the vector alone control. The cell cycle delay phenotype of Bcl-x_L was restored by the re-introduction of Myc into the *myc*$^{-/-}$ cells. Even though cell cycle is very prolonged in *myc*$^{-/-}$ cells (54 hours versus 24 hours), and S phase entry does not occur until about 24 hours following serum stimulation, we showed that *myc*$^{-/-}$ cells can be further delayed by overexpression of p27. The inability of Bcl-2/Bcl-x_L to delay *myc*$^{-/-}$ cell cycle entry can be interpreted in several ways. One possibility is that the cell cycle delay function of Bcl-2/Bcl-x_L is dependent directly on one of Myc's functions, such as downregulation of p27, inhibition of cdks, or regulation of cell growth. Another possibility is that Bcl-2/Bcl-x_L has no effect on alternative, Myc-independent pathways of cell cycle entry, as *myc*$^{-/-}$ cell are able to grow and divide, albeit slowly.

<u>p27 is not elevated in Bcl-2/Bcl-x_L expressing *myc*$^{-/-}$ cells</u>

Since Bcl-2 did not delay S phase entry of *myc*$^{-/-}$ cells, we wished to know whether p27 was elevated by Bcl-2 in these cells. HO15/GFP and HO15/Bcl-2 cells arrested by serum starvation, and stimulated to enter the cell cycle by serum were Western blotted for p27. As expected, p27 was increased in arrested cells and decreased as cells entered cycle. However, the levels of p27 protein were not different between vector control and

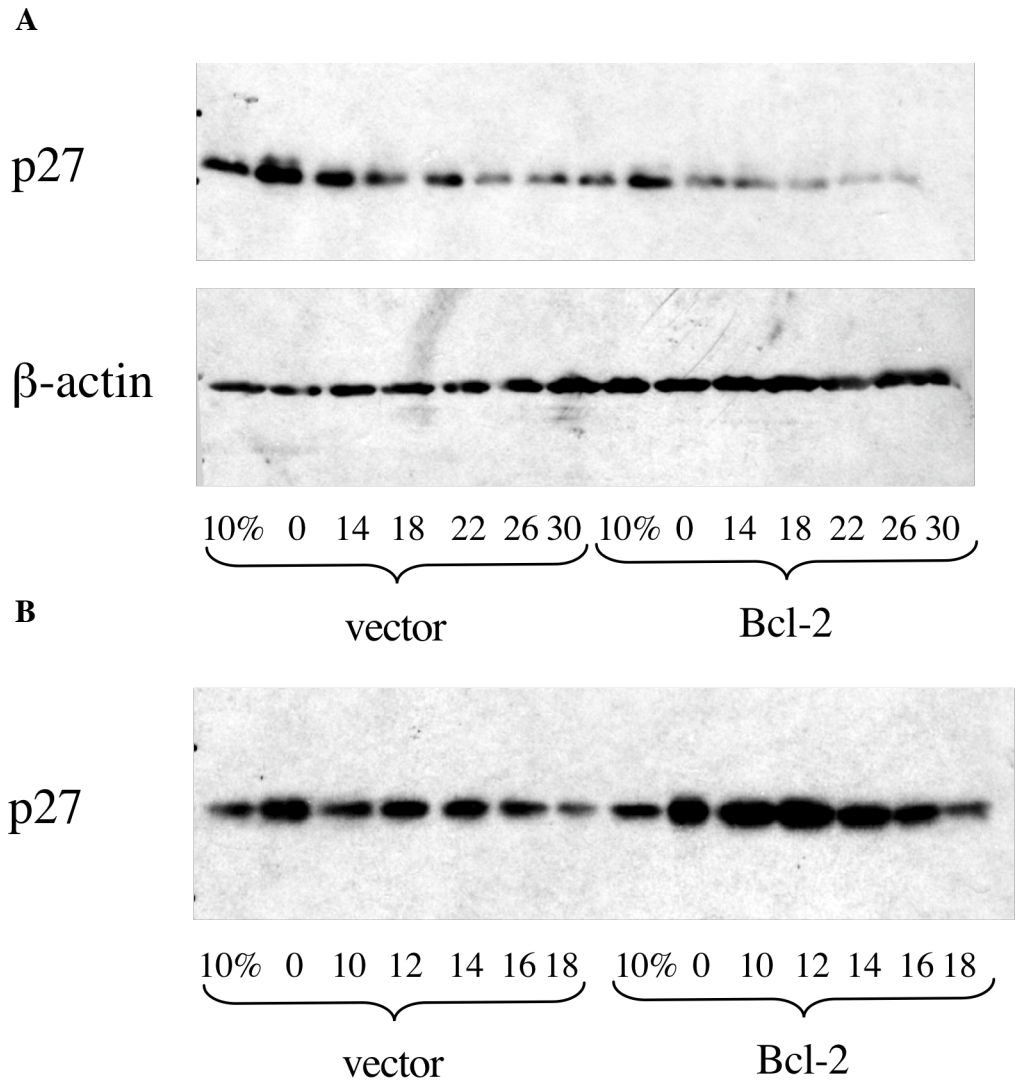

Figure 17: Bcl-2 expression in *myc*$^{-/-}$ cells did not result in p27 elevation. (**A**) HO15 (*myc*$^{-/-}$) cells were serum starved in 0.2% FBS medium for four days, then were stimulated to re-enter the cell cycle by serum re-addition. Equal amounts of protein were immunoblotted for p27 and β-actin to control for loading. (**B**) HOMyc3 cells (*myc*$^{-/-}$ with reconstituted Myc) were serum starved for three days, then serum stimulated to re-enter cell cycle. Equal amounts of protein were immunoblotted for p27. Representative experiments of at least three are shown.

Bcl-2 $myc^{-/-}$ cells (Figure 17 A). HOMyc3 cells expressing Bcl-2 exhibit upregulation of p27 following cell cycle arrest (Figure 17 B). These data suggested that elevation of p27 by Bcl-2 depends on the presence of Myc, supporting the idea that Bcl-2 acts on Myc-dependent cell cycle pathway.

Bcl-2/Bcl-x_L does not affect the ability of Myc to transcriptionally regulate p27

Myc is able to downregulate expression of p27 by several mechanisms, including transcriptional repression of p27, sequestration of p27 away from cyclin E/cdk2 complexes, and transcriptional activation of proteins involved in degradation of p27. To test whether Bcl-2/Bcl-x_L interferes with Myc's transcriptional regulation of p27, we transiently transfected p27 promoter-luciferase reporter construct and CMV-driven Myc in the presence or absence of Bcl-x_L. The p27 promoter expressed alone showed the luciferase activity of about 6500 units (Figure 18). The expression of Myc with the p27 promoter resulted in the suppression of p27 promoter activity to 700 units. The expression of Bcl-xL with Myc and the p27 promoter had very little effect on the ability of Myc to repress p27 promoter activity (from 700 to 1000 units). The experiment showed that Bcl-x_L did not interfere with the ability of Myc to transcriptionally repress p27 (Figure 18 A). Other known Myc targets such as Cul1 (Figure 18 B), cdc25, major late adenoviral promoter, platelet derived growth factor receptor (PDGFR), Gadd45, and p21 were tested. The activity of Cul1 promoter alone (5,000 units), is repressed by Myc (450 units). Expression of Bcl-x_L with Myc and Cul1 results in 2,300 units of activity. The activity of adenoviral major late promoter (14,500 units) is repressed by Myc (3,000 units), and the repression is not affected by Bcl-x_L expression (4,900 units). The activity

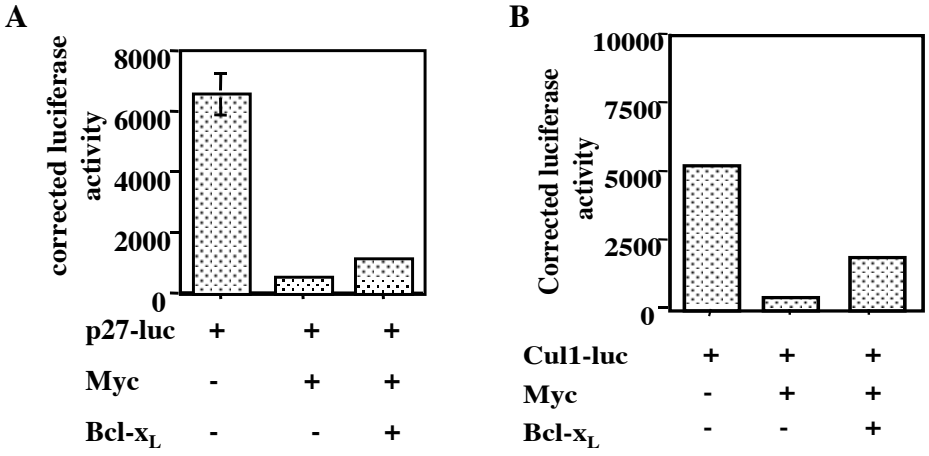

Figure 18: Bcl-x_L does not affect the transcriptional repression of p27 by Myc. (**A**) p27 promoter-luciferase reporter construct and CMV-driven Myc construct were transiently transfected into NIH3T3 cells in the presence or absence of Bcl-x_L. Luciferase activity is normalized against CMV-SEAP. Standard deviation is derived from three experiments. (**B**) Cul1 promoter-luciferase reporter construct and CMV-driven Myc construct were transiently transfected into NIH3T3 cells in the presence or absence of Bcl-x_L. A representative experiment of three is shown. Luciferase activity is normalized against CMV-SEAP.

of cdc25 promoter alone (1.5×10^6 units) is repressed by the expression of Myc (1.5×10^5 units). The expression of Bcl-x_L cannot reverse (5×10^5 units) the repression of cdc25 promoter by Myc. The activity of Gadd45 (1500 units) is repressed by Myc (300 units), the repression is not affected by Bcl-x_L expression (640 units). The activity of p21 (1.6×10^6 units) is repressed by Myc (1.6×10^5 units), and this repression is unaffected by Bcl-x_L (1.4×10^5 units). We concluded that Bcl-x_L does not affect that activity of Myc at these promoters. Dr. C. Sansam confirmed these results using Northern blotting and RealTime-PCR. These experiments indicate that Bcl-x_L does not directly interfere with the transcriptional function of Myc, and suggest that Bcl-x_L may regulate other Myc functions such as cell growth.

Overexpression of p27 in $myc^{-/-}$ cells slows cell cycle time

Deletion of Myc results in prolonged cell cycle time (from about 24 hours to about 54 hours) and overexpression of p27. This raises the question whether Bcl-x_L is unable to delay cell cycle because it requires the Myc pathway or is Bcl-x_L unable to delay cell cycle because these cells are already slow and Bcl-x_L cannot slow them down any further. To address this issue, we tested whether the HO15*myc*$^{-/-}$ cells can be delayed further by exogenous overexpression of p27. pBabe and pBabep27 were retrovirally introduced into HO15*myc*$^{-/-}$ cells, and stable clones were selected. The cells were plated in 6-well dishes at a density of 100,000 cells per well. Cell numbers were counted daily, and the cells were split up as needed. The data showed that the parental HO15 and vector control cells grew at comparable rates, while HO15p27 cells were much slower and did not show significant growth for up to 12 days (Figure 19 A). Similarly, when these cells

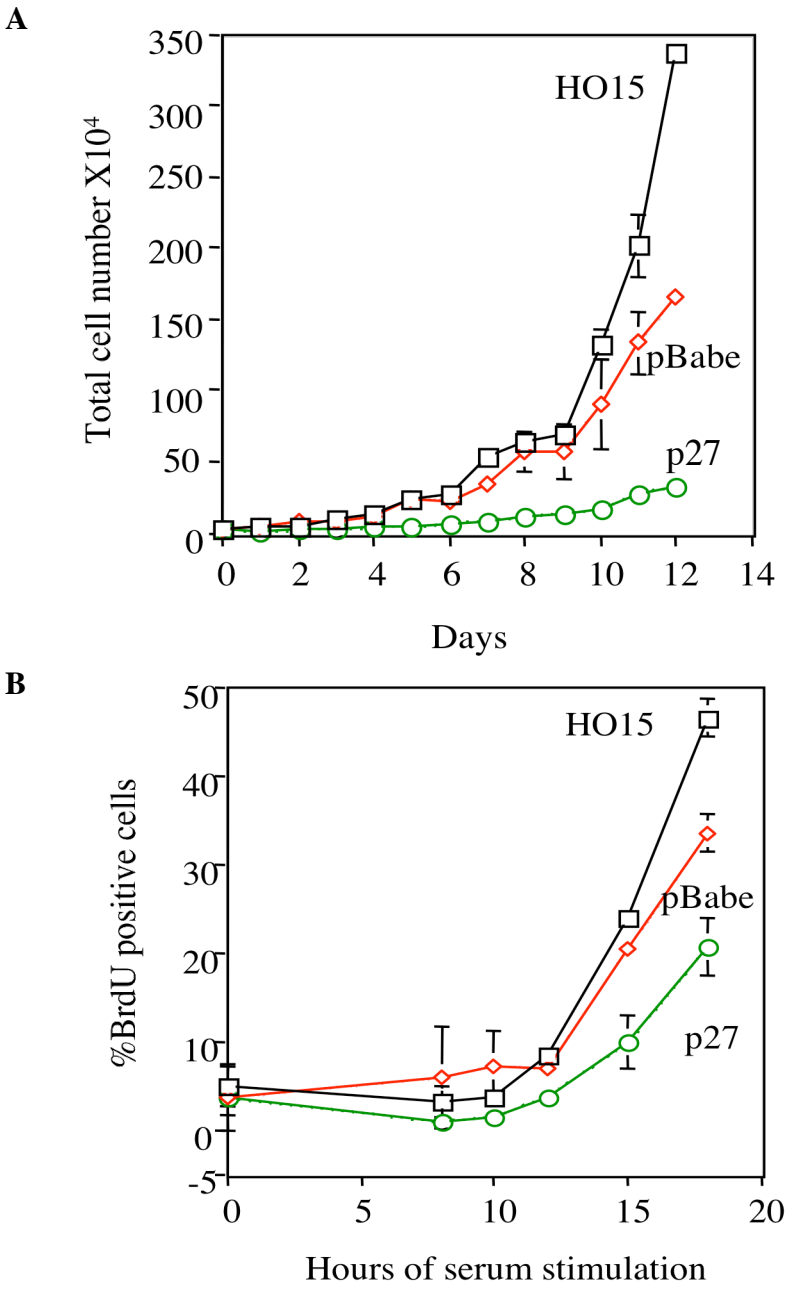

Figure 19: *myc*$^{-/-}$ cells overexpressing p27 exhibit a slowed growth rate and a delayed cell cycle re-entry. (**A**) Comparison of growth rates between HO15, HO15pBabe, and HO15p27 cells. (**B**) BrdU analysis of HO15, HO15pBabe, and HO15p27 cells that were arrested for 4 day□s in 0.1% FCS, and serum stimulated to re-enter cell cycle. Standard deviations were derived from three experiments. At some points standard deviation is so small that the error bars are not visible.

were cell cycle arrested by culturing in 0.1% FCS for 4 days and then serum stimulated to re-enter cell cycle the cells overexpressing p27 were significantly slowed in entering S phase (Figure 19 B). These data indicate that HO15*myc*$^{-/-}$ cells can be slowed down further by overexpression of p27, suggesting that the inability of Bcl-x_L to delay cell cycle entry in HO15*myc*$^{-/-}$ cells may be due to the absence of Myc.

Bcl-x_L expression delays S phase entry in cells with reduced Myc expression

To verify the data from *myc*$^{-/-}$ cells, we expressed siRNA targeted to Myc. The DNA encoding siRNA were inserted into a pSuper retroviral vector. NIH3T3 pBabe or pBabe Bcl-x_L cells were retrovirally infected with pSuper or pSuper siMyc. The cells were arrested in 0.5% CS medium for three days, then stimulated to re-enter cell cycle by re-addition of serum. The data showed that in the absence of Myc, cells exhibited slower rate of cell cycle entry consistent with *myc*$^{-/-}$ cells (Figure 19). However, cells expressing both Bcl-x_L and siMyc entered S phase slower than the siMyc cells alone, indicating that Bcl-x_L was able to delay cell cycle entry in cells expressing very low levels of Myc protein. NIH3T3 cells expressing vector controls, siMyc, Bcl-x_L, and siMyc/Bcl-x_L were verified for reduction of Myc expression by Western blotting (Figure 20). Immunoblotting for p27 showed that reduction of Myc expression resulted in upregulation of p27, however activation of cyclin D1 and p130 was unaffected (Figure 21). These data suggest that Bcl-2/Bcl-x_L does not delay cell cycle by acting on the Myc pathway alone.

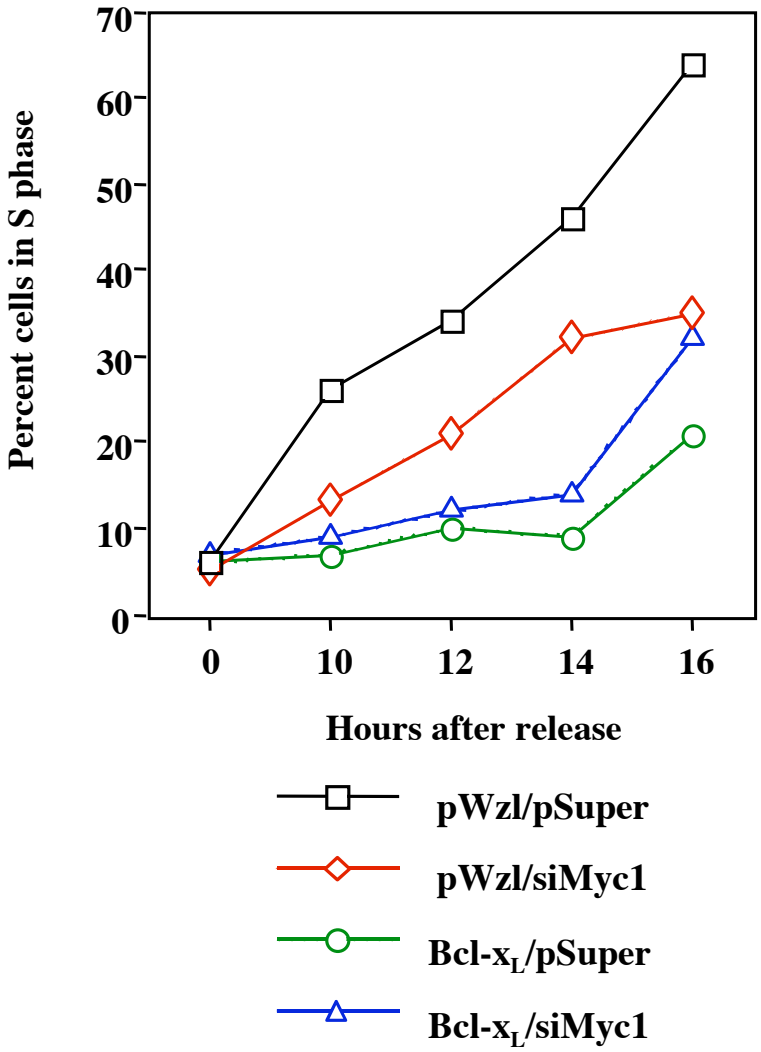

Figure 20: Bcl-x_L delays cell cycle entry in cells with knocked down Myc. NIH3T3 cells were serum starved for 3 days then released by serum stimulation. Cells with reduced Myc expression (pWzl/siMyc1) are entering cell cycle slower than control cells (pWzl/pSuper). Bcl-x_L overexpression in cells with knocked down Myc (Bcl-x_L/siMyc1) exhibit delayed cell cycle re-entry as compared to cells with knocked down Myc (pWzl/siMyc1).

Summary

We observed that Bcl-2/Bcl-x_L is unable to delay cell cycle in *myc*$^{-/-}$ cells, and does not elevate p27 in *myc*$^{-/-}$ cells, suggesting that Bcl-2/Bcl-x_L may affect some function of Myc. Our siRNA data were not consistent with the myc$^{-/-}$ data. There are several reasons for this inconsistency. First, one model is genetically modified to knockout Myc; in the other, Myc is downregulated at the transcriptional level. Second, in each case the cells were derived from different animal; the myc$^{-/-}$ cells are rat fibroblasts, while NIH3T3 are mouse fibroblasts. Third, while the knockout cells lack all Myc protein, the siMyc cells exhibit expression that is downregulated. We were unable to show that Bcl-x_L interferes with the transcriptional function of Myc. At the present the data does not allow for a firm conclusion; however, if Bcl-2/Bcl-x_L acts on the Myc pathway it does not interfere with Myc's transcriptional function. It is still possible that Bcl-2/Bcl-x_L antagonizes the cell growth function of Myc, such as blocking eIF2α, a Myc transcriptional target gene.

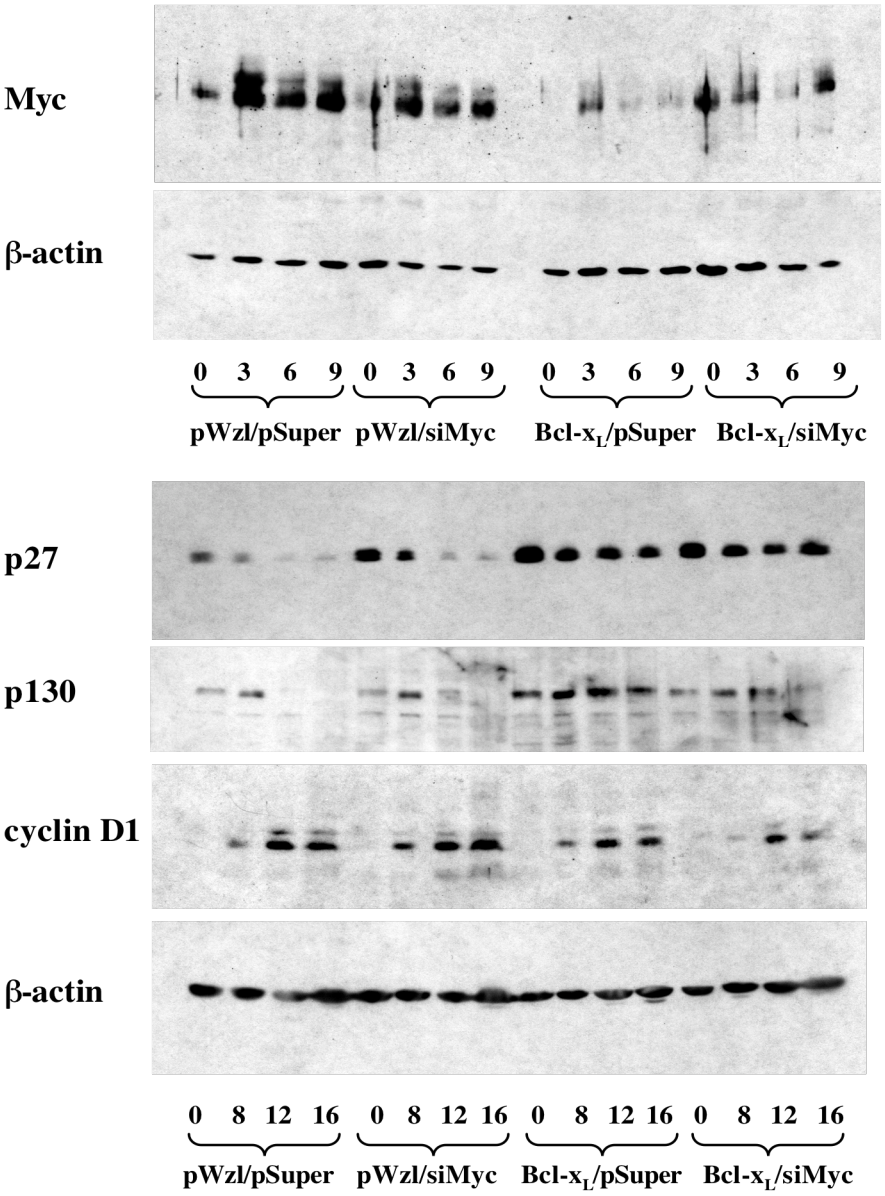

Figure 21: Knocking down Myc results in elevation of p27. Cells were arrested in 0.75% CS for 3 days, then stimulated by serum addition. Cells were collected following arrest and at indicated time points during release. Equal amounts of protein were loaded and immunoblotted for Myc, p27, p130, cyclin D1, and β-actin.

CHAPTER V

BCL-2/BCL-X_L REGULATES CELL CYCLE BY MECHANISMS INDEPENDENT OF APOPTOSIS INHIBITION

Introduction

Bcl-2 and its homologue Bcl-x_L are anti-apoptotic and anti-proliferation. During stimulation of cell cycle entry from cell cycle arrest, Bcl-2 and Bcl-x_L expression causes a delay of S phase entry. An extensive mutational analysis demonstrated that cell cycle entry delay co-segregated with anti-apoptosis in all 23 alleles tested (Janumyan, et al., 2003). We found that Bcl-x_L expression does not alter the induction of the early G_1 genes Myc and cyclin D1 during entry into G_1, but cyclin/cdk activities are inhibited, possibly by upregulation of p27 (Greider, et al., 2002). Assessment of cell size and RNA accumulation during cell cycle entry suggested that Bcl-x_L/Bcl-2 expression retained cells in G_0 and delayed the initiation of cell growth during the G_0-G_1 transition. These data suggest that Bcl-x_L inhibits progression into G_1 despite the occurrence of early G_1 cell cycle events, and that apoptosis and cell cycle regulation by Bcl-2/Bcl-x_L may not be separable. During cell cycle arrest, cells expressing Bcl-x_L reached a smaller size and lower RNA content than control cells, indicating that Bcl-x_L allowed cells to enter an enhanced G_0 state. A possible mechanism for the enhanced G_0 phenotype would be Bcl-x_L's ability to lower the threshold at which cells begin to die due to lack of growth factors, allowing cells to further decrease their size and RNA content. Through sorting experiments, we found that enhancement of G_0 arrest by Bcl-x_L is a major cause of delayed cell cycle entry. Arrested NIH3T3 vector control and Bcl-x_L cells were sorted

based on size into small and large populations. The sorted cells were released back into cell cycle by serum stimulation. We found that small vector control cells entered cell cycle at a similar rate to unsorted Bcl-x_L cells. These data indicated that enhanced G_0 arrest, defined by small cell size and low RNA content, is the mechanism of Bcl-x_L cell cycle delay. We hypothesize that enhanced G_0 arrest is an intrinsic function of Bcl-2/Bcl-x_L, and that Bcl-2/Bcl-x_L enhances G_0 arrest by regulating the same mitochondrial functions as in inhibition of apoptosis. However, it is unlikely that the enhanced G_0 arrest is a direct consequence of anti-apoptosis because in the absence of an apoptotic stimulus such as during contact inhibition, Bcl-2/Bcl-x_L still results in enhanced G_0 arrest and cell cycle entry delay. Our previously published data (Greider, et al., 2002) showed that Bcl-2 and Bcl-x_L can delay cell cycle entry induced by serum stimulation, Myc induction, but not E2F iduction, while protecting cells from Myc-induced and E2F-induced cell death; supporting the notion that cell cycle function is not always a consequence of anti-apoptosis. An important question in understanding the dual role of Bcl-2/Bcl-x_L is whether the cell cycle function of Bcl-2/Bcl-x_L is distinct from the anti-apoptotic function or whether the cell cycle activity is a consequence of enhanced survival. If the cell cycle activity of Bcl-2/Bcl-x_L is a consequence of its anti-apoptotic function, then inhibition of cell death during cell cycle arrest by means other than Bcl-2/Bcl-x_L will result in enhanced G_0 arrest and delayed cell cycle entry. We inhibited cell death in fibroblasts during serum starvation by suppressing caspase activity to elucidate the mechanism of enhanced G_0 arrest by Bcl-2/Bcl-x_L. Cell death independent of the Bcl-2/Bcl-x_L pathway was inhibited by mAkt overexpression. Other effects of Bcl-2/Bcl-x_L at the mitochondria during apoptosis such as maintenance of ATP/ADP exchange and the initial maintenance

of mitochondrial membrane potential were tested as possible mechanisms of enhanced G_0 arrest.

Results

zVAD-fmk partially recapitulates the Bcl-x_L cell cycle delay phenotype

Effects of Bcl-2/Bcl-x_L on mitochondria during apoptosis include inhibition of the release of apoptogenic factors, maintenance of mitochondrial membrane potential, and maintenance of ATP/ADP exchange (Vander Heiden, et al., 1999; Plas, et al., 2001). These effects are of particular interest because they have been shown in growth factor-withdrawal mediated apoptosis. We asked whether Bcl-2/Bcl-x_L enhances G_0 through the same mitochondrial functions as in inhibition of apoptosis. We hypothesize that Bcl-2/Bcl-x_L functions to enhance G_0 by inhibition of apoptotic caspases.

Bcl-2/Bcl-x_L inhibits the release of cytochrome c from mitochondria and activation of caspases. To test whether the Bcl-x_L cell cycle function was a consequence of cell death inhibition, we inhibited cell death in NIH3T3 cells during cell cycle arrest with the pan-caspase inhibitor zVAD-fmk. NIH3T3 cells stably expressing Bcl-x_L or empty vector (pBabe puro) were arrested in low serum for 3 days in the presence of 40uM zVAD or DMSO. Cells were stimulated to re-enter the cell cycle by addition of 10% serum. Cell cycle was measured by FACS profiles of propidium iodide stained cells collected at consecutive time points (Figure 22 A). As expected, the time to reach S phase was prolonged in Bcl-x_L cells. DMSO-treated control cells showed a rise in S phase cells at 10 hrs after serum addition, which reached 60% by 16 hours. Bcl-x_L cells

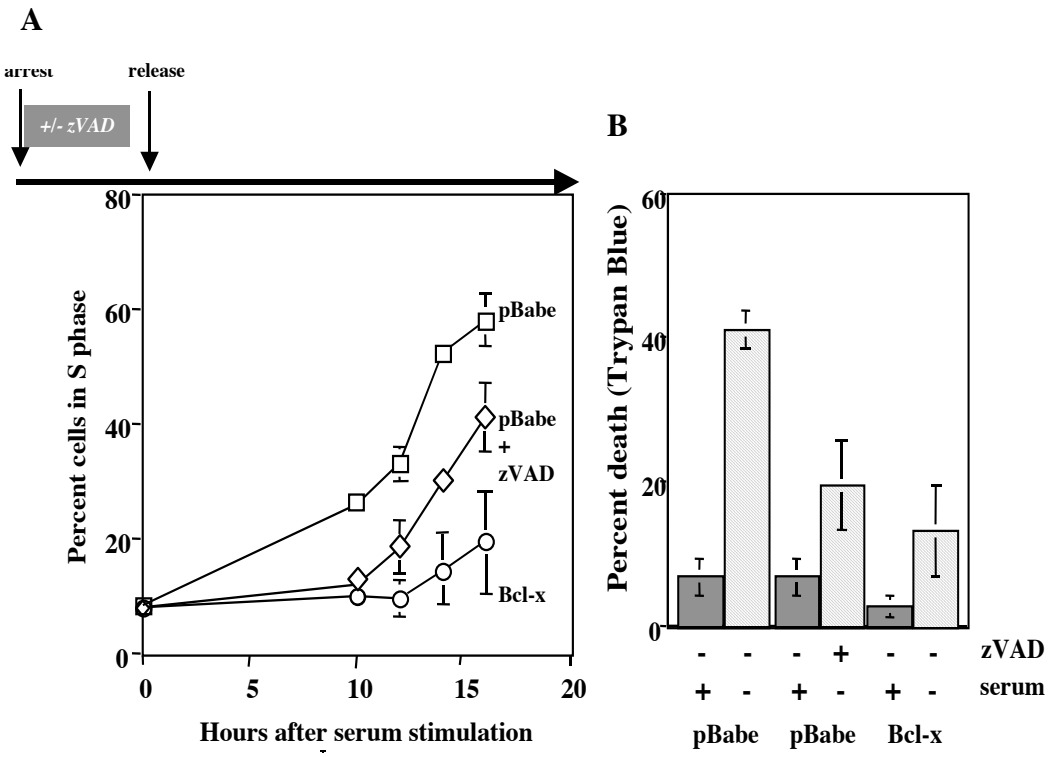

Figure 22: zVAD-fmk-treated NIH3T3 cells exhibit a partial cell cycle phenotype. (**A**) NIH3T3pBabe cells were serum starved in 0.75% CS medium and treated with either zVAD-fmk or DMSO for three days. NIH3T3 Bcl-x_L cells were serum starved and treated with DMSO for three days. The cells were stimulated to enter cell cycle by re-addition of 10% CS medium (no treatment). DNA contents of cells were obtained by PI and FACS analysis. Standard deviations are derived from three experiments. For some of the time points the standard deviation is so small that the error bars are not visible. (**B**) Viability of NIH3T3 cells treated with zVAD-fmk or DMSO or expressing Bcl-x_L was assessed by Trypan Blue staining. Standard deviations are derived from three experiments.

showed no change in S phase until 14-16 hours following cell cycle stimulation, at which time the S phase cells were still less than 20%. Interestingly, zVAD-treated cells exhibited an intermediate rate of cell cycle entry, showing an initial rise in the percentage of S phase cells at 12 hours after serum addition and reaching ~40% at 16 hours. Viability determinations of serum starved 3T3 cells showed that zVAD rescued cell death nearly as efficiently as Bcl-x_L, confirming that the caspase inhibitor was functional in these cells (Figure 22 B).

We previously reported that the major mechanism of the Bcl-x_L cell cycle delay - was enhancement of G_0arrest (Janumyan et al., 2003). The decreases in RNA content and cell size signifying entry into G_0 were accentuated and the increases in ribosomal RNA synthesis and cell size accompanying transition from G_0 to G_1 were delayed in Bcl-x_L cells (Janumyan et al., 2003). To determine whether treatment with zVAD also retained cells in G_0, we compared RNA content and cell size between zVAD treated cells and Bcl-x_L cells. We stained asynchronously growing and arrested cells for total RNA content with the fluorescent dye pyronin Y and measured PY fluorescence of cells gated for 2N DNA content (Figure 23). Consistent with our previous data, Bcl-x_L cells exhibited about 40% reduction ($p= 0.003$ significantly different from control) in mean pyronin Y fluorescence following cell cycle arrest, while DMSO treated control cells showed no reduction in RNA content. Whereas treatment of control cells with zVAD resulted in partial cell cycle delay, it did not cause further reduction of RNA content compared to DMSO treatment ($p=0.327$ not different from control) (Figure 23 A, C). Cell size, as measured by mean FSC, was largely unchanged in cells treated with zVAD ($p=0.74$ as compared to control), while it decreased by 20% in Bcl-x_L cells during cell cycle arrest

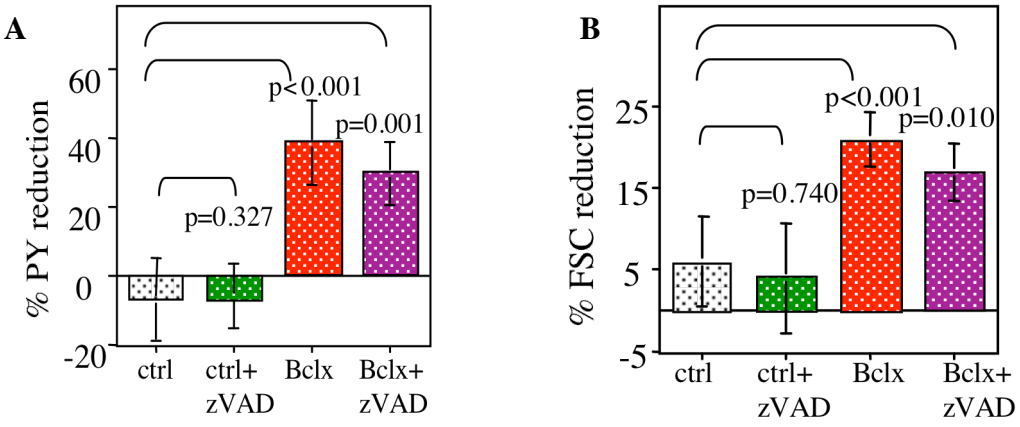
A
% PY reduction
60
40
20
0
-20
p<0.001
p=0.001
p=0.327
ctrl
ctrl+ zVAD
Bclx
Bclx+ zVAD
B
% FSC reduction
25
15
5
-5
p<0.001
p=0.010
p=0.740
ctrl
ctrl+ zVAD
Bclx
Bclx+ zVAD

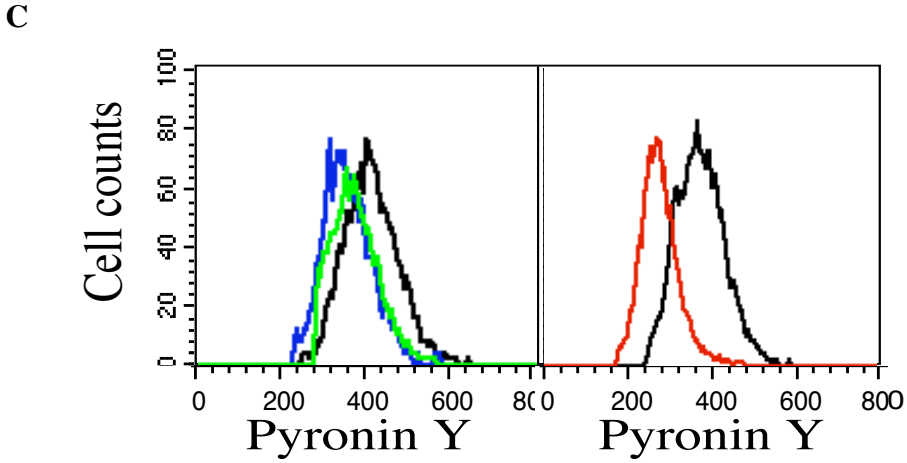
C
Cell counts
0
20
40
60
80
100
0
200
400
600
800
Pyronin Y
Pyronin Y

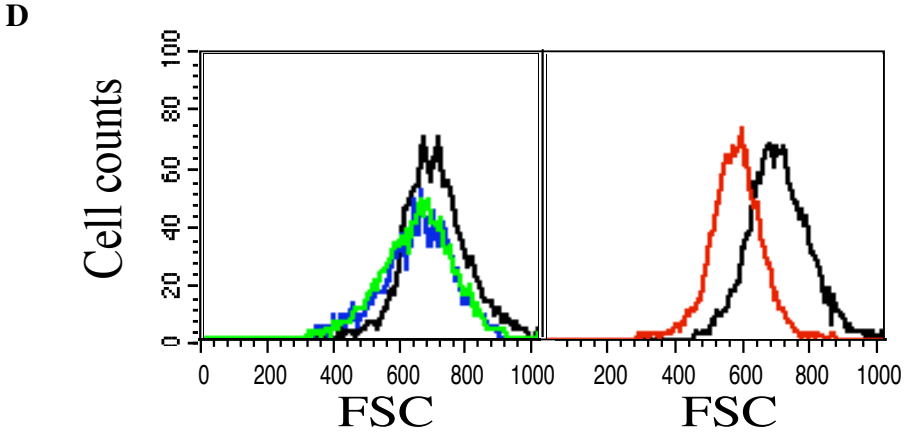
D
Cell counts
0
20
40
60
80
100
0
200
400
600
800
1000
FSC
FSC

Figure 23: zVAD-fmk-treated NIH3T3 cells do not exhibit enhanced G_0 arrest. NIH3T3 cells were arrested in 0.75% CS medium and treated with zVAD-fmk or DMSO for three days. NIH3T3 Bcl-x_L cells were serum starved and treated with DMSO for three days. Cells were collected and fixed in 70% ethanol. Cells were stained with 7-AAD and pyronin Y, and analyzed by flow cytometry. (**A**) The bar graph represents the percent reduction in pyronin Y fluorescence from asynchronously growing cells to arrested cells. (**B**) The bar graph represents the percent reduction in forward scatter from asynchronously growing cells to arrested cells. Standard deviations are derived from three experiments. (**C**, **D**) Histograms of pyronin Y fluorescence or forward scatter are overlaid. Asynchronously growing pBabe (black) are overlaid with arrested DMSO-treated pBabe cells (blue) and arrested zVAD-treated pBabe cells (green) in the left panel. Asynchronously growing Bcl-x_L cells (black) are overlaid with arrested DMSO-treated Bcl-x_L cells (red) in the right panel.

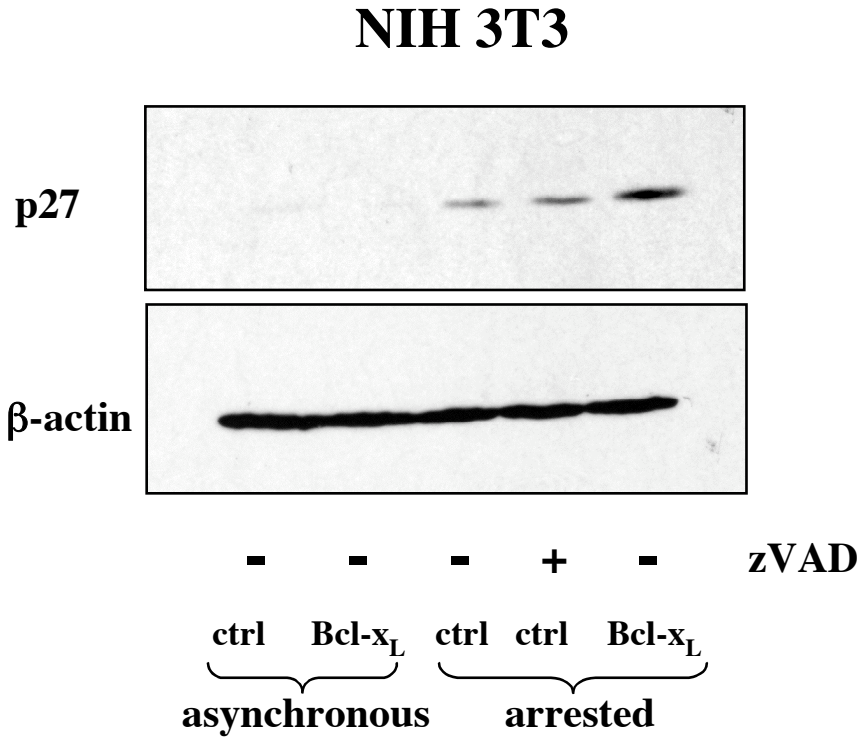

Figure 24: zVAD-fmk-treated NIH3T3 cells do not upregulate p27 during cell cycle arrest. NIH3T3 vector control cells were treated with zVAD or DMSO and NIH3T3 Bcl-x_L cells were treated with DMSO during cell cycle arrest for three days. Cells were collected before and after cell cycle arrest and immunoblotted for p27 and β-actin. A representative experiment of three is shown.

($p<0.000$ as compared to control) (Figure 23 B, D). These results showed that inhibition of caspase-dependent apoptosis did not push cells into G_0, suggesting that the enhanced G_0 state observed in Bcl-x_L cells was not simply a result of cell death inhibition.

Quiescent Bcl-2/Bcl-x_L expressing cells express significantly elevated p27 levels compared to control cells (Greider et al., 2002), and we and others showed that Bcl-2/Bcl-x_L required p27 to mediate its cell cycle effect (Linette et al., 1996; Vairo et al., 2000; Greider et al., 2002). To determine whether high p27 expression was a result of cell death inhibition during cell cycle arrest, cells treated with zVAD-fmk or DMSO during serum starvation were Western blotted for p27. As expected, p27 was elevated in Bcl-x_L cells compared to DMSO-treated vector control cells. zVAD-treated cells exhibited levels of p27 comparable to DMSO-treated control cells, suggesting that Bcl-x_L upregulates p27 by a function other than inhibition of caspase activation (Figure 24).

zVAD-fmk treatment of Rat1MycER cells does not recapitulate the Bcl-2 cell cycle phenotype

In addition to serum stimulation, we tested the effect of caspase inhibition on Myc-induced cell cycle entry. Rat1MycER cells stably expressing Bcl-2 or empty vector (pBabe puro) were serum starved for 3 days in the presence of 40uM zVAD-fmk or an equal volume of DMSO and stimulated to enter cell cycle by the addition of 4-OHT. Following induction of MycER, DMSO-treated vector control cells showed a significant rise in S phase cells by 8 hrs and continued to rise to 35% at 10 hours, while Bcl-2 cells showed no rise in S phase cells by 10 hrs, as expected (Figure 25 A). Surprisingly, zVAD treatment of Rat1MycER cells had no effect on cell cycle entry, unlike the partial

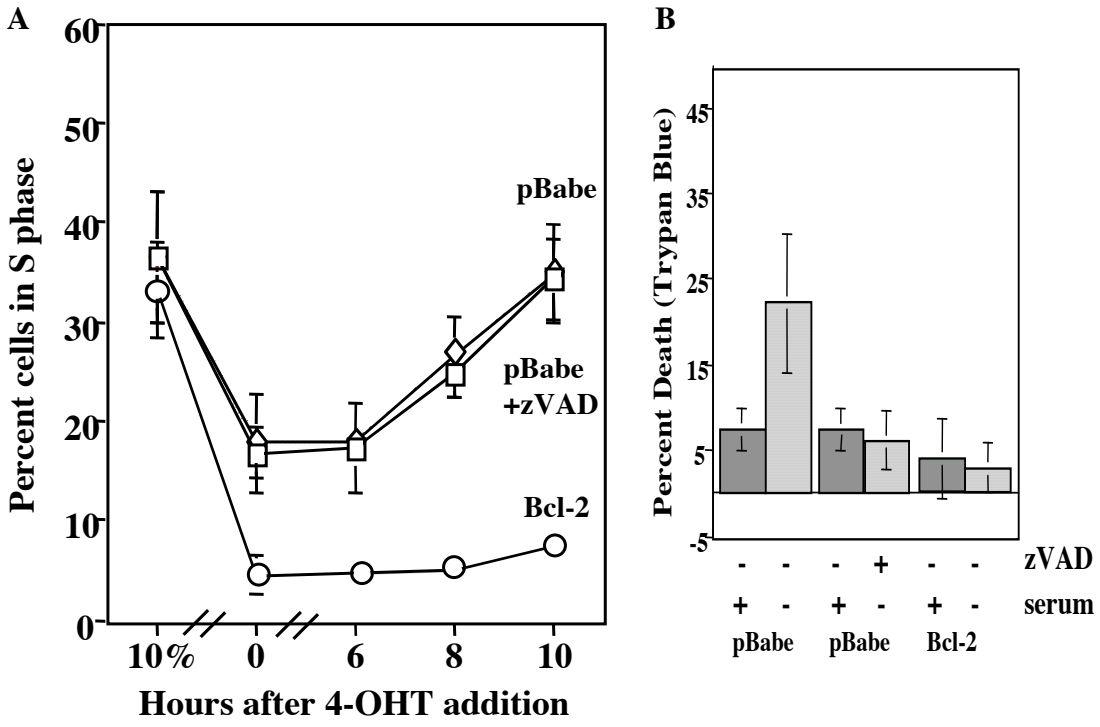

Figure 25: zVAD-fmk-treated Rat1MycER cells do not exhibit delayed cell cycle entry. Rat1MycER pBabe cells were arrested in 0.05% FBS medium and treated with zVAD or DMSO for three days. Rat1MycER Bcl-2 cells were arrested in 0.05% FBS medium and treated with DMSO for three days. (**A**) DNA contents of cells were obtained by PI and FACS analysis. Error bars are derived from three experiments. For some of the time points the standard deviation is so small that the error bars are not visible. (**B**) Viability of Rat1MycER cells treated with zVAD-fmk or DMSO or expressing Bcl-2 was assessed by Trypan Blue staining. Error bars are derived from three experiments.

effect seen in serum-induced cell cycle entry. MycER cells do not arrest in G_0/G_1 well, typically showing 10-20% S phase cells after 3 days of low serum, which was not affected by zVAD treatment. Viability in 0.05% serum confirmed that zVAD inhibited cell death almost as well as Bcl-2 (Figure 25 B).

The experiments using zVAD showed that caspase inhibition was not sufficient to recapitulate enhanced G_0 arrest or delayed cell cycle entry seen in Bcl-2/Bcl-x_L cells. Data from MycER cells were consistent with our findings in NIH3T3 cells that caspase inhibition cannot be the sole mechanism of Bcl-2's cell cycle function.

Caspase 9 dominant negative mutant partially recapitulates the Bcl-x_L cell cycle delay phenotype in NIH3T3 cells

Since Bcl-2/Bcl-x_L regulates the release of cytochrome c from the mitochondria, and cytochrome c binds Apaf-1 and pro-caspase 9 to form the apoptosome, we used a caspase 9 dominant negative (DN) mutant to test whether promoting survival by genetic inhibition of the apoptosome can enhance G_0 arrest. A caspase 9 dominant negative (DN) or Bcl-x_L cDNA was stably expressed in NIH3T3 cells. Caspase 9 DN expression was confirmed by western blotting, and caspase 9 DN function was confirmed by inhibition of caspase 3 cleavage after serum deprivation (Figure 26 A). Vector control, caspase 9 DN, and Bcl-x_L cells were cultured in 0.75% calf serum for 3 days, and stimulated to enter cell cycle by re-addition of 10% serum (Figure 26 B). Propidium iodide staining data showed that vector control cells enter S phase between 9 and 11 hrs, while Bcl-x_L cells enter S phase between 13 and 15 hrs. The caspase 9 DN expressing cells exhibit an intermediate rate of S phase entry. Consistent with data from zVAD treated cells, caspase 9 DN cells exhibited an approximately 20% decrease in RNA content similar to

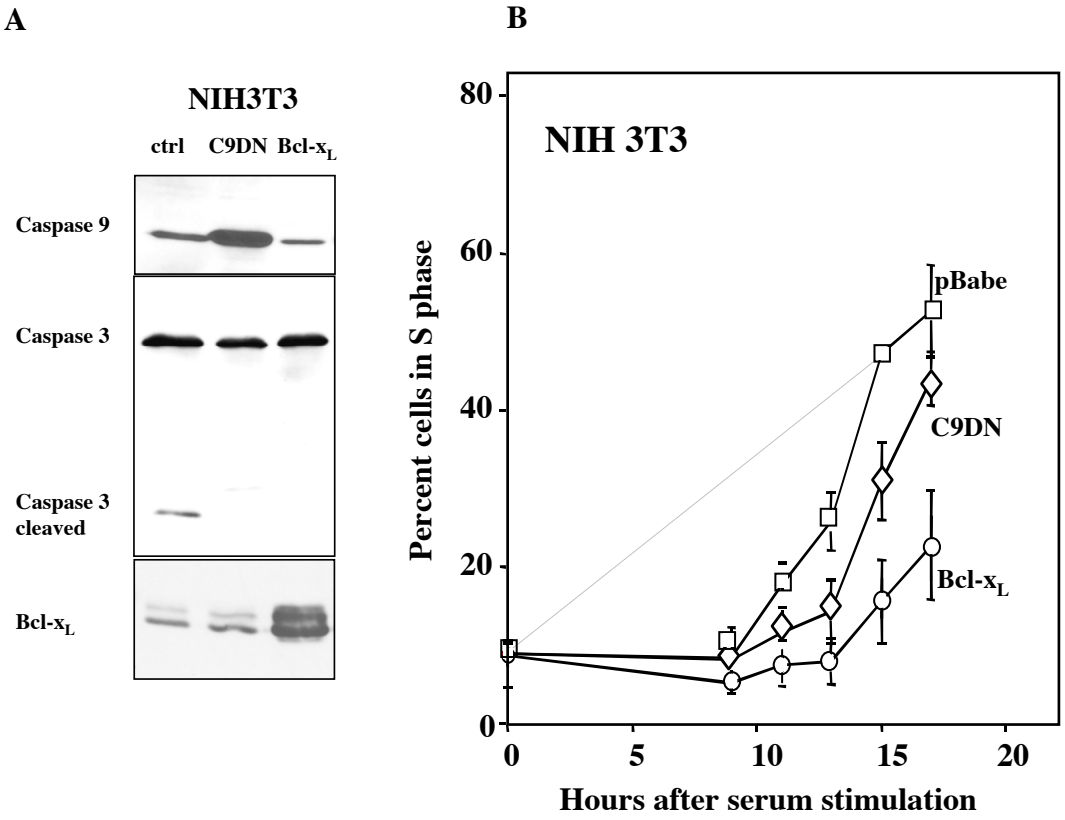

Figure 26: NIH3T3 caspase 9 DN exhibit a partial cell cycle delay phenotype. (**A**) Western blots of NIH3T3 cells showing overexpression of caspase 9 DN or Bcl-x_L. Cells were cultured in the absence of serum for 24 hours and immunoblotted for caspase 3 to verify function of the caspase 9 DN. (**B**) Caspase 9 DN was stably transfected into NIH3T3 pBabe cells. Cells were serum starved in 0.75% CS medium for three days and stimulated to enter cell cycle by serum re-addition. DNA contents of cells were obtained by PI and FACS analysis. Standard deviations are derived from three experiments. For some of the time points the standard deviation is so small that the error bars are not visible.

vector control cells (p=0.154 as compared to control), while Bcl-x_L expressing cells showed a further reduction in RNA of 42% (p=0.012 as compared to control) (Figure 27 A, C). The FSC results are consistent with the RNA data, in that there was no significant difference in the FSC change between control and caspase 9 DN cells, while Bcl-x_L cells reduced their size by 13% (p=0.012 as compared to control), significantly more than the cell size reduction in vector control and the caspase 9 DN cells (Figure 27 B, D). Western blotting for p27 revealed that, unlike Bcl-x_L expression, caspase 9 DN expression did not lead to further upregulation of p27 compared to vector control cells (Figure 27 E).

Caspase 9 dominant negative mutant does not affect cell cycle arrest or entry in Rat1MycER cells

Caspase 9 DN or Bcl-2 or empty vector were stably expressed in Rat1MycER cells. Western blotting for caspase 9 and caspase 3 cleavage, respectively, confirmed Caspase 9 DN expression and function (Figure 28 A). Caspase 9 DN is as efficient as Bcl-2 at protecting cell survival in low serum conditions (Figure 28 B). Vector control, caspase 9 DN, or Bcl-2 cells were arrested by serum starvation in 0.05% serum for 3 days. Arrested cells were stimulated to enter cell cycle by addition of 4-OHT. Cells were collected at serial time points and were subjected to BrdU analysis. The data showed that cells expressing caspase 9 DN enter S phase at a rate comparable to vector control cells, while Bcl-2 cells remain in G_0/G_1 longer (Figure 28 C). The pyronin Y and FSC data show that in Rat1MycER cells, expression of caspase 9 DN has no effect on the change in RNA content or cell size during cell cycle arrest. The reduction in RNA content following arrest was on average 20% in vector control cells, 22% in caspase 9

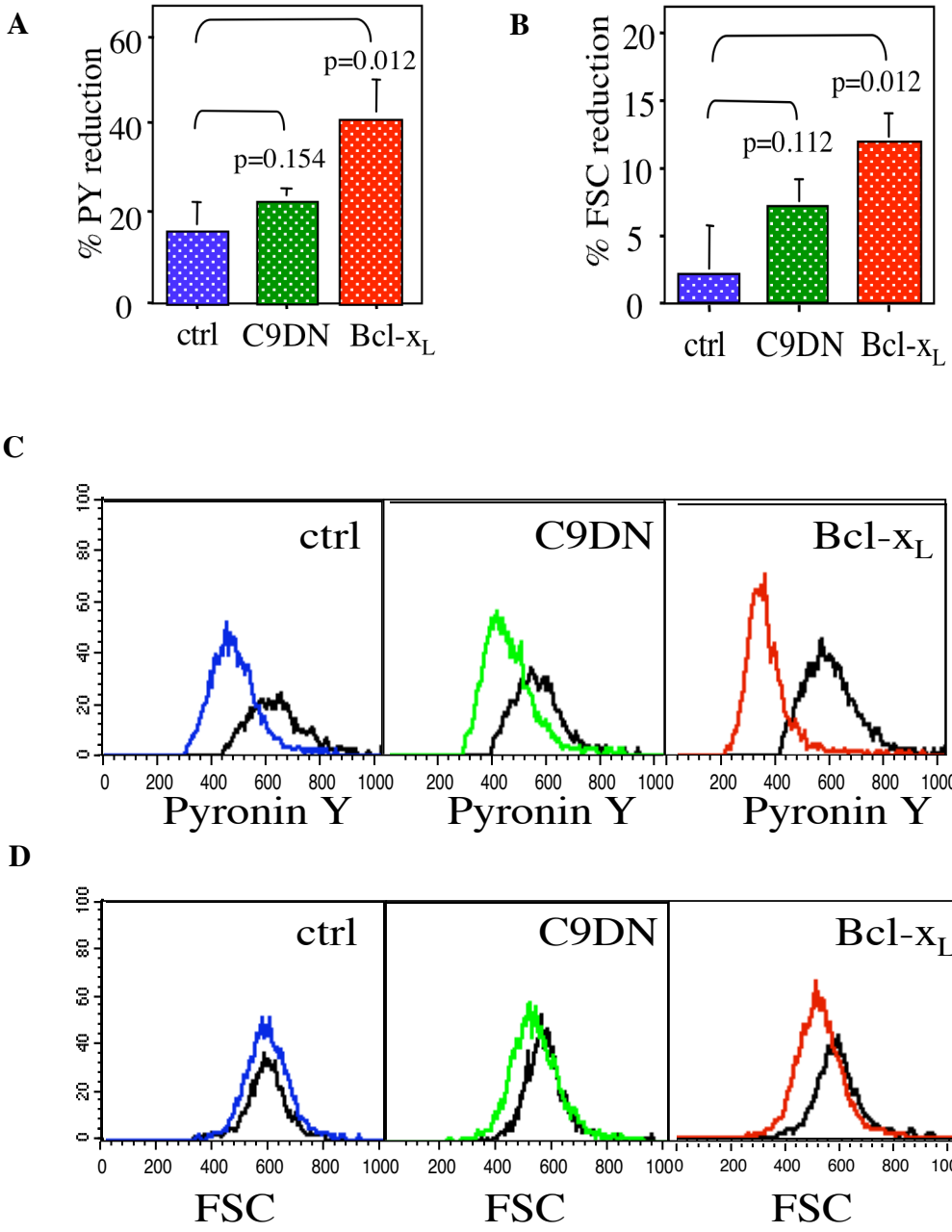
A
% PY reduction
60
40
20
0
p=0.012
p=0.154
ctrl
C9DN
Bcl-x_L
B
% FSC reduction
20
15
10
5
0
p=0.012
p=0.112
ctrl
C9DN
Bcl-x_L
C
ctrl
C9DN
Bcl-x_L
0
20
40
60
80
100
0
200
400
600
800
1000
Pyronin Y
Pyronin Y
Pyronin Y
D
ctrl
C9DN
Bcl-x_L
FSC
FSC
FSC

E

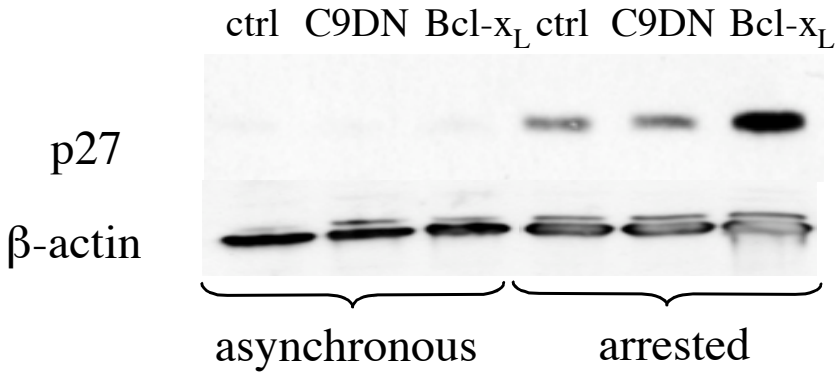

Figure 27: NIH3T3 caspase 9 DN do not exhibit enhanced G_0 arrest. NIH3T3 vector control, caspase 9 DN, and Bcl-x_L cells were arrested in 0.75% CS medium for three days. Cells were collected and fixed in 70% ethanol, then cells were stained with 7-AAD and pyronin Y, and analyzed by flow cytometry. (**A**) The bar graph represents the percent reduction in pyronin Y fluorescence from asynchronously growing cells to arrested cells. (**B**) The bar graph represents the percent reduction in forward scatter from asynchronously growing cells to arrested cells. Standard deviations are derived from three experiments. (**C**, **D**) Asynchronously growing pBabe (black) are overlaid with arrested pBabe cells (blue), growing caspase 9 DN cells (black) are overlaid with arrested caspase 9 DN cells (green), and asynchronously growing Bcl-x_L cells (black) are overlaid with arrested Bcl-x_L cells (red). (**E**) NIH3T3 vector control, caspase 9 DN, and Bcl-x_L cells were serum starved for three days and immunoblotted for p27 and β-actin.

DN cells (p>0.9 as compared to control cells), and 44% in Bcl-2 expressing cells (p=0.028 as compared to control cells) (Figure 29 A, C). The reduction in cell size in control cells was on average 10%, and 8% in caspase 9 ND (p=0.600), while in Bcl-2 cells it was 20% (p=0.030) (Figure 29 B, D). Western blotting for p27 in asynchronously growing and arrested Rat1MycER cells showed that caspase 9 DN upregulated p27 during arrest to a level comparable to control cells (Figure 29 E). These data suggest that inhibition of caspase 9 is not involved in the cell cycle arrest function of Bcl-2/Bcl-x_L.

Inhibition of cell death in FL5.12 cells by mAkt does not recapitulate the Bcl-x_L cell cycle phenotype

To test whether increasing cell survival by pathways independent of Bcl-2/Bcl-x_L can lead to enhanced cell cycle arrest, we used FL5.12 cells containing a doxycyclin-inducible, myristoylated Akt (mAkt), a survival kinase with many targets, only one of which is the Bcl-2 family member, Bad. Western blotting of phospho-Ser 473 and total Akt confirmed expression of phosphorylated Akt 12 hours after addition of doxycyclin (Figure 30). Assaying viability of cells cultured in low (25% of IL-2 in complete medium) IL-3 for three days showed that mAkt was as efficient as Bcl-x_L at promoting cell survival (Figure 31 A). IL-3-dependent FL5.12 cells were cultured in low IL-3 medium for 3 days such that 90% of control cells were in G_0/G_1 and only 4% of cells were in S phase. The cells were stimulated to enter cycle by resuspending in complete IL-3 medium. After 3 days in low IL-3 medium, cells with induced mAkt still exhibited 18% S phase cells (Figure 31 B). BrdU/PI analysis was performed to determine whether mAkt expression prevented cell cycle arrest in low IL-3 or caused S phase arrest (Figure 31 C). In low IL-3, PI staining showed most of the control and Bcl-x_L cells to have 2N

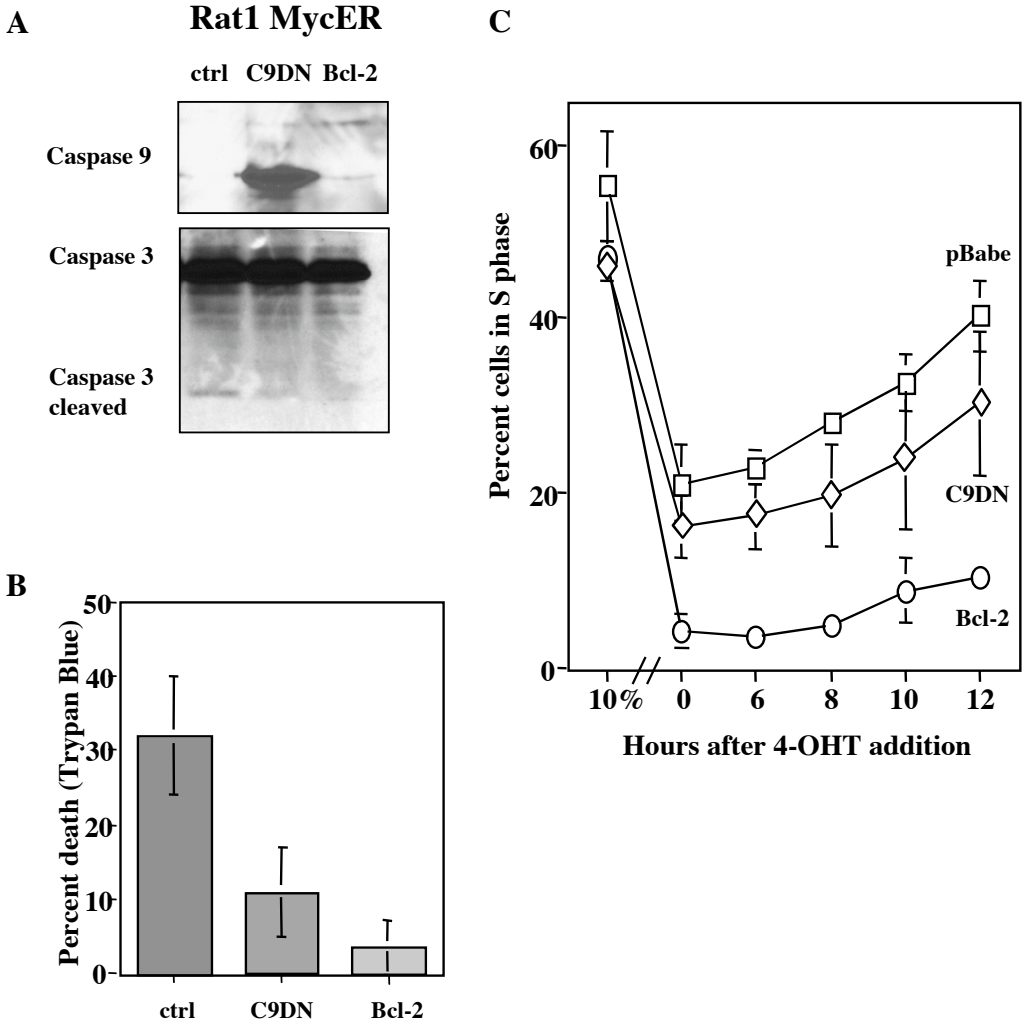

Figure 28: Rat1 caspase 9 DN cells do not exhibit a cell cycle delay phenotype. (**A**) Western blots of Rat1MycER cells showing overexpression of caspase 9 DN. Cells were cultured in the absence of serum for 24 hours and immunoblotted for caspase 3 to verify function of the caspase 9 DN. (**B**) Bar graph represents the percentage of dead cells following serum starvation in vector control, caspase 9 DN and Bcl-2 cells. (**C**) Caspase 9 DN was retrovirally introduced into Rat1MycER cells. Cells were serum starved in 0.05% FBS medium for three days and stimulated to enter cell cycle by serum re-addition. DNA contents of cells were obtained by PI and FACS analysis. Error bars are derived from three experiments. For some of the time points the standard deviation is so small that the error bars are not visible.

DNA content, and very few cells incorporated BrdU, as expected for a G_0/G_1 arrested culture. However, a significant proportion of the cells with doxycyclin-induced mAkt had S phase DNA content by PI and did not incorporate BrdU, indicating S phase arrest. Other cells in the culture had S phase DNA content and incorporated BrdU, indicating active S phase progression. Pyronin Y staining of cells with 2N DNA content cultured in low IL-3 revealed that the decrease in RNA content in mAkt cells was not significantly different from control cells ($p=0.148$), while Bcl-x_L cells exhibited a significantly greater decrease in RNA content ($p=0.033$ as compared to controls), indicating G_0 arrest (Figure 32 A). The decrease in cell size of mAkt cells in low IL-3 also was not statistically different from the decrease in control cells (Figure 32 B). Consistently, p27 was not elevated (Figure 32 C). Thus, in response to low survival factor concentration, mAkt-expressing cells either continued to proliferate or arrested in mid-cycle, rather than entering G_0. While mAkt maintained cell survival in low IL-3 medium nearly as well as Bcl-x_L, the two survival proteins had very different effects in cell cycle arrest. These data indicate that the enhancement of G_0 arrest and delay of cell cycle entry seen in Bcl-2/Bcl-x_L cells cannot simply be the result of cell death inhibition.

Bcl-2/Bcl-x_L delays the increase in ATP content during cell cycle entry in NIH3T3, Rat1MycER, and primary T cells

Our published data suggested that the initiation of cell cycle events occurs normally in Bcl-x_L/Bcl-2 cells, but downstream processes are delayed. In cells undergoing growth factor depletion-induced apoptosis, oxidative phosphorylation and mitochondrial membrane potential are reduced, and defective ADP/ATP exchange results in low cellular ATP leading to collapse of the mitochondrial membrane integrity.

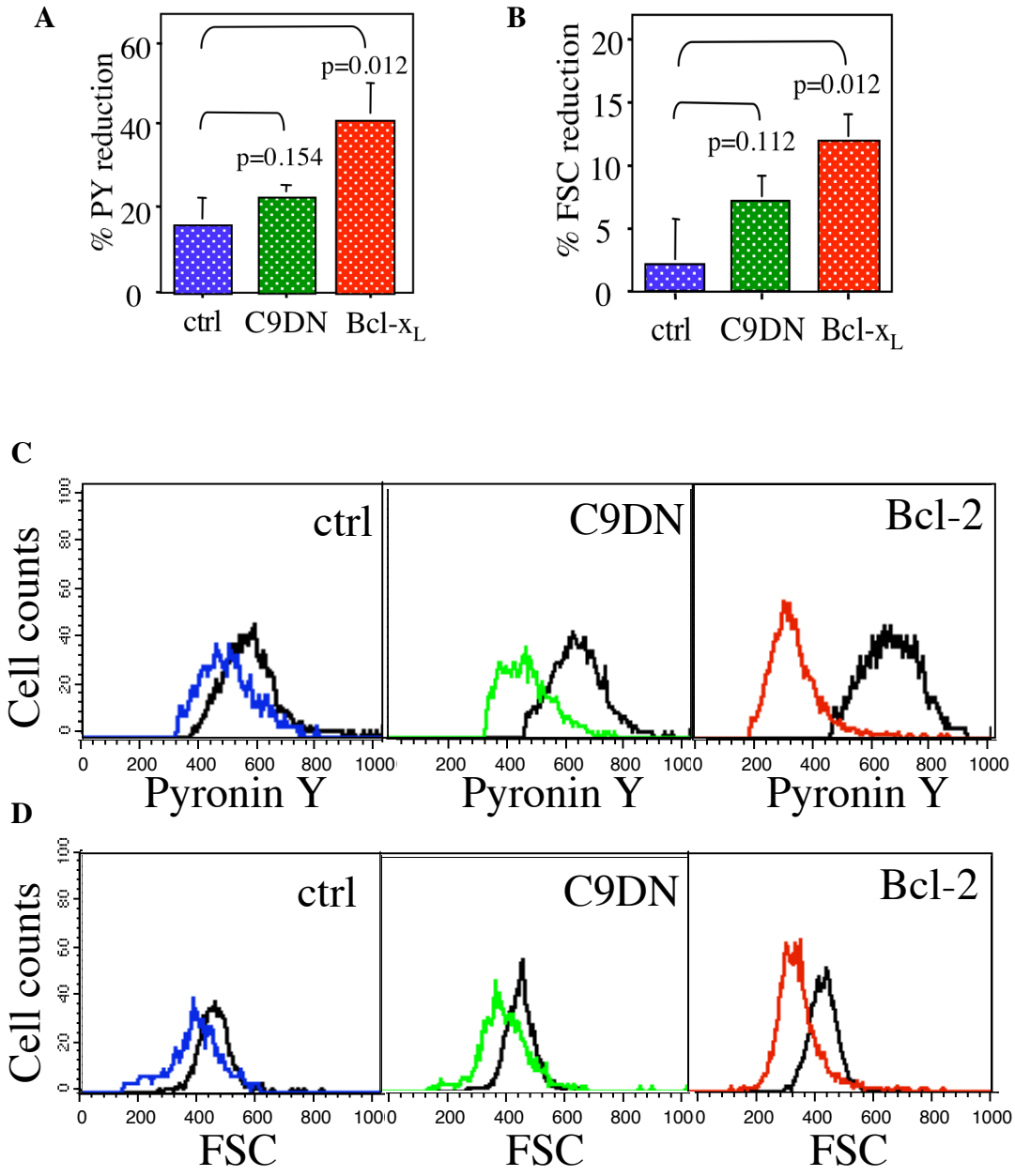
A
% PY reduction
60
40
20
0
p=0.012
p=0.154
ctrl
C9DN
Bcl-x_L
B
% FSC reduction
20
15
10
5
0
p=0.012
p=0.112
ctrl
C9DN
Bcl-x_L
C
Cell counts
ctrl
C9DN
Bcl-2
Pyronin Y
Pyronin Y
Pyronin Y
D
Cell counts
ctrl
C9DN
Bcl-2
FSC
FSC
FSC

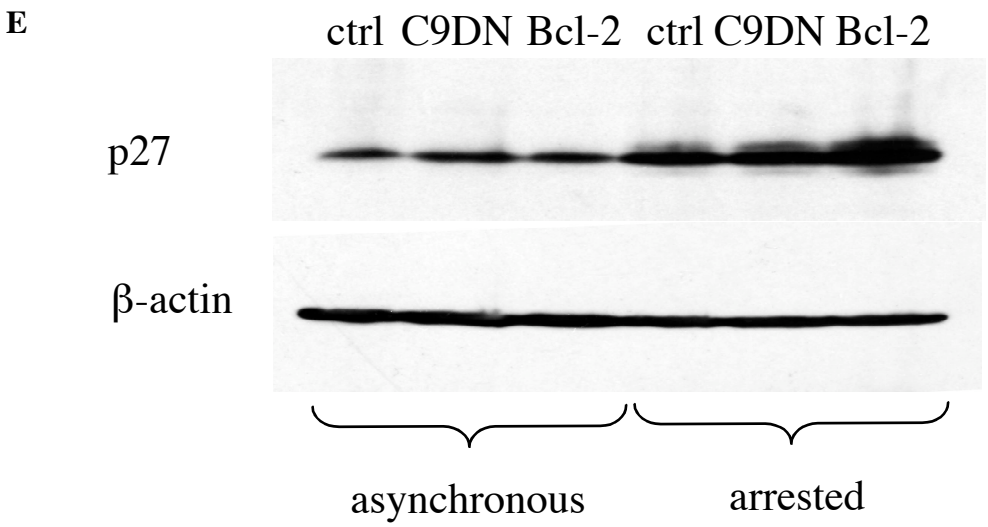

Figure 29: Rat1MycER caspase 9 DN cells do not exhibit enhanced G_0 arrest. Rat1MycER control, caspase 9 DN, and Bcl-2 cells were arrested in 0.05% FBS medium for 3 days. (**A**) The bar graph represents the percent reduction in pyronin Y fluorescence from asynchronously growing cells to arrested cells. (**B**) The bar graph represents the percent reduction in forward scatter from asynchronously growing cells to arrested cells. The error bars are derived from three experiments. (**C**, **D**) Histograms of pyronin Y fluorescence or forward scatter are overlaid, asynchronously growing (black) are overlaid with arrested cells (control-blue, caspase 9 DN-green, Bcl-2-red). (**E**) Rat1MycER vector control, caspase 9 DN, and Bcl-2 cells were serum starved for three days in 0.05% FBS medium. Cells were collected before and after cell cycle arrest and immunoblotted for p27 and β-actin.

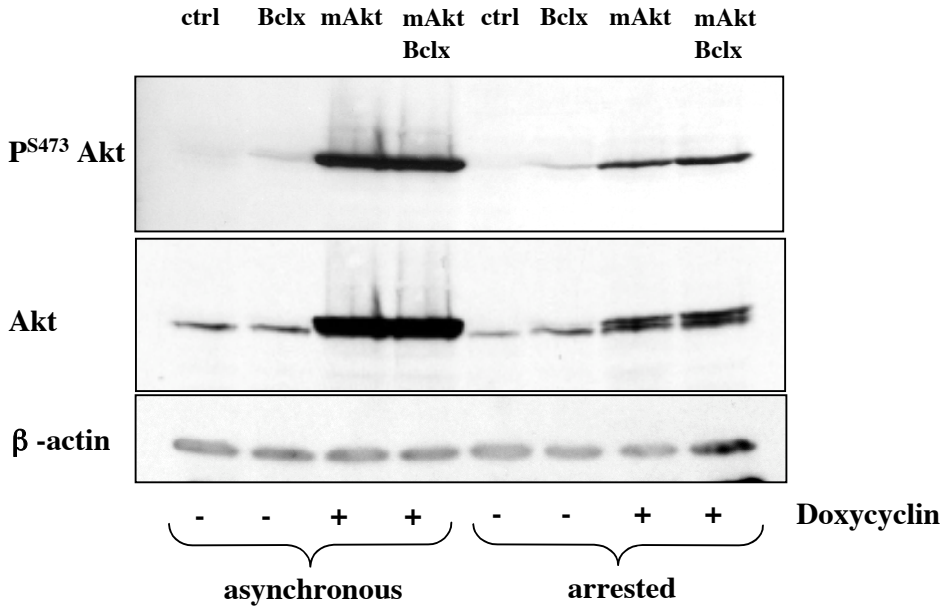

Figure 30: Induction of mAkt in the FL5.12 cells. Cells were treated with 2ug/ml doxycyclin for 16 hrs before they were cultured in reduced IL-3 medium in the presence of doxycyclin for three days. Cells were collected before and after arrest and immunoblotted for pS473 Akt, total Akt, and β-actin.

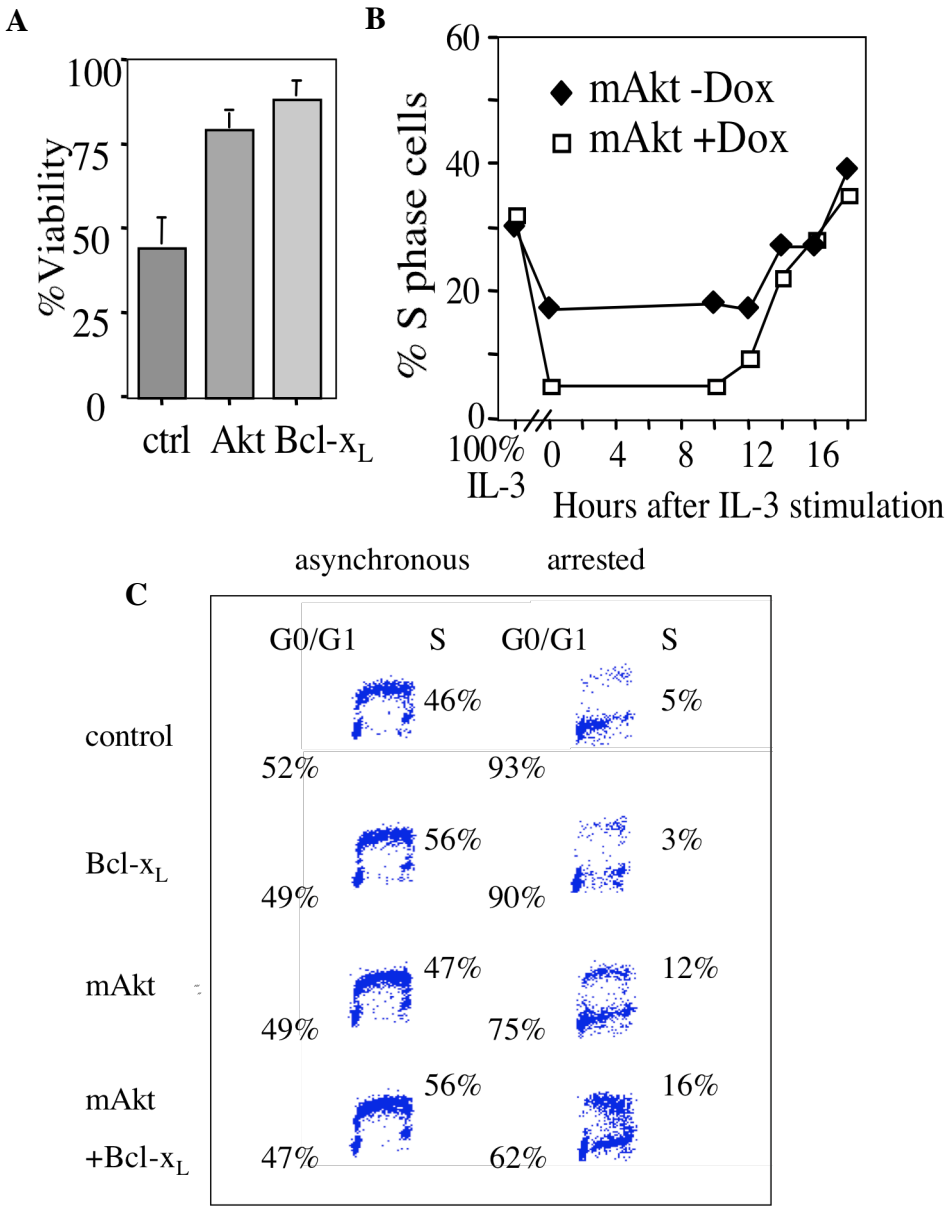

Figure 31: FL5.12 cells expressing mAkt are protected from cell death. (**A**) The bar graph represents the percent viability as measured by Trypan Blue of FL5.12 cells cultured in low IL-2 for three days. (**B**) Cells were treated with doxycyclin, then cultured in low IL-3 medium for three days with doxycyclin. DNA contents of cells were obtained by PI and FACS analysis. (**C**) BrdU analysis of asynchronous and arrested FL5.12 control, Bcl-x_L, mAkt, and Bcl-x_L/mAkt.

Maintenance of ADP/ATP exchange by Bcl-x_L allows mitochondria to remain coupled at a lower level of cellular metabolism (Plas et al., 2002; Plas et al., 2001). Regulation of ADP/ATP exchange may play a role in Bcl-x_L-mediated cell cycle arrest. We examined the effects of Bcl-2/Bcl-x_L on total cellular ATP content during arrest and cell cycle entry. In serum starved control NIH3T3 cells stimulated to re-enter the cell cycle by serum, maximal ATP content was measured at 13 hours, when cells were entering S phase (Figure 33 A, Aa). In Bcl-x_L cells, peak ATP level was delayed until 16 hours, coincident with delayed S phase entry in these cells. Similarly, in control Rat1MycER cells stimulated with 4-OHT, cellular ATP content peaked at 8 hours, just prior to S phase entry. In Bcl-2 expressing MycER cells, progression to S phase was delayed to 12-14 hours, and peak cellular ATP was also delayed until 12 hours (Figure 33 B, Ba).

The delay in peak ATP associated with Bcl-2/Bcl-x_L expression was confirmed in primary murine T cells. ATP content was measured in wildtype and Bcl-2 transgenic splenic T cells stimulated to enter cell cycle by anti-CD3 activation (Figure 33 C, Ca). In wild type T cells, ATP levels began to rise after 20 hours and peaked around 40 hours when robust entry into S phase was evident. The rise in ATP levels in Bcl-2 transgenic T cells was delayed until after 40 hours, paralleling delayed S phase entry. Thus, in cell lines and primary cells, cell cycle delay by Bcl-2/Bcl-x_L was associated with delayed rise in cellular ATP.

Elevated ATP does not reverse the cell cycle effect of Bcl-x_L

Could the delay in peak ATP content in Bcl-x_L/Bcl-2 cells be the mechanism of cell cycle delay? If Bcl-x_L regulated cell cycle entry by delaying ATP increase, then

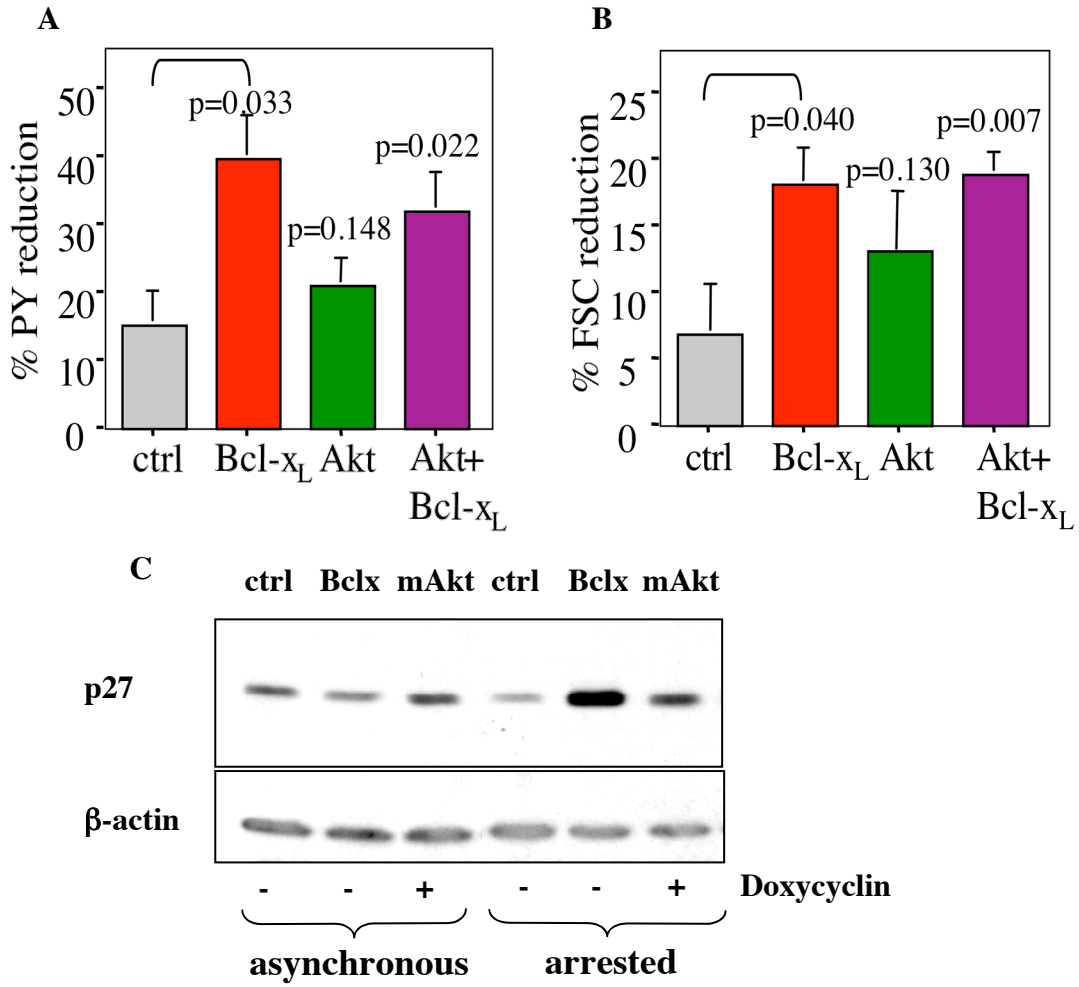

Figure 32: FL5.12 mAkt cells do not exhibit enhanced G_0 arrest. FL5.12 vector control, Bcl-x_L, and Bcl-x_L/mAkt cells were pre-treated with doxycyclin and arrested in low IL-3 medium for three days in the presence of doxycyclin. Cells were collected and fixed in 70% ethanol, then cells were stained with 7-AAD and pyronin Y, and analyzed by flow cytometry. (**A**) The bar graph represents the percent reduction in pyronin Y fluorescence from asynchronously growing cells to arrested cells. (**B**) The bar graph represents the percent reduction in forward scatter from asynchronously growing cells to arrested cells. The error bars are derived from three experiments. (**C**) Western blot for p27 and β-actin on asynchronously growing (pre-treated with doxycyclin) and arrested FL5.12 cells (pre-treated with doxycyclin).

exogenous elevation of ATP in Bcl-x_L cells should reverse cell cycle delay. Addition of adenine to NIHT3 cells during cell cycle entry raised cellular ATP in Bcl-x_L cells to levels higher than in untreated control cells (Figure 34 A). However, the cell cycle PI profiles showed that the rate of S phase entry of Bcl-x_L cells with higher ATP levels was identical to the untreated Bcl-x_L cells. Higher ATP levels also did not alter S phase entry in control cells (Figure 34 B). These results showed that cell cycle delay by Bcl-2/Bcl-x_L expression could not be overcome by higher cellular ATP levels, suggesting that Bcl-x_L regulates cell cycle independently of ADP/ATP exchange.

Bcl-x_L cells exhibit lower MMP during cell cycle arrest

Bcl-2/Bcl-x_L is able to prevent the disintegration of mitochondrial membrane potential and inhibit the formation of reactive oxygen species both the processes contribute to cells death (Gottlieb, et al., 2000; Harris, et al., 2000; Ferri, et al., 2001). Our data indicating a dissociation between cell cycle events and cell growth suggest two possible modes of action for Bcl-2/Bcl-x_L. First, cells expressing Bcl-2/Bcl-x_L arrest at a different metabolic state (smaller size, less protein and RNA, lower mitochondrial membrane potential) than controls because of the ability of Bcl-2/Bcl-x_L to maintain mitochondrial function and keep cells alive, so that the other processes of cell cycle arrest can continue. Therefore, when the Bcl-2/Bcl-x_L cells are stimulated to re-enter cell cycle they take longer to reach critical mass for G_1 and S phase to occur. Second, Bcl-2/Bcl-x_L inhibits the proliferation of mitochondria, decreasing the rate of cell growth. To distinguish between these two models, we monitored mitochondrial membrane potential (MMP) and mitochondrial mass in asynchronously growing and arrested cells. TMRE

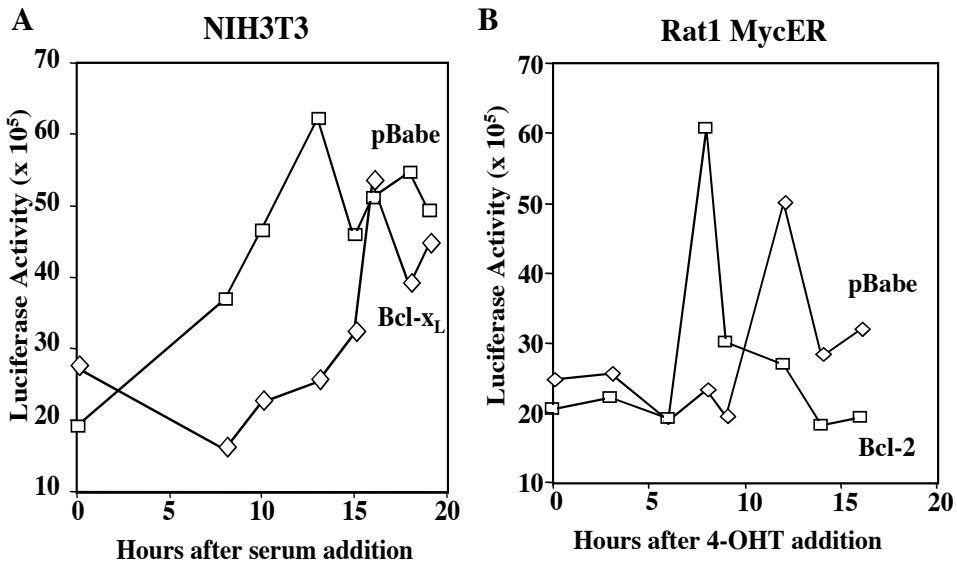
A
NIH3T3
Luciferase Activity (x 10^5)
70
60
50
40
30
20
10
0
5
10
15
20
pBabe
Bcl-x_L
Hours after serum addition
B
Rat1 MycER
Luciferase Activity (x 10^5)
pBabe
Bcl-2
Hours after 4-OHT addition

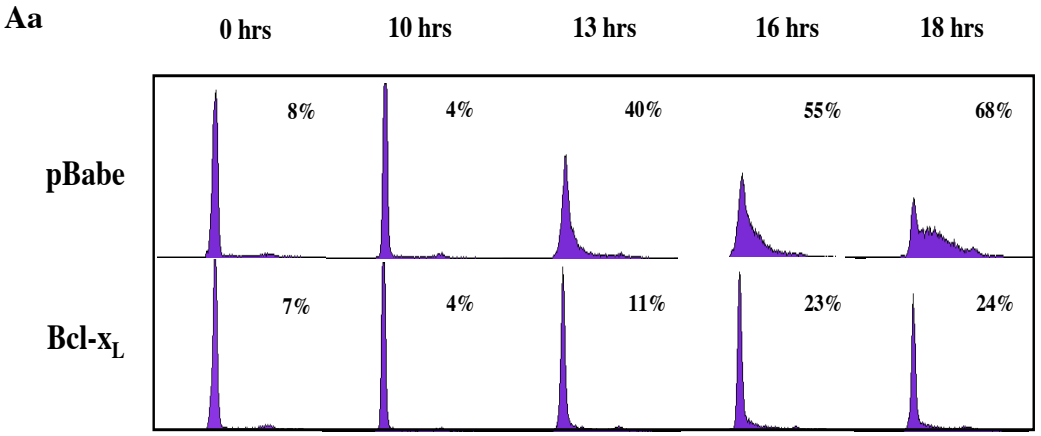
Aa
0 hrs
10 hrs
13 hrs
16 hrs
18 hrs
pBabe
8%
4%
40%
55%
68%
Bcl-x_L
7%
4%
11%
23%
24%

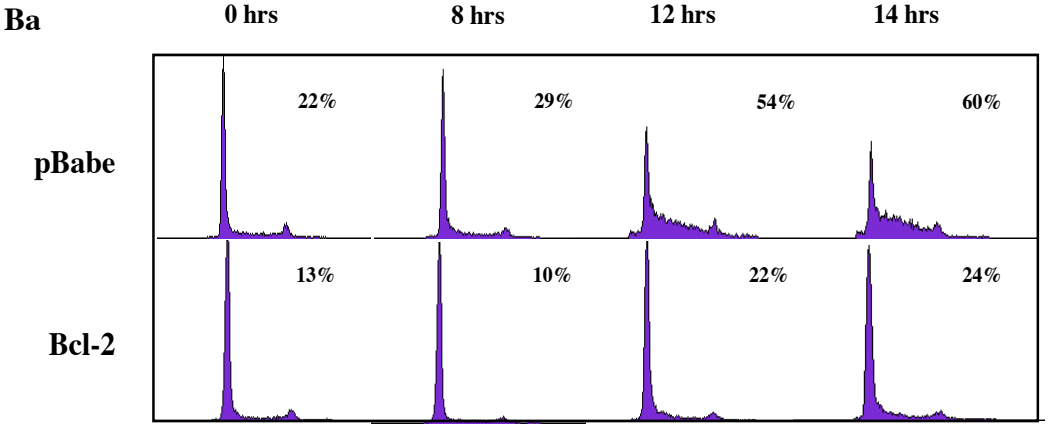
Ba
0 hrs
8 hrs
12 hrs
14 hrs
pBabe
22%
29%
54%
60%
Bcl-2
13%
10%
22%
24%

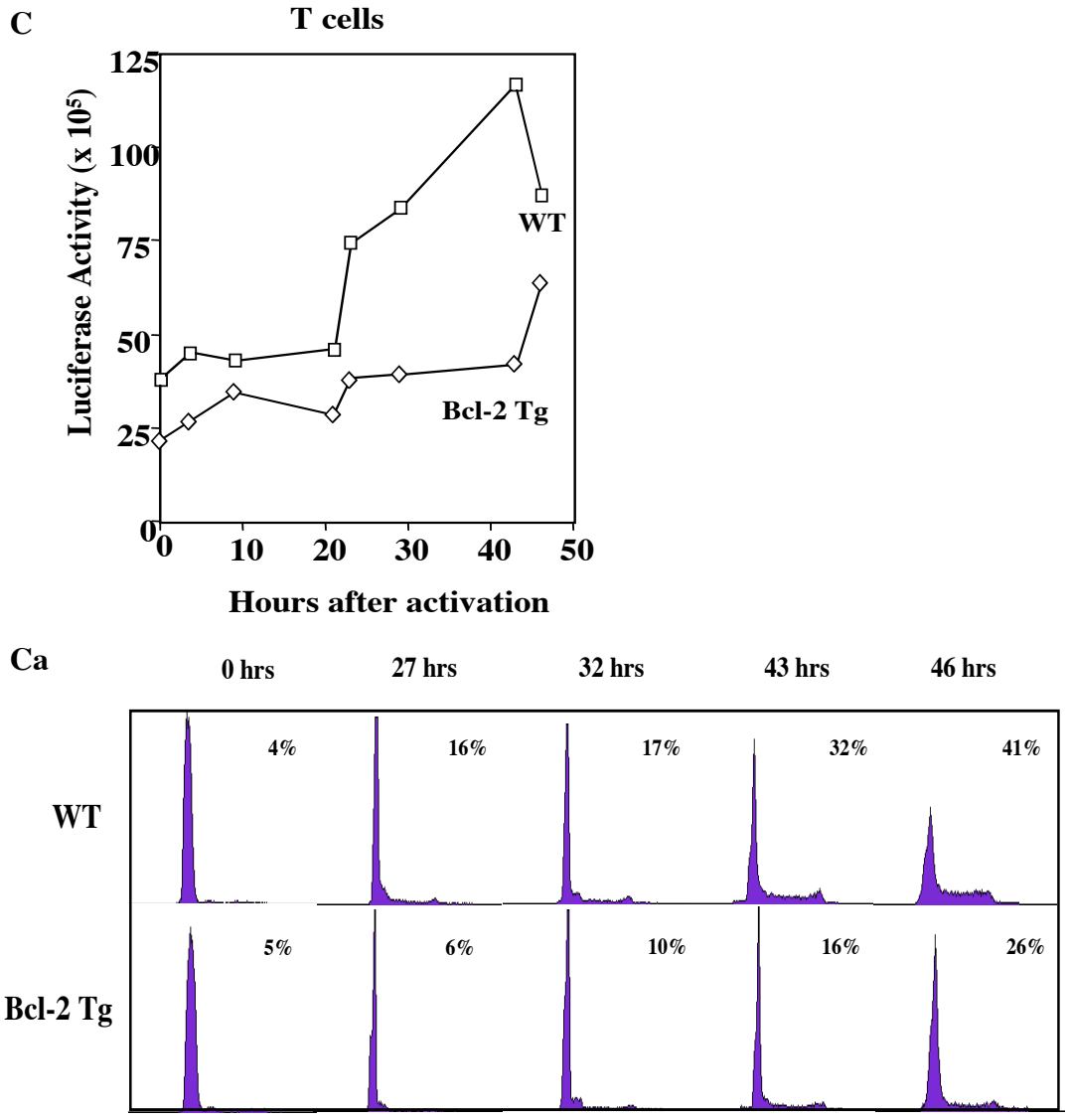

Figure 33: Peak ATP is delayed in cell lines and primary T cells expressing Bcl-x_L/Bcl-2. (**A**) NIH3T3 control and Bcl-x_L cells were cultured in 0.75% CS medium for three days, then released from arrest by serum stimulation. Total cellular ATP content was determined using Roche ATP Bioluminescence assay at the indicated time points. (**Aa**) DNA content was obtained by PI and FACS analysis. (**B**) Rat1MycER control and Bcl-2 cells were cultured in 0.05% FBS medium for three days, then released from arrest by activation of MycER. Total cellular ATP and (**Ba**) DNA content were determined at the indicated time points. (**C**) Wild type and Bcl-2 transgenic T cells were activated with α-CD3. Total cellular ATP and (**Ca**) DNA content were determined at the indicated time points.

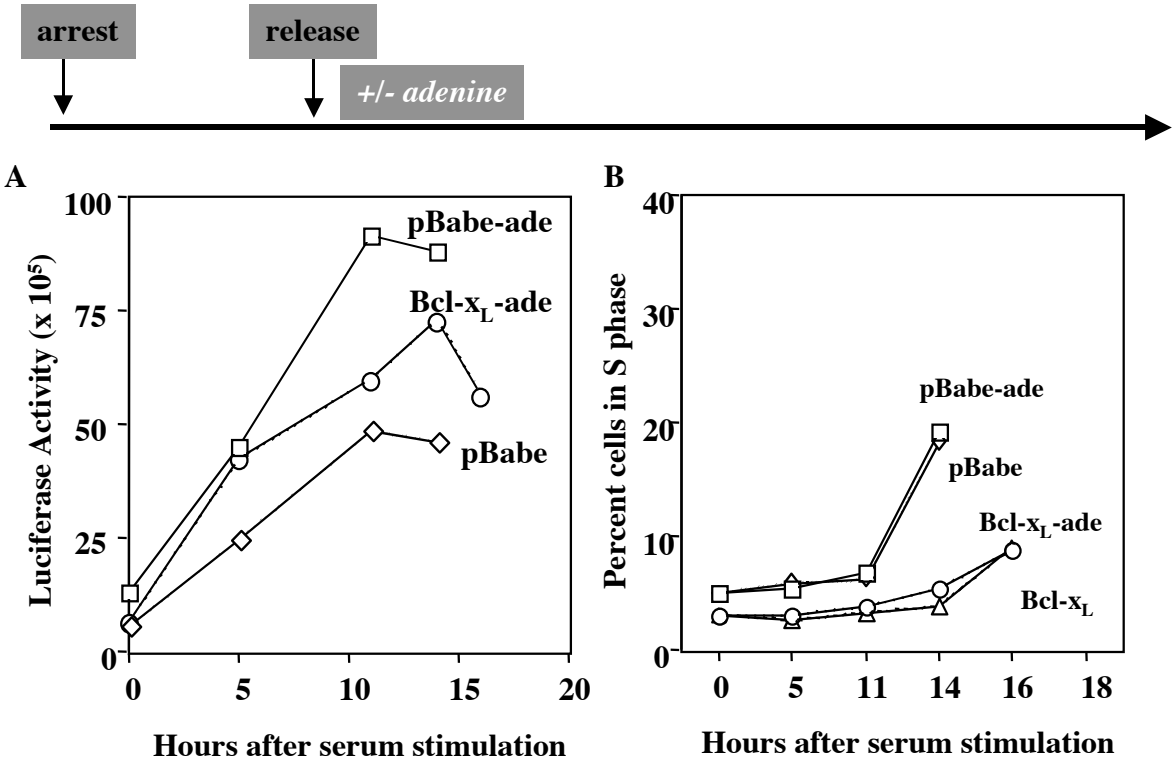

Figure 34: Elevation of cellular ATP does not reverse the cell cycle delay phenotype of Bcl-x_L. NIH3T3 vector control and Bcl-x_L cells were cultured in 0.75% CS medium for three days, and then released from arrest by re-addition of 10% CS medium in the presence of 50μM adenine or vehicle. (**A**) ATP content of NIH3T3 control and Bcl-x_L cells treated with adenine and control cells treated with vehicle alone. (**B**) DNA content of NIH 3T3 vector control and Bcl-x_L cells treated with adenine or vehicle.

stains mitochondria in a potential-dependent manner, while MitoTracker Green stains mitochondria independently of potential. FL5.12 cells expressing vector control or Bcl-x_L were washed three times with PBS and cultured in low IL3 medium for three days. Cells were incubated with 50nM TMRE or 500nM MitoTracker Green for 30 minutes, then analyzed by flow cytometry. TMRE staining showed that following arrest mitochondrial membrane potential is lower in Bcl-x_L cells than in control cells (Figure 35 A). MTG staining showed that while mitochondrial number in control cells either increases or remains the same after cell cycle arrest, the mitochondrial number in Bcl-x_L cells tends to decrease (Figure 35 B). The ratio of mitochondrial membrane potential per mitochondrion showed that in arrest, Bcl-x_L cells tend to have higher potential per mitochondrion than control cells, however this does not reach significance (Figure 35 C). These data suggest that Bcl-x_L regulates either mitochondrial membrane potential or mitochondrial number during cell cycle arrest.

Bcl-x_L delays cell cycle entry in 143B ρ0 cells

Bcl-2/Bcl-x_L has been shown to prevent the disintegration of mitochondrial membrane potential which contributes to cell death (Gottlieb et al., 2000). We have shown that Bcl-2/Bcl-x_L-expressing cells were delayed in reaching the restriction point in G_1 due to a lag in accumulation of RNA and cell size, consistent with prolonged G_0 (Janumyan et al., 2003). We also found that the induction of early G_1 molecules Myc and cycling D1 are not affected by Bcl-2/Bcl-x_L, indicating that the initiation of early cell cycle events is normal in Bcl-2/Bcl-x_L cells. We hypothesized that cells expressing Bcl-2/Bcl-x_L arrest at a different metabolic state (smaller size, less RNA, lower mitochondrial

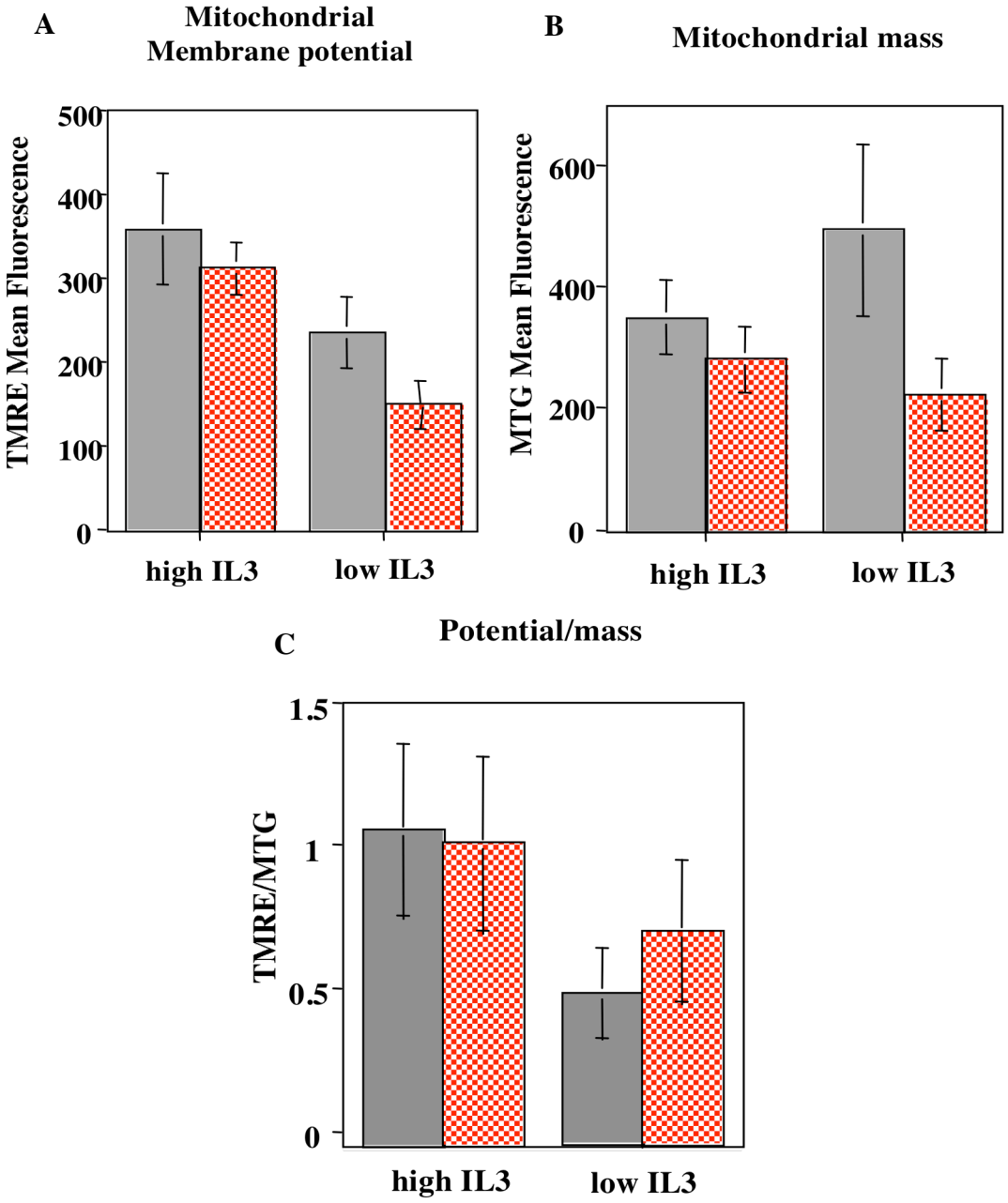

Figure 35: Bcl-x_L may regulate mitochondrial membrane potential or number. Control (grey, solid bar) cells and Bcl-x_L (red, checkered bar) cells were stained with TMRE (**A**) or MTG (**B**) while growing asynchronously (high IL-3) and following cell cycle arrest (low IL-3). (**C**) The ratio of mitochondrial membrane potential per mitochondrial mass. Standard deviation is derived from five experiments.

membrane potential) than controls, because of the ability of Bcl-2/Bcl-x_L to maintain mitochondrial function keeping cells alive, so that the other processes of cell cycle arrest can continue. mtDNA-free 143B ρ0 cells stably expressing empty vector or Bcl-x_L were serum starved for 4 days and then released into cell cycle by serum stimulation. Viability of these cells in low serum confirmed that Bcl-x_L rescued cell death (Figure 36 A). 143B ρ0 vector control cells began to enter S phase before 10 hrs, while Bcl-x_L cells did not show S phase entry until 12 to 14 hrs following serum stimulation (Figure 36 B). These data showed that Bcl-x_L does not require normal mitochondrial membrane potential to delay cell cycle entry, and that Bcl-x_L regulates cell cycle entry independently of mitochondrial membrane potential. Analysis of RNA content and cell size showed that Bcl-x_L can enhance G_0 arrest in parental 143B cells, but not in 143Bρ0 (Figure 36 C). The data indicate that Bcl-x_L regulates G_0 arrest through mechanisms requiring an intact electron transport chain.

Summary

To determine the relationship between cell cycle control and apoptosis inhibition by Bcl-2 and Bcl-x_L, we sought to inhibit cell death during cell cycle arrest by means other than Bcl-2/Bcl-x_L overexpression. Surprisingly, we found that inhibition of cell death contributes to some, but not most of the cell cycle phenotypes of Bcl-2/Bcl-x_L. Our findings show that inhibition of caspases during cell cycle arrest results in a delay of cell cycle entry as compared to control cells. However, caspase inhibition does not result in the small cell size, reduced RNA content, or upregulated p27 phenotypes observed in cells overexpressing Bcl-2/Bcl-x_L, indicating that caspase inhibition may not be the

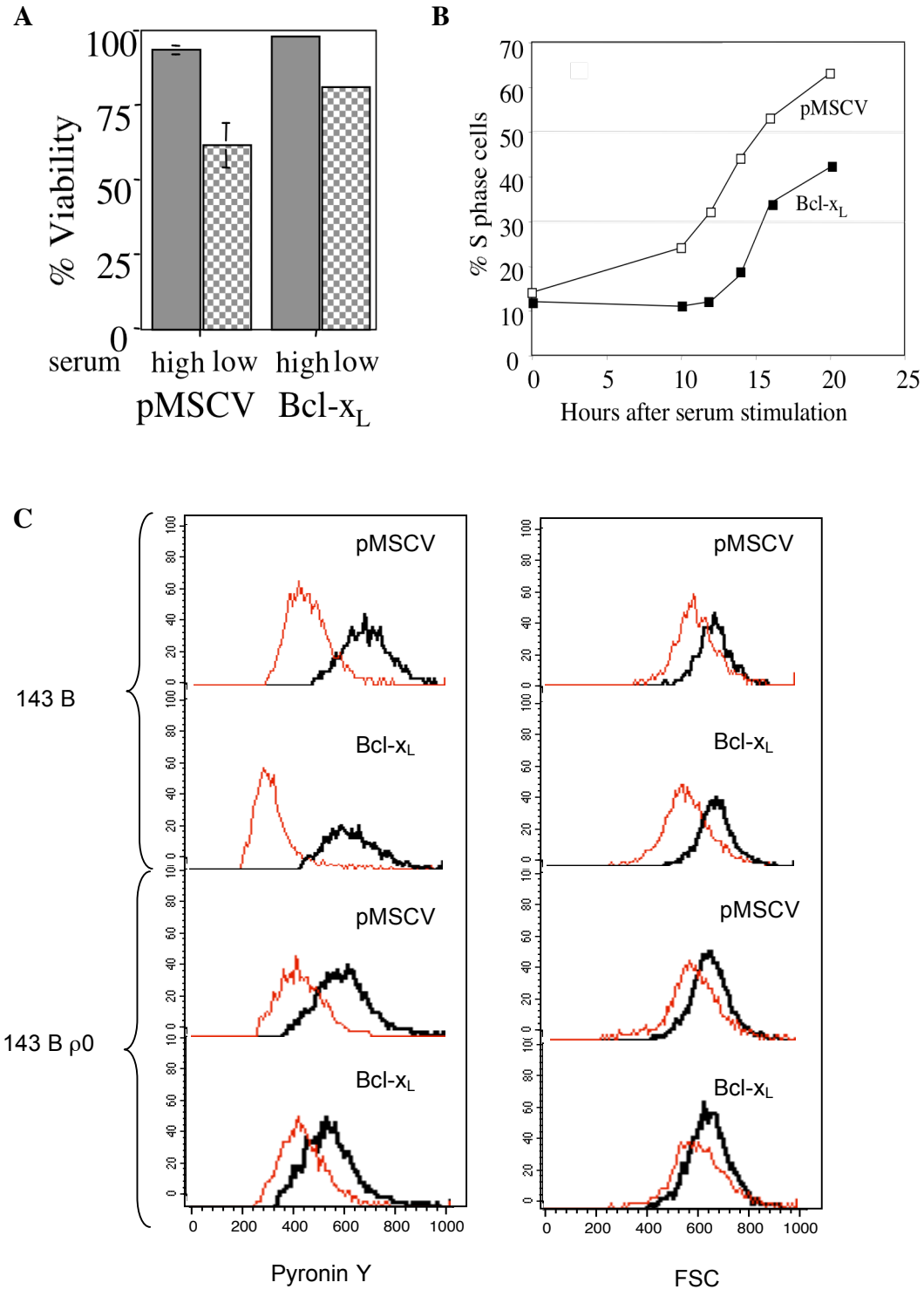
A
100
75
50
25
0
% Viability
serum
high low high low
pMSCV Bcl-xL
B
70
60
50
40
30
20
10
0
% S phase cells
pMSCV
Bcl-xL
0 5 10 15 20 25
Hours after serum stimulation
C
143 B
143 B ρ0
pMSCV
Bcl-xL
pMSCV
Bcl-xL
pMSCV
Bcl-xL
pMSCV
Bcl-xL
0 200 400 600 800 1000
Pyronin Y
0 200 400 600 800 1000
FSC

Figure 36: Bcl-x_L does not enhance cell cycle arrest in 143B ρ0 cells. (**A**) Viability of vector control and Bcl-x_L 143B ρ0 cells in low serum as assessed by Trypan Blue. Standard deviation is derived from three experiments. At some time points the standard deviation is so small that the error bars are not visible. Vector control and Bcl-x_L 143B ρ0 cells were arrested in low serum then serum stimulated to re-enter cell cycle. (**B**) DNA content of vector control and Bcl-x_L 143B ρ0 cells. Average of two experiments is shown. (**C**) Pyronin Y and forward scatter histograms of asynchronously growing (black) and arrested cells (red). Representative experiment of three is shown.

mechanism of enhanced G_0 arrest by Bcl-2/Bcl-x_L. Our data from the caspase inhibition experiments is consistent with the emerging evidence, which suggests that caspases may regulate cell cycle in addition to apoptosis. Caspase 3 has been implicated as a negative regulator of B cell cycling (Woo et al., 2003). Splenic B cells from *casp3*$^{-/-}$ mice exhibit normal apoptosis, but increased proliferation due to increased associated of p21 with PCNA. The activities of caspases 6 and 8 were shown to be upregulated following B cell activation, but caspase 3 activity and apoptosis were decreased (Olson, et al., 2003). Additional evidence for the role of caspases in cell cycle is provided by patients with a genetic deficiency in caspase 8, who exhibit defects in apoptosis as well as activation of T, B, and NK cells (Chun, et al., 2002).

Inhibitors of caspase 9 and 3, LEHD, DEVD, or DQMD, did not inhibit cell death of NIH3T3 and Rat1MycER cells during serum starvation at a range of concentrations; therefore, these inhibitors could not be used to answer the question of whether inhibition of cell death during arrest leads to cell cycle delay.

Although our arrest data from NIH3T3 and Rat1MycER cells are consistent, the reasons for different cell cycle entry results with either zVAD treatment or caspase 9 DN expression are not obvious. One explanation for the differences between zVAD and caspase 9 DN is that one is a drug treatment and the other is genetic inhibition. Another possibility is that the cell cycle entry stimuli are different. The extent to which caspases are inhibited as well as the length of time varies in each case. NIH3T3 cells were induced to enter cell cycle from quiescence by serum stimulation; however, the Rat1MycER cells were stimulated by induction of Myc.

We previously reported that the delay of cell cycle entry phenotype of Bcl-2/Bcl-

x_L is mostly due to the enhanced state of G_0 (Janumyan et al., 2003). The data presented here showed that NIH3T3 control cells treated with zVAD during arrest or expressing caspase 9 DN exhibit partially delayed cell cycle entry in the absence of decreased cell size or decreased RNA content. We believe the data indicate that while enhanced arrest is the major contributor to delayed cell cycle entry by Bcl-2/Bcl-x_L, the anti-apoptotic function of Bcl-2/Bcl-x_L may also be partially responsible. However, there must be mechanisms independent of or upstream from caspase inhibition that are responsible for the enhanced G_0 phenotype. What are the possible mechanisms of action for Bcl-2/Bcl-x_L in cell cycle arrest? It has been shown that $Bak^{-/-}/Bax^{-/-}$ hematopoietic cells are able to survive for weeks in the absence of growth factor by activating autophagy; which results in decreased cell size; however, the longer the cells were deprived of growth factor the more impaired the proliferative potential of these cells becomes (Lum et al., 2005). Bcl-2/Bcl-x_L may activate autophagy during starvation conditions to maintain prolonged survival. Upon a cell cycle stimulus, the Bcl-2/Bcl-x_L cells would take longer to synthesize enough organelles for cell cycle entry. Our data indicating a dissociation between cell cycle events and cell growth, suggest three possible modes of action for Bcl-2/Bcl-x_L. First, Bcl-2/Bcl-x_L arrests cells at a different metabolic state than controls, because of the ability of Bcl-2/Bcl-x_L to maintain mitochondrial function keeping cells alive, so that the other processes of cell cycle arrest can continue. Therefore, when the Bcl-2/Bcl-x_L cells are stimulated to re-enter cell cycle they take longer to reach critical mass for G_1 and S phase to occur. Second, Bcl-2/Bcl-x_L may inhibit mitochondrial biogenesis, decreasing the rate of cell growth. Third, Bcl-2/Bcl-x_L may have an inhibitory effect on a cell growth pathway, such as the mTOR pathway.

The major source of energy for cellular metabolism is a high ATP/ADP ratio, which is maintained by oxidative phosphorylation. Mitochondrial ATP/ADP exchange is a regulated event critical for cell survival. Lack of ADP in the mitochondrial matrix prevents the F_1F_0 ATPase from using the H^+ ion gradient and results in mitochondrial hyperpolarization and generation of ROS (Figure 37). Hyperpolarization of mitochondria leads to matrix swelling, loss of outer mitochondrial membrane integrity and cytochrome c release. Bcl-x_L expression enhances cell survival by maintaining ATP/ADP exchange, allowing mitochondria to remain coupled at a lower level of cellular metabolism (Vander Heiden et al., 1999). The effect of Bcl-2 on ATP/ADP exchange also relates to our cell growth hypothesis (Chapter V). It has been shown that mTOR is an ATP sensor (Dennis et al., 2001). Signaling through mTOR is influenced by intracellular ATP concentration, and is independent of amino acid abundance. mTOR functions as a homeostatic sensor, regulating the rate of ribosomal biogenesis to reflect intracellular ATP concentration. To determine whether Bcl-2/Bcl-x_L affect cell cycle by regulating cellular bioenergetics, we monitored cellular ATP levels during arrest and cell cycle entry. The data showed that cells expressing Bcl-2/Bcl-x_L exhibited delayed peak ATP content, suggesting that Bcl-2/Bcl-x_L may delay cell cycle entry by maintaining low cellular ATP content. The data were consistent in both the cell lines and primary murine T cells. To test whether low cellular ATP levels in Bcl-2/Bcl-x_L were responsible for the cell cycle effect, we exogenously elevated ATP levels in Bcl-x_L cells. The data showed that elevation of ATP in Bcl-x_L does not reverse the cell cycle effect of Bcl-x_L, indicating that low ATP levels are not causal to the Bcl-2/Bcl-x_L cell cycle effect. The data showed that peak ATP levels correlate with S phase entry. It is possible that the maintenance of low ATP levels

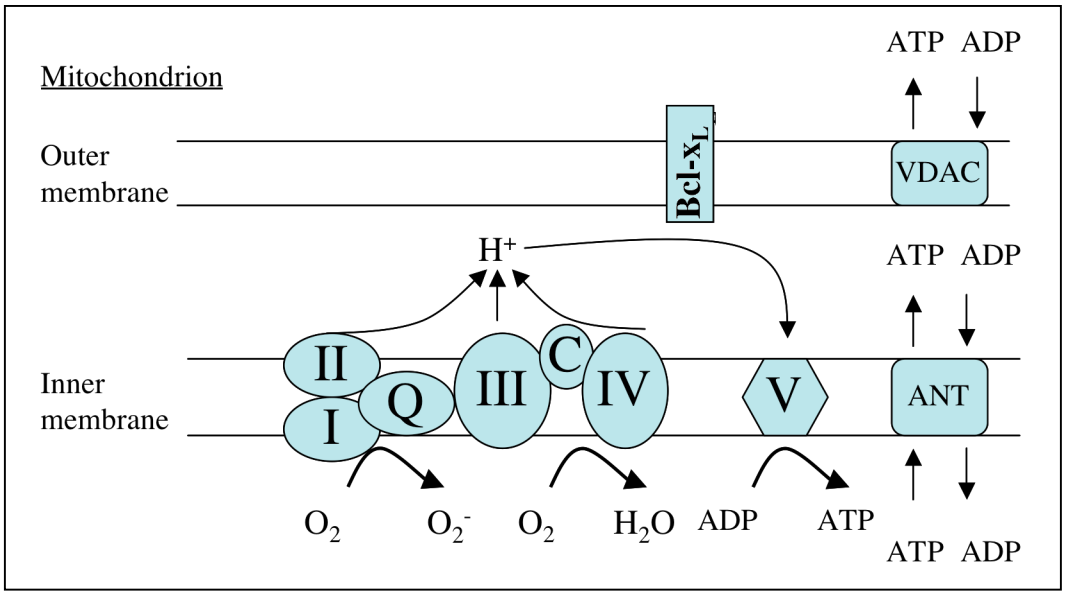

Figure 37: Diagram of the electron transport chain and other major components of mitochondrial membranes. Under normal conditions the H^+ electrochemical gradient is generated by the electron transport chain, across the inner mitochondrial membrane. This gradient provides the energy for ATP synthesis by complex V (ATP synthase) and is the basis of the mitochondrial membrane potential ($\Delta\Psi_m$). ANT exchanges ATP for cytosolic ADP. Single electrons leak from the electron transport chain, especially at the level of CoQ, and can reduce O_2 to superoxide radical, $O_2.^-$ ADP: adenosine diphosphate; ATP: adenosine triphosphate; Q: coenzyme Q (CoQ, ubiquinone); I: complex I (NADH-CoQ reductase); II: complex II (succinate-CoQ reductase); III: complex III (CoQ-cytochrome *c* reductase); IV: complex IV (cytochrome *c* oxidase); V: complex V (F_0F_1-ATPase, ATP synthase); ANT: adenine nucleotide transporter.

in Bcl-2/Bcl-x_L cells is a result of delayed S phase entry.

Our data and others have suggested that Bcl-2/Bcl-x_L may regulate either mitochondrial membrane potential or mitochondrial number. To determine whether Bcl-2/Bcl-x_L mediates its cell cycle function by regulating mitochondrial membrane potential, we tested the ability of Bcl-2/Bcl-x_L to delay cell cycle entry in cells lacking normal mitochondrial membrane potential. Although Bcl-2/Bcl-x_L has been found to prevent the initial disintegration of mitochondrial membrane potential during cell death (Gottlieb et al., 2000), our data showed that Bcl-2/Bcl-x_L can still delay cell cycle entry in the absence of normal mitochondrial membrane potential. However, Bcl-x_L cannot enhance G_0 arrest in 143Bρ0 cells, suggesting that Bcl-x_L regulates cell cycle arrest by mechanisms requiring an intact electron transport chain.

CHAPTER VI

CONCLUDING REMARKS AND FUTURE DIRECTIONS

Concluding Remarks

Experiments presented in this dissertation show that cell death and cell cycle functions of Bcl-2/Bcl-x_L are regulated by independent but possibly overlapping mechanisms. Cell death and cell cycle functions could not be genetically separated and do not depend on subcellular localization of Bcl-2/Bcl-x_L. We showed that overexpression of Bcl-2/Bcl-x_L does not affect the activation of Myc and Cyclin D, but causes an inhibition in the activities of Cyclin E/cdk2 and Cyclin D/cdk4 (work of C. Greider). Analysis of cell size and RNA content during cell cycle arrest and entry revealed that Bcl-2/Bcl-x_L caused an enhanced G_0 arrest and that the delay in cell cycle entry occurred in G_0. When arrested control cells are sorted by size, the small population enters cell cycle slower than the large population. The sorting experiment suggested that Bcl-2/Bcl-x_L entered cell cycle slower than control cells because they were in a more enhanced state of arrest. The use of the pro-apoptotic protein Bad antagonized the cell death and the cell cycle functions of Bcl-x_L, suggesting that the two functions are due to one integral mechanism.

Bcl-2 was more efficient at delaying Myc-induced than serum-induced cell cycle entry, suggesting that Bcl-2 may act on the Myc pathway. We found that Bcl-2 was not able to delay cell cycle entry in Myc knockout cells. Through promoter-reporter assays, we determined that Bcl-2/Bcl-x_L did not interfere with Myc's ability to transcriptionally

regulate its target genes. Although we did not find how or if Bcl-2/Bcl-x_L affects the Myc pathway, we speculate that Bcl-2/Bcl-x_L may act on the cell growth function of Myc (see Future Directions).

To test whether the cell cycle phenotype was an effect of the cell death function of Bcl-2/Bcl-x_L, we inhibited cell death by the caspase inhibitor zVAD or caspase 9 DN. We found that caspase inhibition partially mimics the cell cycle delay but not the cell cycle arrest phenotype. Inhibition of cell death by the survival kinase Akt did not result in cell cycle delay or enhanced cell cycle arrest. These data suggest that inhibition of cell death may not be the only mechanism by which Bcl-2/Bcl-x_L enhance G_0 arrest. However, it is possible that cell cycle entry delay and enhanced G_0 arrest are the results of two separate mechanisms. Bcl-2/Bcl-x_L may cause cell cycle delay by inhibition of basal caspase activity, while enhanced G_0 arrest is the result of a different mechanism of action.

To find that mechanism, we monitored ATP content of Bcl-x_L cells during arrest and cell cycle entry. We found that Bcl-x_L expression results in a delay in peak ATP during cell cycle entry. However, this delay does not appear to be responsible for the Bcl-2/Bcl-x_L cell cycle phenotype because exogenous elevation of ATP in Bcl-x_L cells does not reverse the cell cycle affect of Bcl-2/Bcl-x_L.

Our data and others have suggested that Bcl-2/Bcl-x_L may regulate either mitochondrial membrane potential or mitochondrial number. By staining mitochondrial mass and potential, we found that Bcl-x_L cells arrest with lower mitochondrial mass and potential than control cells, providing evidence for the hypothesis that Bcl-x_L regulates cell cycle arrest through control of mitochondrial bioenergetics or proliferation. In cells

lacking normal mitochondrial membrane potential, Bcl-x_L can inhibit growth factor withdrawal-induced cell death, delay cell cycle re-entry; however, Bcl-x_L cannot enhance G_0 arrest; indicating that normal mitochondrial membrane potential or an intact electron transport chain are necessary for the cell cycle arrest by Bcl-2/Bcl-x_L.

Together, these data suggest that Bcl-2/Bcl-x_L have two distinct phenotypes in the cell cycle, first, enhancement of G_0 and second, delay of cell cycle re-entry. The cell death and cell cycle functions are not genetically separable, suggesting that both are due to integral Bcl-2/Bcl-x_L actions at the mitochondria. It is possible that Bcl-2/Bcl-x_L delays cell cycle entry by inhibiting basal caspase activity or that delayed cell cycle entry is a consequence of suppressed caspase activity by Bcl-2/Bcl-x_L. However, it is still possible that another mechanism of action contributes to cell cycle entry delay, since only partial cell cycle delay was observed with caspase inhibition. This contributing mechanism could be enhanced G_0 arrest or Bcl-2/Bcl-x_L may affect cell growth. Enhanced G_0 arrest by Bcl-2/Bcl-x_L is executed through novel mechanisms involving an intact electron transport system and independent of caspase inhibition (Figure 38). Enhanced G_0 arrest by Bcl-2/Bcl-x_L could be accomplished through the regulation of mitochondrial bioenergetics, reactive oxygen species, or retrograde signaling (see Models of Bcl-2/Bcl-x_L Function), all of which depend on or are affected by the electron transport chain.

Future Directions

The experiments presented here contribute to a better understanding of the relationships between cell growth, cell metabolism, and cell death. If we find that Bcl-

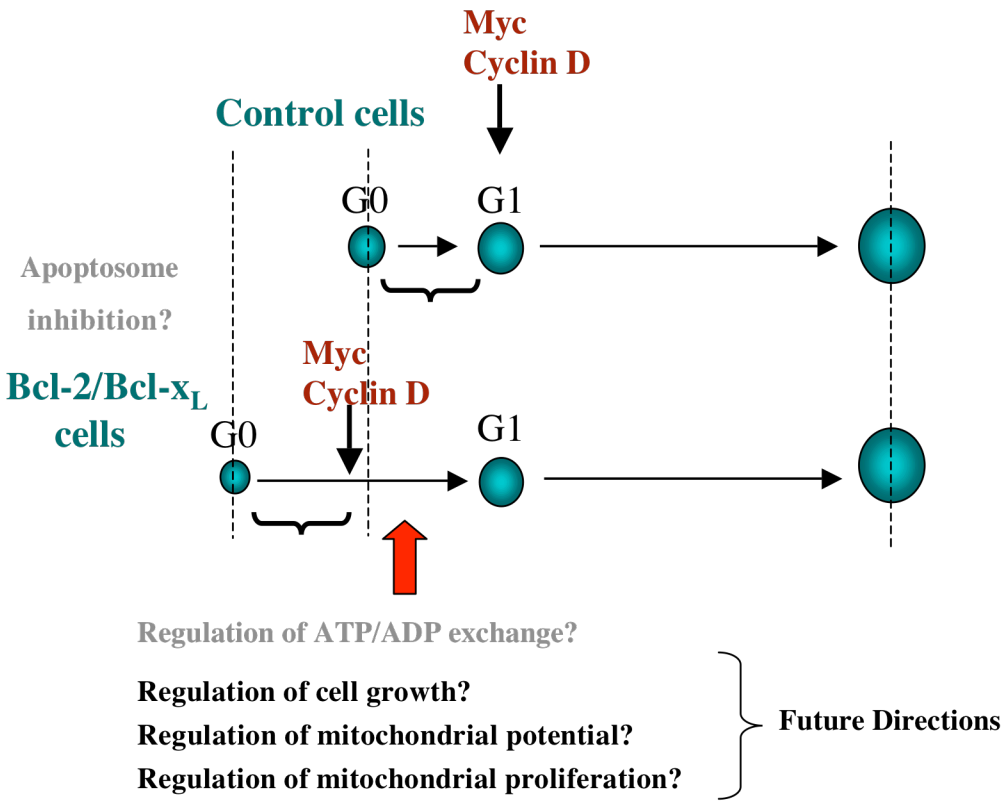

Figure 38: Bcl-2/Bcl-x_L regulates cell cycle arrest by mechanisms in addition to cell death inhibition. Apoptosis inhibition is sufficient to partially recapitulate the cell cycle delay phenotype, but not the cell cycle arrest phenotype of Bcl-2/Bcl-x_L. Our data excludes ATP/ADP exchange as a possible mechanism of cell cycle arrest regulation. More studies are needed to determine whether Bcl-2/Bcl-x_L controls cell cycle arrest through the regulation of mitochondrial bioenergetics, mitochondrial biogenesis, or cell growth.

2/Bcl-x_L regulates cell growth, it will be necessary to determine the mechanism of this regulation in detail. We may also be able to apply our new understanding of cell growth control to animal models of various cancers. We know that cell division is dependent on attainment of a critical mass or growth rate to assure the survival of daughter cells. Repressing cell growth may result in inhibition of cell division. However, cancer cells lose growth control and the ability to respond to their environment, suggesting that their growth control mechanisms are abnormal. Restoration of normal growth control to transformed cells will require a better understanding of this field.

The effect of Bcl-2/Bcl-x_L on cell growth pathway regulators

Our data indicated that in Bcl-2/Bcl-x_L cells, early cell cycle entry signals are activated but increases in cell size and RNA content are delayed, suggesting that Bcl-2/Bcl-x_L may work through a cell growth pathway. TSC1/TSC2 (tuberous sclerosis complex) tumor suppressors act downstream of Akt and upstream of mTOR (target of rapamycin). TSC1/TSC2 represses mTOR activity by inhibiting Rheb (Ras homologue enriched in brain) activity and is phosphorylated and inactivated by Akt. Knocking out TSC1 or TSC2, overexpressing Rheb, or overexpressing myristoylated Akt results in activation of the mTOR growth pathway.

We have shown that Bcl-2/Bcl-x_L expressing cells were delayed in reaching the restriction point in G_1 due to a lag in accumulation of RNA and cell size, consistent with prolonged G_0. We also found that the induction of early G_1 molecules Myc and cyclin D1 are not affected by Bcl-2/Bcl-x_L, indicating that the initiation of early cell cycle events is normal in Bcl-2/Bcl-x_L cells. Our data suggest that progression through G_1 in Bcl-2/Bcl-

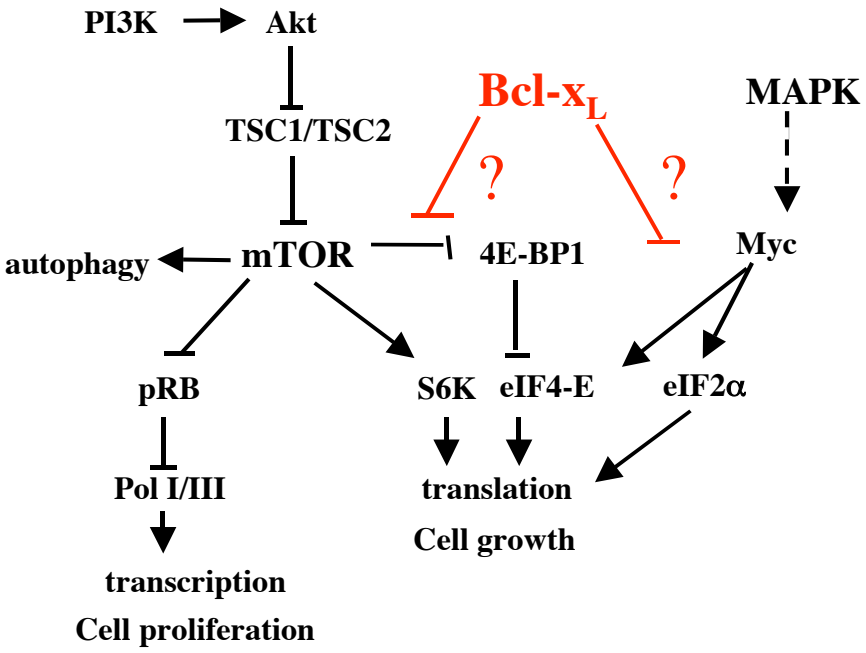

Figure 39: Bcl-x_L may control cells growth by affecting the pathways that regulate cell growth, such as the mTOR or the c-Myc pathways. Upon stimulation with growth factors or nutrients Akt is activated by translocation to the plasma membrane and phosphorylation. Akt phosphorylates the tuberous sclerosis complex, allowing activation of mTOR, which in turn activates protein translation resulting in cell growth. Bcl-2/Bcl-x_L may inhibit cell growth by acting on the mTOR pathway.

x_L cells may be delayed due to retardation of metabolic processes, such as cell growth. We hypothesize that Bcl-2/Bcl-x_L delays the G_0-G_1 transition through the regulation of cell growth.

Protein synthesis during the cell cycle is a highly regulated cellular process (Dennis, 1999). mTOR (mammalian target of rapamycin) is a central player in the pathway that regulates transcription/translation and autophagy in response to the cellular environment (Figure 38). mTOR positively regulates translation by phosphorylating 4E-BP1. When hypophosphorylated, 4E-BP1 (eIF4-E binding protein) binds eIF4-E, preventing the formation of the translation initiation complex. mTOR also phosphorylates S6K (40S ribosomal S6 kinase). S6K increases the translation of mRNAs that encode ribosomal proteins and other elements of the translation machinery. mTOR may also regulate the transcription of rRNA and tRNA, because the functions of pol I and pol III, which transcribe large rRNA genes and 5S rRNA/tRNA genes, are inhibitable by rapamycin (Dennis, 1999). TSC1/TSC2 represses mTOR activity, and TSC1/TSC2 is phosphorylated and inactivated by Akt (Marygold et al., 2002). TSC1/TSC2 complex negatively regulates cell growth and cells size (Inoki et al., 2003) through inhibition of mTOR function. Cells lacking TSC2 increase in cell size following glucose deprivation (Inoki et al., 2003), indicating that TSC2 mediates the energy limitation signal to regulate cell size. TSC2 also protects cells from glucose deprivation induced-apoptosis. In the absence of TSC2, cells undergo massive apoptosis in glucose-free conditions, while expression of TSC2 rescues cells from cell death by glucose starvation (Inoki et al., 2003). Overexpression of either TSC1 or TSC2 leads to growth arrest and increased levels of p27 (Soucek et al., 2001; Benvenuto et al., 2000; Miloloza et al., 2000).

NIH3T3 control and Bcl-2/Bcl-x_L expressing cells will be synchronized in G_0 and released into cell cycle by serum stimulation. Western blots will be performed during the time course of cell cycle entry to compare the induction of regulators of cell growth (4EBP1, S6K, NRF, PRC and CREB total protein and phospho-specific antibodies at Calbiochem and Santa Cruz). CREB is phosphorylated at approximately 1 hour (Herzig, 2000), and PRC expression is upregulated at about 3 hours following serum stimulation of BALB/3T3 cells (Andersson et al., 2001). Northern blots will be performed on those regulators of rRNA synthesis (S6K, 4EBP1) and mitochondrial biogenesis (NRF, PRC, and CREB) that showed a difference in protein levels between Bcl-2 and control cells. If we find that Bcl-2 affects these regulators of rRNA synthesis and mitochondrial biogenesis, we will verify the specificity of Bcl-2's action by comparing the activation of 4EBP1, S6K, NRF, PRC and CREB in bcl-$2^{-/-}$ cells. If Bcl-2 has no effect on ribosomal or mitochondrial biogenesis, then there should be no difference in the activation of these regulators between wild type and bcl-$2^{-/-}$ cells.

NIH3T3 control and Bcl-2/Bcl-x_L expressing cells will be infected with a retroviral vector expressing myristoylated Akt (gift from D. Plas) or empty vector. Myristoylated Akt is targeted to the plasma membrane and is constitutively active. Active Akt will phosphorylate the TSC1/TSC2 complex causing derepression of mTOR, allowing us to assay the cell cycle function of Bcl-2/Bcl-x_L in the presence of active mTOR pathway. The cells will be synchronized in G_0 and released into cell cycle by serum stimulation. Cells will be analyzed for cell cycle entry, cell size, RNA and protein content. This experiment will show whether Bcl-2/Bcl-x_L can mediate cell cycle delay in conditions of enhanced growth. Some of these experiments have been done in FL5.12

cells (see chapter IV). We show that arresting FL5.12 cells that express both mAkt and Bcl-x_L in low IL-3 results in a mixed population that contains cycling cells, S phase arrested cells, and G_0/G_1 arrested cells; while Fl5.12 cells expressing only Bcl-x_L arrest in G_0. However, the mAkt/Bcl-x_L cells that are G_0/G_1 arrested are similar to Bcl-x_L cells in size and RNA content. These data suggest that Bcl-x_L is not as efficient at arresting cells in G_0 in conditions of enhanced growth.

A similar but more direct approach to testing the affect of Bcl-x_L on cell growth in the presence of active mTOR would be to use $TSC1^{-/-}$ cells. Bcl-2/Bcl-x_L or vector control will be introduced into $TSC1^{-/-}$ cells. Cells will be synchronized in G_0 and released into cell cycle by serum stimulation. Cells will be collected during arrest and following stimulation, and analyzed for cell cycle entry, cell size, RNA and protein content. Preliminary data showed that overexpression of Bcl-x_L in $TSC1^{-/-}$ cells resulted in no cell cycle delay as compared to $TSC1^{-/-}$ cells expressing vector control, suggesting that Bcl-2/Bcl-x_L may delay cell cycle by inhibiting the TSC/mTOR pathway. Arrest of the $Tsc1^{-/-}$ cells in the presence and absence Bcl-2/Bcl-x_L overexpression needs to be assessed to determine whether Bcl-2/Bcl-x_L enhances G_0 arrest by shutting off the mTOR pathway. If Bcl-x_L inhibits cell cycle progression by blocking the mTOR pathway, then Bcl-x_L should not have an effect in cells with constitutively activated mTOR pathway. If Bcl-x_L inhibits cell cycle progression through a pathway other than mTOR, particularly if that pathway is downstream of mTOR pathway, Bcl-x_L overexpression will be able to delay cell cycle entry in cells with activated mTOR pathway. The proposed experiments will allow us to elucidate whether Bcl-x_L acts on mTOR-mediated growth pathway or whether Bcl-x_L affects mitochondrial biogenesis. The proposed experiments will be done

on a cell culture model. Results will be verified in primary T cells and hepatocytes in the presence or absence of a Bcl-2 transgene by assaying the activation of molecules such as TSC1/TSC2.

The effect of Bcl-2/Bcl-x_L on Myc's cell growth function

Our previous data showed that in the absence of Myc, Bcl-2/Bcl-x_L was unable to delay cell cycle entry. Myc is an oncogene that induces both apoptosis and proliferation (Leone, 2001). Myc controls cell growth independently of cell proliferation (Schmidt, 1999). Cell growth refers to the accumulation of mass by a cell, which is reflected in cell size and the amount of protein accumulated. Generally, overexpression of Myc leads to increased cell size, while loss of Myc results in reduced cell size (Johnston, et al., 1999; Piedra, et al., 2002; Iritani, et al., 1999). Myc exerts its growth-enhancing function through the regulation of the mRNA cap-binding protein eIF4E, a key regulator in the initiation of translation (Figure 37) (Stocker, 2000). Myc has also been shown to directly activate RNA pol III, which is responsible for transcribing rRNAs (Gomez-Roman, et al., 2003). In addition to direct transcriptional targets, Myc may also regulate cell growth through protein-protein interactions. Myc was shown to bind pRB *in vitro* and alter transcription of target genes such as pol I (Schmidt, 1999). Our data from cell size and RNA assessments indicated that Bcl-2/Bcl-x_L may delay cell cycle entry through the regulation of cell growth. Bcl-2/Bcl-x_L inhibits Myc-dependent apoptosis and is able to delay Myc-induced cell cycle entry (Greider, et al., 2002). We also showed that in *myc*$^{-/-}$ cells, Bcl-2/Bcl-x_L is not able to inhibit cell cycle entry. Our data in myc$^{-/-}$ cells show that Bcl-x_L cell cycle delay is diminished in cells with reduced Myc expression. We

hypothesize that Bcl-2/Bcl-x_L delays the G_0-G_1 transition through the regulation of Myc's control of cell growth. To determine whether Bcl-2 has an effect on Myc-induced cell growth, we will assess cell size and protein content of Rat1MycER/pBabe and Rat1MycER/Bcl-2 cells. In this system, following serum starvation, cell cycle entry is induced by the addition of 4-(OHT) in the absence of serum. Thus, the Myc pathway is the only one activated. We will compare Rat1MycER/pBabe and Rat1MycER/Bcl-2 cells cultured in 10%FBS, arrested for 3 days in 0.1%FBS, and induced to enter S phase by addition of 4-OHT. Cells will be harvested at 2, 4, 6, 8, and 10 hours following Myc-induced cell cycle entry. Vector control cells begin to enter S phase at about 8 hours following Myc-induction, while Bcl-2 overexpressing Rat1 cells begin to enter S phase at about 14 hours. The cells will be stained with 15 ug/ml PI (propidium iodide) and 0.1ug/ml FITC and 50 ug/ml RNase A. The cells will be analyzed by flow cytometry on a FACSCalibur (BD) with a 488nm excitation laser. Forward scatter (cell size), PY fluorescence (RNA content) and FITC fluorescence (total protein) will be compared between cell populations in the same phases of the cell cycle by gating on the PI cell cycle profile. We will also measure protein synthesis by quantification of total TCA-precipitable material. Cells will be either continuously labeled for total protein synthesis or labeled for 1 hour prior to harvest for rate of protein synthesis at a given time. Cells will be released from arrest in medium containing 1uM 4-OHT and radiolabeled amino acids (200 uCi/ml of Trans^{35}S-label).

The translation initiation factors eIF4E and eIF2α are Myc targets and are upregulated by Myc at the level of mRNA and protein (Schmidt, 1999). To determine whether Bcl-2/Bcl-x_L affects the induction of eIF4E and eIF2α by Myc, we will perform

Western and Northern blots of Rat1MycER pBabe and Bcl-2 cells. Rat1MycER pBabe and Bcl-2 cells will be serum starved (0.1% FBS) and cell cycle entry will be induced by addition of 4-OHT. Cells will be collected at 10%, 0, 1, 2, 4, and 8 hours following induction of Myc. Western blots will be performed with antibodies from Transduction Labs and Santa Cruz, and Northern blot probes are a gift from Dr. Hann. To confirm our results from the above-mentioned experiments, we will test the action of Bcl-2/Bcl-x_L on eIF4E and eIF2α in *myc* $^{-/-}$ cells. We expect that expression of Bcl-2/Bcl-x_L will delay the increase in cell size and protein accumulation in MycER cells after Myc induction. If we find that Bcl-2/Bcl-x_L expression affects the induction of eIF4-E and eIF2α by Myc, then this data will support the hypothesis that Bcl-2/Bcl-x_L inhibits the cell growth function of Myc. The advantage of using the MycER system is that it allows us to isolate the effects of Myc without activating other mitogenic pathways. This is important to sorting out the effects of Bcl-x_L/Bcl-2 on the cell growth function of Myc versus other mitogenic pathways.

Models of Bcl-2/Bcl-x_L Function

The effects of Bcl-2/Bcl-x_L on autophagy

Autophagy is the major regulated pathway responsible for degrading cellular organelles to generate free amino acids and nucleotides to sustain macromolecular synthesis and cellular ATP. Environmental stressors such as nutrient starvation or pathogen infection can induce autophagy. Autophagy starts with the isolation of double-membrane bound vesicles inside a cell. As these autophagosomes mature, microtubule-

associated protein 1 light chain 3 (LC3) is recruited to their membranes. Autophagosomes sequester proteins and organelles and fuse with lysosomes. The PI(3)K/Akt/mTOR pathway is a major regulator of autophagy. mTOR inhibits autophagy in the presence of nutrients. mTOR causes hyperphosphorylation of Atg13, resulting in its lower affinity for Atg1 (reviewed in Klionsky, 2005). However, in Drosophila, S6K, a downstream target of mTOR, has been shown to promote autophagy under starvation conditions (Scott, et al., 2004). mTOR is a central player in the pathway that regulates transcription/translation and autophagy in response to the cellular environment. mTOR is activated through the class I PI(3)K pathway, which phosphorylates phosphotidyl inositol lipids, allowing for the recruitment and activation of Akt at the plasma membrane. PTEN antagonizes the action of Akt, thus promoting autophagy. The TSC1/TCS2 complex acts as a GTPase activating protein (GAP) for Rheb, and the GTP-bound form of Rheb stimulates mTOR activity.

Based on the data that Bcl-2/Bcl-x_L results in smaller cells, containing less RNA during nutrient deprivation or contact inhibition, it is plausible to hypothesize that Bcl-2/Bcl-x_L may be regulating autophagy to keep cells viable longer. In fact, it has been shown through yeast two-hybrid and confirmed by FRET analysis that the autophagy protein Beclin 1 interacts with Bcl-2 (Liang, et al., 1998). Taken together with our data, it is conceivable that during nutrient limited conditions, the expression of Bcl-2/Bcl-x_L prevents apoptotic cell death and promotes autophagy by binding Beclin 1 (Figure 40). This would result in Bcl-2/Bcl-x_L cells getting progressively smaller in size during nutrient starvation, which is exactly what our data showed. However, the same group recently showed that yeast as well as mammalian cells exhibit reduced autophagy in

starvation conditions when Beclin1 is co-transfected with Bcl-2 or viral Bcl-2 (Pattingre, et al., 2005). The reduction in autophagy is abolished if mutant Bcl-2, which cannot bind Beclin 1, is used or if mitochondria-targeted Bcl-2, is used (Pattingre, et al., 2005). The authors hypothesize that nutrient conditions regulate the Bcl-2 and Beclin1 interaction at the endoplasmic reticulum, and suggest that Bcl-2 may be phosphorylated by the nutrient sensor mTOR during basal conditions to bind Beclin 1 and suppress autophagy.

The effects of Bcl-2/Bcl-x_L on mitochondrial fusion/fission

Mitochondria take different shapes depending on cell type and the state of the cell. Mitochondria can undergo fusion to form a network of connected mitochondria or can be divided by fission. The purpose of mitochondrial fusion may be even distribution of energy throughout the cell or to exchange mtDNA. Drp1 (dynamin-related protein 1), a GTPase, regulates mitochondrial fission in mammalian cells. A mutation in the GTP-binding site of Drp1 (Drp1 K38A) results in a dominant-negative mutant and causes interconnected, fused mitochondria (Smirnova, et al., 2001). Mitofusins 1 and 2 (Mfn1 and Mfn2) regulate mitochondrial fusion in mammalian cells. Knock out of Mfn1 or Mfn2 results in cells with highly fragmented mitochondria, indicating suppression of mitochondrial fusion (Chen, et al., 2003). The pro-apoptotic protein Bax has been shown to co-localize with Mfn2 and Drp1 at the scission site of mitochondria in apoptotic cells, suggesting that Bax participates in mitochondrial fission (Karbowsky, et al., 2002). Activation of Bax leads to excessive mitochondrial fission, which can be rescued by the overexpression of Bcl-2 (Karbowsky, et al., 2002).

It is possible that Bcl-2/Bcl-x_L plays a role in mitochondrial fusion or fission also,

since it antagonizes the cell death function of Bax. Bcl-2/Bcl-x_L may also counter the mitochondrial fission function of Bax. Interestingly, it was found that cells lacking Mfn1 or Mfn2 had a greater number of mitochondria with lower mitochondrial membrane potential as measured by MitoTracker Red (Chen, et al., 2003). Data presented in this dissertation also showed that overexpression of Bcl-x_L in FL5.12 cells causes lower MMP than in control cells during cell cycle arrest. In this model, Bcl-2 may associate with the mitochondria fusion or fission machinery to prevent fission that occurs during cell death (Figure 40). Bcl-2 may also regulate the bioenergetic state of the cells through the control of mitochondrial fusion or fission.

Retrograde signaling

Retrograde signaling refers to the communication from mitochondria to the nucleus that influences many cellular activities. These adaptive signaling pathways result in changes in nuclear gene expression. Most of our knowledge about retrograde signaling pathways comes from studies in budding yeast. The comparison of respiratory-competent (ρ+) to yeast lacking mtDNA (ρ0), showed that the ρ0 cells upregulated genes involved in mitochondrial biogenesis and function (Traven et al., 2001). In *Saccharomyces cerevisiae*, substrates of the tricarboxylic acid (TCA) cycle signal from the mitochondria to the nucleus to adjust metabolic activities in response to changes in the mitochondria potential (Liu et al., 1999). In mammalian cells, loss of mitochondrial DNA altered nuclear gene expression (Marusich et al., 1997; Wang and Morais, 1997). Induction of altered mitochondrial membrane potential in C2C12 skeletal myoblasts or human lung carcinoma A549 cells resulted in elevation of cytosolic free calcium,

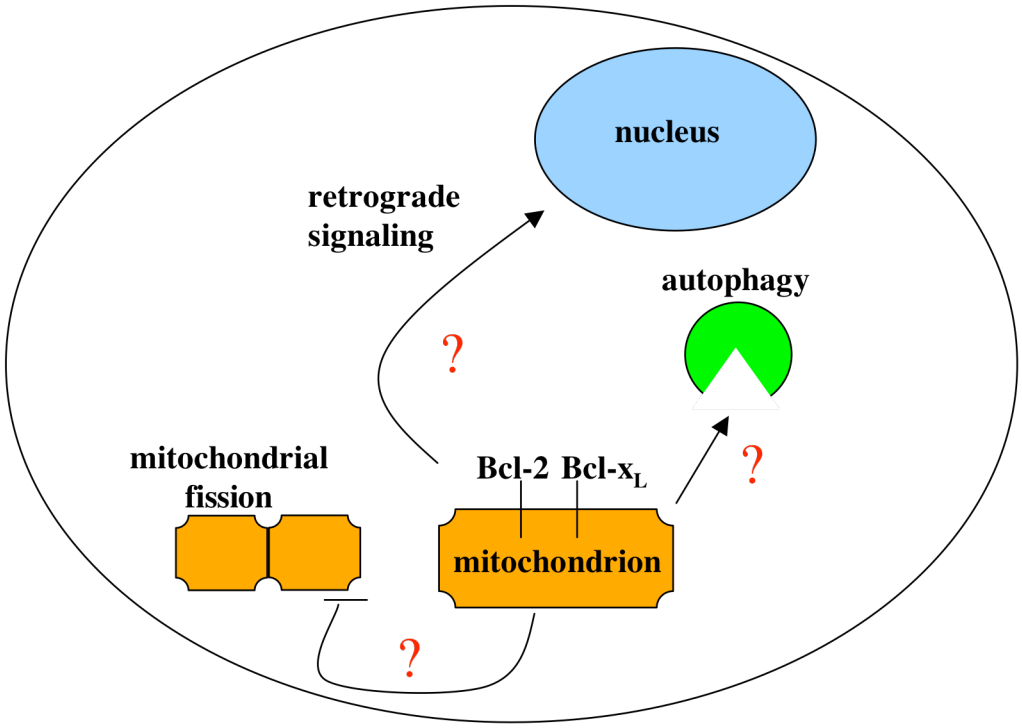

Figure 40: Possible modes of action for Bcl-2/Bcl-x_L in cell cycle arrest. Bcl-2/Bcl-x_L could promote autophagy in nutrient limiting conditions resulting in smaller cells. Bcl-2/Bcl-x_L could affect the state of cell cycle arrest by regulating mitochondrial fusion/fission. Retrograde signaling may be altered by Bcl-2/Bcl-x_L to result in changes in gene expression leading to an enhanced G_0 arrest.

activation of calcineurin, and upregulation of a number of genes involved in calcium storage and transport (Biswas et al., 1999; Amuthan et al., 2001).

Based on the data presented in this dissertation, the final model of Bcl-2/Bcl-x_L function in cell cycle arrest would involve signaling from mitochondria to the nucleus. During cell cycle arrest, Bcl-2/Bcl-x_L may affect the mitochondria in such a way as to result in signaling from the mitochondrial to the nucleus, causing enhanced G_0 arrest (Figure 40). We have shown that Bcl-x_L maintains mitochondrial membrane potential per mitochondrion higher than control cells in cell cycle arrest. This altered state of mitochondrial membrane potential and possibly function may signal the nucleus that nutrients are limited resulting in entry into quiescence. This could occur through the upregulation of p27 stability by repression of the ubiquitin degradation pathway.

Mitochondria are the major site of ROS generation due to electron transfer to oxygen in the respiratory chain. An excess of ROS in the mitochondria results in oxidative stress, which causes intramolecular crosslinking, and release of calcium from mitochondria. Evidence supports that Bcl-2 may act as an antioxidant to block a putative ROS-mediated step in the apoptotic pathway. Following glucose deprivation and H_2O_2 treatment, Bcl-2 prevents accumulation of ROS and the subsequent steps in the apoptosis pathway (Ouyang et al., 2002). It is possible that in control cells during conditions in which nutrients are limited mitochondria try to compensate for the lack of nutrients resulting in overproduction of ROS. The excess of ROS may damage mitochondria in control cells leading to cell death. Bcl-x_L may shuttle ROS to the cytosol where they may stimulate retrograde signaling, resulting in the maintenance of certain levels of ATP production and allow cells to activate the quiescence program.

Bcl-2 and Bcl-x_L are molecules with two functions: inhibition of apoptosis and inhibition of proliferation. Elucidation of the relationship between these functions as well as the mechanism of action will allow for better understanding of cell cycle as well as cancer pathogenesis. Separation of the anti-apoptotic and anti- proliferative functions of Bcl-2/Bcl-x_L will allow for the development of novel cancer treatments. The data presented in this thesis attempts to elucidate the relationship between the functions of Bcl-2/Bcl-x_L and contributes to a better understanding of the mechanisms of their action.

REFERENCES

Akao, Y., Otsuki, Y. S., Kataoka, S., Ito, Y., and Y. Tsujimoto. (1994) Multiple subcellular localization of Bcl-2: detection in nuclear outer membrane, endoplasmic reticulum, and mitochondrial membrane. *Cancer Research*, **54**: 2468-2471.

Alam, A., Cohen, L., Aouad, S., and R.-P. Sekaly. (1999) Early activation of caspases during T lymphocyte stimulation results in selective substrate cleavage in nonapoptotic cells. *Journal of Experimental Medicine*, **190**: 1879-89.

Amuthan, G., Biswas, G., Zhang, S.Y., Klein-Szanto, A., Vijayasarathy, C., and N.G. Avadhani. (2001) Mitochondria-to-nucleus stress signaling induces phenotypic changes, tumor progression and cell invasion. *EMBO Journal*, **20**: 1910-1920.

Andersson, U. and R.C. Scarpulla. (2001) PGC-1-Related coactivator, a novel, serum-inducible coactivator of nuclear respiratory factor 1-dependent transcription in mammalian cells. *Molecular and Cellular Biology*, **21**: 3738-3749

Arabi, A., Wu, S., Ridderstrale, K., Bierhoff, H., Shiue, C., Fatyol, K., Fahlen, S., Hydbring, P., Soderberg, O., Grummt, I., Larsson, L.G., and A.P. Wrigh. (2005) c-Myc associates with ribosomal DNA and activates RNA polymerase I transcription. *Nature Cell Biology*, **3**: 303-310.

Bakhshi, A., Jensen, J.P., Goldman, P., Wright, J.J., McBride, O.W., Epstein, A.L. and S.J. Korsmeyer. (1985) Cloning the chromosomal breakpoint of t(14;18) human lymphomas: Clustering around Jh on Chromosome 14 and near a transcriptional unit on 18. *Cell*, **41:** 899-906.

Bello-Fernandez, C., Packham, G., and J. Cleveland. (1993) The ornithine decarboxilase gene is a transcriptional target of c-Myc. *Proceedings of the National Academy of Science USA*, **90**: 7804-7808.

Benvenuto, G., Li, S., Brown, S., Braverman, R., Vass, W., Cheadle, J., Halley, D., Sampson, J., Wienecke, R., and J. DeClue. (2000) The tuberous sclerosis-1 (TSC1) gene product hamartin suppresses cell growth and augments the expression of TSC2 product tuberin by inhibiting its ubiquitination. *Oncogene*, **19**: 6306-6316.

Biswas, G., Adebanjo, O.A., Freedman, B.D., Anandatheerthavarada, H.K., Vijayasarathy, C., Zaidi, M., Kotlikoff, M., and N.G. Avadhani. (1999) Retrograde Ca2+ signaling in C2C12 skeletal myocytes in response to mitochondrial genetic and metabolic stress: a novel mode of inter-organelle crosstalk. *EMBO Journal*, **18**: 522-33.

Boise, L.H., Gonzalez-Garcia, M., Postema, C.E., Ding, L., Lindsten, T., Turka, L.A., Mao, X., Nunez, G. and C.B. Thompson. (1993) bcl-x, a bcl-2-related gene that functions as a dominant regulator of apoptotic cell death. *Cell*, **74**: 597-608.

Brady, H.J., Gil-Gomez, G., Kirberg, J., and A.J. Berns. (1996) Bax alpha perturbs T cell development and affects cell cycle entry of T cells. *EMBO Journal*, **15**: 6991-7001.

Chattopadhyay, A., Chiang C.W., and E. Yang. (2001) Bad/Bcl-x_L heterodimerization leads to bypass of G_0/G_1 arrest. *Oncogene*, **20**: 4507-4518.

Chen, H., Detmer, S.A., Ewald, A.J., Griffin, E.E., Fraser, S.E., and D.C. Chan. (2003) Mitofusins Mfn1 and Mfn2 coordinately regulate mitochondrial fusion and are essential for embryonic development. *Journal of Cell Biology*, **160:** 189-200.

Cheng, N., Janumyan, Y.M., Didion, L., Van Hofwegen, C., Yang, E., and C.M. Knudson. (2004) Bcl-2 inhibition of T-cell proliferation is related to prolonged T-cell survival. *Oncogene*, **21**: 3770-3780.

Chen-Levy, Z., Nourse, J. and M. Cleary. (1989) The bcl-2 candidate proto-oncogene product is a 24 kilodalton integral-membrane protein highly expressed in lymphoid cell lines and lymphomas carrying the t(14;18) translocation. *Molecular and Cellular Biology*, **9**: 701-710.

Chittenden, T., Flemington, C., Houghton, A.B., Ebb, R.G., Gallo, G.J., Elangovan, B., Chinnadurai, G. and Lutz, R.J. (1995) A conserved domain in Bak, distinct from BH1 and BH2, mediates cell death and protein binding functions. *Embo Journal*, **14:** 5589-5596.

Chun, H., L. Zheng, M. Ahmad, J. Wang, C. Speirs, R. Seigel, J. Dale, J. Puck, J. Davis, C. Hall, S. Skoda-Smith, T.P. Atkinson, S. Straus, and M. Lenardo. (2002) Pleiotropic defects in lymphocyte activation caused by caspase-8 mutations lead to human immunodeficiency. *Nature*, **419**: 395-9.

Darzynkiewicz, Z. (1994) Simultaneous analysis of cellular RNA and DNA content. *Methods Cell Biology*, **41**: 401-420.

de Alboran, I.M., O'Hagan, R.C., Gartner, F., Malynn, B., Davidson, L., Rickert, R., Rajewsky, K., DePinho, R.A. and F.W. Alt. (2001) Analysis of C-MYC function in normal cells via conditional gene-targeted mutation. *Immunity*, **14:** 45-55.

De La Coste, A., Mignon, A., Fabre, M., Gilbert, E., Porteu, A., Van Dyke, T., Kahn, A., and C. Perret. (1999) *Cancer Research*, **59**: 5017-5022.

del Peso, L., Gonzalez-Garcia, M., Page, C., Herrera, R., and G. Nunez. (1997) Interleukin-3-induced phosphorylation of BAD through the protein kinase Akt.

Science, **278**: 687-689.

Fabre, S., Lang, V., Harriague, J., Jobart, A., Unterman, T.G., Trautmann, A., and G. Bismuth. (2005) Stable activation of phosphatidylinositol 3-kinase in the T cell immunological synapse stimulates Akt signaling to FoxO1 nuclear exclusion and cell growth control. *Journal of Immunology*, **7**: 4161-4171.

Fero, M.L., Rivkin, M., Tasch, M., Porter, P., Carow, C.E., Firpo, E., Polyak, K., Tsai, L. H., Broudy, V., Perlmutter, R.M., Kaushansky, K., and J.M. Roberts. (1996) A syndrome of multiorgan hyperplasia with features of gigantism, tumorigenesis, and female sterility in p27-deficient mice. *Cell*, **85:** 733–744.

Ferri, K.F., and G. Kroemer. (2001) Organelle-specific initiation of cell death pathways. *Nature Cell Biology*, **3**: E255-E263.

Gibson, L., Holmgreen, S.P., Huang, D.C., Bernard, O., Copeland, N.G., Jenkins, N.A., Sutherland, G.R., Baker, E., Adams, J.M. and S. Cory. (1996) bcl-w, a novel member of the bcl-2 family, promotes cell survival. *Oncogene*, **13**: 665-675.

Grandori, C., Gomez-Roman, N., Felton-Edkins, Z.A., Ngouenet, C., Galloway, D.A., Eisenman, R.N., and R.J. White. (2005) c-Myc binds to human ribosomal DNA and stimulates transcription of rRNA genes by RNA polymerase I. *Nature Cell Biology*, **3**: 311-318.

Gomez-Roman, N., Grandori, C., Eisenman, R., and R. White. (2003) Direct activation of RNA polymerase III transcription by c-Myc. *Nature*, **421**: 290-294.

Gottlieb, E., Vander Heiden, M.G., and C. B. Thompson. (2000) Bcl-x_L prevents the initial decrease in mitochondrial membrane potential and subsequent reactive oxygen species production during tumor necrosis factor alpha-induced apoptosis. *Mol Cell Biol*, **20**: 5680-5689.

Greider, C., Chattopadhyay, A., Parkhurst, C. and E. Yang. (2002) Bcl-xL and Bcl-2 delay Myc-induced cell cycle entry through elevation of p27 and inhibition of G1 cyclin-dependent kinases. *Oncogene*, **21**: 7765-7775.

Grewal, S.S., Li, L., Orian, A., Eisenman, R.N., and B.A. Edgar. (2005) Myc-dependent regulation of ribosomal RNA synthesis during Drosophila development. *Nature Cell Biology*, **3**: 295-302.

Gross, A., McDonell, J. M., and S. J. Korsmeyer. (1999) Bcl-2 family members and the mitochondria in apoptosis. *Genes & Development*, **13**: 1899-1911.

Grummt, I. (1999) Regulation of mammalian ribosomal gene transcription by RNA polymerase I. *Progress in nucleic acid research and molecular biology*, **62**: 109-

54.

Grummt, I. (2003) Life on a planet of its own: regulation of RNA polymerase I transcription in the nucleolus. *Genes and Development*, **14**: 1691-1702.

Han, J., Sabbatini, P. and E. White. (1996) Induction of apoptosis by human Nbk/Bik, a BH3-containing protein that interacts with E1B 19K. *Molecular and Cellular Biology*, **16:** 5857-5864.

Harbour, J. (2000) The Rb/E2F pathway: expanding roles and emerging paradigms. *Genes and Development*, **14**: 2393-2409.

Harris, M.H. and C. B. Thompson. (2000) The role of the Bcl-2 family in the regulation of outer mitochondrial membrane permeability. *Cell Death and Differentiation*, **7**: 1182-1191.

Hatakeyama, M., Brill, J., Fink, G., and R. Weinberg. (1994) Collaboration of G1 cyclins in the functional inactivation of the retinoblastoma protein. *Genes and Development*, **8**: 1759-1771.

Herzig, R. Scacco, S., and R. Scarpulla. (2000) Sequential serum-dependent activation of CREB and NRF-1 leads to enhanced mitochondrial respiration through the induction of cytochrome c. *The Journal of Biological Chemistry*, **275**: 13134-13141.

Ho, A., and S.F. Dowdy. (2002) Regulation of G(1) cell-cycle progression by oncogenes and tumor suppressor genes. *Current Opinion in Genetics and Development*, **12**: 47-52.

Hockenberry, D.M., Oltvai, Z.N., Yin, X.M., Milliman, C.M. and S.J. Korsemeyer. (1993) Bcl-2 functions in an antioxidant pathway to prevent apoptosis. *Cell*, **75**: 241-51.

Hunter, J.J., and T.G. Parslow. (1996) A peptide sequence from Bax that converts Bcl-2 into an activator of apoptosis. *Journal of Biological Chemistry*, **271**: 8521.

Iritani, B.M. and R.N. Eisenman. (1999) c-Myc enhances protein synthesis and cell size during B lymphocyte development. *Proceedings of the National Academy of Sciences of the USA*, **96:** 13180-13185.

Jager, R., Herzer, U., Schenckel, J., and H. Weiher. (1997) Overexpression of Bcl-2 inhibits alveolar cell apoptosis during involution and accelerates c-myc-induced tumorigenesis of the mammary gland in transgenic mice. *Oncogene*, **15**: 1787-1795.

Janumyan, Y., Sansam, C., Chattopadhyay, A., Cheng, N., Soucie, E., Penn, L., Andrews,

D., Knudson C. M., and E. Yang. (2003) Bcl-x_L/Bcl-2 coordinately regulates apoptosis, cell cycle arrest and cell cycle entry. *EMBO Journal*, **22**: 5459-5470.

Johnstom, L.A., Prober, D.A., Edgar, B.A., Eisenman, R.N. and P. Gallant. (1999) Drosophila myc regulates cellular growth during development. *Cell*, **98**: 779-90.

Karbowski, M., Lee, J., Gaume, B., Jeong, S., Frank, S., Nechushtan, A., Santel, A., Fuller, M., Smith, C.L., and R.J. Youle. (2002) Spatial and temporal association of Bax with mitochondrial fussion sites, Drp1, and Mfn2 during apoptosis. *Journal of Cell Biology*, **159**: 931-938.

Kelekar, A., Chang, B.S., Harlan, J.E., Fesik, S.W., and C.B. Thompson. (1997) Bad is a BH3 domain-containing protein that forms an inactivating dimer with Bcl-x_L. *Molecular Cell Biology*, **17**: 7040-7046.

Kennedy, N., Kataoka, T., Tschopp, J., and R. Budd. (1999) Caspase activation is required for T cell proliferation. *Journal of Experimental Medicine*, **190**; 1891-1895.

Kiefer, M.C., Brauer, M.J., Powers, V.C., Wu, J.J., Umansky, S.R., Tomei, L.D. and P.J. Barr. (1995) Modulation of apoptosis by the widely distributed Bcl-2 homologue Bak. *Nature*, **374**: 736-739.

Klionsky, D.J. (2005) The molecular machinery of autophagy: unanswered questions. *Journal of Cell Science*, **118**(Pt 1): 7-18.

Kozopas, K.M., Yang, T., Buchan, H.L., Zhou, P. and R.W. Craig. (1993) MCL1, a gene expressed in programmed myeloid cell differentiation, has sequence similarity to BCL2. *Proceedings of the National Academy of Science U S A*, **90:** 3516-3520.

Kutay, V., Hartman, E., and T. Rapoport. (1993) A class of membrane proteins with a C-terminal anchor. *Trends in Cell Biology*, **3**: 72-75.

Kwiatkowski, D.J. (2003) Tuberous sclerosis: from tubers to mTOR. *Annals of Human Genetics*, **67**: 87-96.

Lee, A.M., Whyte, K.B., and C. Haslette. (1993) Inhibition of apoptosis and prolongation of neutrophil longevity by inflammatory mediators. *Journal of Leukocyte Biology*, **54**: 283-288.

Lee, S.T., Hoeflich, K.P., Wasfy, G.W., Woodget, J.R., Leber, B., Andrews, D.W., Hedley, D.W., and L. Z. Penn. (1999) Bcl-2 targeted to the endoplasmic reticulum can inhibit apoptosis induced by Myc but not etoposide in Rat-1 fibroblast. *Oncogene*, **18**: 3520-28.

Leone, G., Sears, R., Huang, E., Rempel, R., Nuckols, F., Park, C., Giagrande, P., Wu,

L., Saavedra, H., Field, S., Thompson, M., Yang, H., Fujiwara, Y., Greenberg, Orkin, S., Smith, C., and J. Nevins. (2001) Myc requires distinct E2F activities to induce S phase and apoptosis. *Molecular Cell*, **8**: 105-13.

Lin, E.Y., Orlofsky, A., Berger, M.S. and M.B. Prystowsky. (1993) Characterization of A1, a novel hemopoietic-specific early-response gene with sequence similarity to bcl-2. *Journal of Immunology*, **151**: 1979-1988.

Liang, X.H., Kleeman, L.K., Jiang, H.H., Gordon, G., Goldman, J.E., Berry, G., Herman, B., and B. Levine. (1998) Protection against fatal Sindbis virus encephalitis by beclin, a novel Bcl-2-interacting protein. *Journal of Virology*, **11**: 8586-8596.

Lind, E.F., Wayne, J., Wang, Q.Z., Staeva, T., Stolzer, A. and H.T. Petrie. (1999) Bcl-2-induced changes in E2F regulatory complexes reveal the potential for integrated cell cycle and cell death functions. *Journal of Immunology*, **162**: 5374-5379.

Linette, G.P., Y. Li, K. Roth, and S. J. Korsemeyer. (1996) Cross talk between cell death and cell cycle progression: Bcl-2 regulates NFAT-mediated activation. *Proceedings of the National Academy of Science of the USA*, **93**: 9545-9552.

Liu, A. and R.A. Butow. (1999) A transcriptional switch in the expression of yeast tricarboxylic acid cycle genes in response to reduction or loss of respiratory function. *Molecular and Cellular Biology,* **19**: 6720-6728.

Lundberg, A., and R. Weinberg. (1998) Functional inactivation of the retinoblastoma protein requires sequential modification by at least two distinct cyclin/cdk complexes. *Molecular Cell Biology*, **18**: 753-761.

Machida S., Spangenburg E.E., and F.W. Booth. (2003) Forkhead transcription factor FoxO1 transduces insulin-like growth factor's signal to p27Kip1 in primary skeletal muscle satellite cells. *Journal of Cell Physiology*, **3**: 523-531.

McDonnell, T.J., Deane, N., Platt, F.M., Nunez, G., Jaeger, U., McKearn, J.P. and S.J. Korsmeyer. (1989) bcl-2-Immunoglobulin transgenic mice demonstrate extended B cell survival and follicular lymphoproliferation. *Cell*, **57:** 79-88.

McDonnell, T.J., Nunez, G., Platt, F.M., Hockenberry, D., London, L., McKearn, J.P. and S.J. Korsmeyer. (1990) Deregulated Bcl-2-immunoglobulin transgene expands a resting but responsive immunoglobulin M and D-expressing B-cell population. *Molecular and Cellular Biology*, **10:**1901-1907.

McDonnell, T.J. and S.J. Korsmeyer. (1991) Progression from lymphoid hyperplasia to high grade malignant lymphoma in mice transgenic for the t(14;18). *Nature,* **349:** 254-256.

Majewski, N., Nogueira, V., Robey, R.B., and N. Hay. (2004a) Akt inhibits apoptosis

downstream of BID cleavage via a glucose-dependent mechanism involving mitochondrial hexokinases. *Molecular and Cellular Biology*. **2**: 730-740.

Majewski, N., Nogueira, V., Bhaskar, P., Coy, P.E., Skeen, J.E., Gottlob, K., Chandel, N.S., Thompson, C.B., Robey, R.B., Hay, N. (2004b) Hexokinase-mitochondria interaction mediated by Akt is required to inhibit apoptosis in the presence or absence of Bax and Bak. *Molecular Cell*, **16**: 819-30.

Malumbres, M., and M. Barbacid. (2001) To cycle or not to cycle: a critical decision in cancer. *Nature Rev Cancer*, **1**: 222-231.

Marin, C.M., Hsu, B., Stephens, L.C., Brisbay, S. and T.J. McDonnell. (1995) The functional basis of c-myc and bcl-2 complementation during multistep lymphomagenesis in Vivo. *Experimental Cell Research*, **217:** 240-247.

Ma, A., Pena, J.C., Chang, B., Margosian, E., Davidson, L., Alt, F.W. and C.B Thompson. (1995) Bclx regulates the survival of double-positive thymocytes. *Proceedings of the National Academy of Science U S A*, **92:** 4763-4767.

Margineantu, D.H., Cox, W.G., Sundell, S., Sherwood, S.W., Beechem, J.M., and R.A. Capaldi. (2002) Cell cycle dependent morphology changes and associated mitochondrial DNA redistribution in mitochondria of human cell lines. *Mitochondrion*, **1**: 425-435.

Marygold, S., and S. Leevers. (2002) Growth signaling: TSC takes its place. *Current Biology*, **12**: R785-R787.

Mazel, S., Burtrum, D., and H.T. Petrie. (1996) Regulation of cell division cycle progression by Bcl-2 expression: a potential mechanism for inhibition of programmed cell death. *Journal of Experimental Medicine*, **183**: 2219-2226.

Mignotte, B. and J.L. Vayssiere. (1998) Mitochondria and apoptosis. *European Journal of Biochemistry*, **252**: 1-15.

Miloloza, A., Rosner, M., Nellist, M., Halley, D., Bernaschek, G., and M. Hengstschlager. (2000) The TSC1 gene product, hamartin, negatively regulates cell proliferation. *Human Molecular Genetics*, **9**: 1721-1727.

Minn, A.J., Velez, P., Schendel, S.L., Liang, H., Muchmore, S.W., Fesik, S.W., Fill, M., and C. B. Thompson. (1997) Bcl-x_L forms an ion channel in synthetic lipid membranes. *Nature*, **385**: 353-357.

Minn, A.J., Kettlun, C.S., Liang, H., Kelekar, A., Vander Heiden, M.G., Chang, B.S., Fesik, S.W., Fill, M., and Thompson, C.B. (1999) Bcl-xL regulated apoptosis by heterodimerization-dependent and -independent mechanisms. *EMBO Journal,* **18:** 632-643.

Moreas, C.T. (2001) What regulates mitochondrial DNA copy number in animal cells? *Trends in Genetics*, **17**: 199-205.

Motoyama, N., Wang, F., Roth, K.A., Sawa, H., Nakayama, K., Negishi, I., Senju, S., Zhang, Q., Fujii, S. et al. (1995) Massive cell death of immature hematopoietic cells and neurons in Bcl-x- deficient mice. *Science*, **267:** 1506-1510.

Muchmore, S.W., Sattler, M., Liang, H., Meadows, R.P., Harlan, J.E., Yoon, H.S., Nettesheim, D., Chang, B.S., Thompson, C.B., Wong, S.B., Ng, S.L., and S. W. Fesik. (1996) X-ray and NMR structure of human Bcl-x_L, an inhibitor of programmed cell death. *Nature*, **381**: 335-341.

Nakayama, K., Negishi, I., Kuida, K., Shinkai, Y., Louie, M.C., Fields, L.E., Lucas, P.J., Stewart, V., and F.W. Alt. (1993) Disappearance of the lymphoid system in Bcl-2 homozygous mutant chimeric mice. *Science*, **261**: 1584.

Nakayama, K., Ishida, N., Shirane, M., Inomata, A., Inoue, T., Shishido, N., Horii, I., and Loh, D. (1996) Mice lacking p27 display increased body size, multiple organ hyperplasia, retinal dysplasia, and pituitary tumors. *Cell,* **85:** 707–720.

Nechushtan, A., Smith, L.C., Hsu, Y.T., and R.J. Youle. (1999) Conformation of the Bax C-terminus regulates subcellular location and cell death. *EMBO Journal*, **18**: 2330.

O'Reiley, L.A., Huang, D.C., and A. Strasser. (1996) The cell death inhibitor Bcl-2 and its homologues influence control of cell cycle entry. *EMBO Journal*, **15**: 6979-6990.

Olson, N.E., Graves, J.D., Shu, G.L., Ryan, E.J., and E.A. Clark. (2003) Caspase activity is required for stimulated B lymphocytes to enter cell cycle. *Journal of Immunology*, **170**: 6065-6072.

Oltvai, Z.N., Milliman, C.L., and S.J. Korsmeyer. (1993) Bcl-2 heterodimerizes in vivo with a conserved homologue, Bax, that accelerates programmed cell death. *Cell*, **74**; 609-619.

Ouyang, Y.-B., Carriedo, S., and R. Giffard. (2002) Effect of Bcl-x_L overexpression on reactive oxygen species, intracellular calcium, and mitochondrial membrane potential following injury in astrocytes. *Free Radical Biology & Medicine*, **33**; 544-551.

Pattingre, S., Tassa, A., Qu, X., Garuti, R., Liang, X.H., Mizushima, N., Packer, M., Schneider, M.D., and B. Levine. (2005) Bcl-2 antiapoptotic proteins inhibit Beclin 1-dependent autophagy. *Cell*, **122**: 927-939.

Piedra, M.E., Delgado, M.D., Ros, M.A., and J. Leon. (2002) c-Myc overexpression increases cell size and impairs cartilage differentiation during chick limb development. *Cell Growth and Differentiation*, **13**:185-93.

Pierce, R.H., Vail, M.E., Ralph, L., Campbell, J.S., and N. Fausto. (2002) Bcl-2 expression inhibits liver carcinogenesis and delays development of proliferating foci. *American Journal of Pathology*, **160**: 1555-1560.

Plas, D.R., Talapatra, S., Edinger, A.L., Rathmel, J.C., and C.B. Thompson. (2001) Akt and Bcl-x_L promote growth factor-independent survival through distinct effects on mitochondrial physiology. *Journal of Biological Chemistry*, **276**: 12041-8.

Plas, D.R., and C.B. Thompson. (2002) Cell metabolism in the regulation of programmed cell death. *Trends Endocrinology and Metabolism,* **13**: 75-8.

Puthalakath, H., Huang, D.C., O'Reilly, L.A., King, S.M. and A. Strasser. (1999) The proapoptotic activity of the Bcl-2 family member Bim is regulated by interaction with the dynein motor complex. *Mol Cell*, **3:** 287-296.

Polymenis, M. and E.V. Schmidt. (1999) Coordination of cell growth with cell division. *Current Opinion in Genetics and Development*, **9**: 76-80.

Ranger, A.M., Malynn, B.A., and S.J. Korsmeyer. (2001) Mouse models of cell death. *Nature Genetics*, **28:** 113-118.

Rathmell, J.C., Vander Heiden, M.G., Harris, M.H., Frauwirth, K.A., and C.B. Thompson (2000) In the absence of extrinsic signals, nutrient utilization by lymphocytes is insufficient to maintain either cell size or viability. *Molecular Cell*, **3**: 683-692.

Rathmell, J.C., Elstrom, R.L., Cinalli, R.M., and C.B. Thompson. (2003) Activated Akt promotes increased resting T cell size, CD28-independent T cell growth, and development of autoimmunity and lymphoma. *European Journal of Immunology*, **8**: 2223-2232.

Reed, J.C. (1997) Cytochrome c: can't live with it-can't live without it. *Cell*, **91:** 559-562.

Reed, J. and D. Green. (2002) Remodeling for demolition: changes in mitochondrial ultrastructure during apoptosis. *Molecular Cell*, **9**: 1-9.

Santoni-Rugiu, E., Falck, F., Mailand, N., Bartek, J., and J. Lukas. (2000) Involvement of Myc activity in a G1/S promoting mechanism parallel of the pRB/E2F pathway. *Molecular and Cellular Biology*, **20**: 3497-3509.

Saraste, A. and K. Pulkki. (2000) Morphological and biochemical hallmarks of apoptosis. *Cardiovascular Research*, **45**: 528-537.

Scarpulla, R.C. (2002) Nuclear activators and coactivators in mammalian mitochondrial biogenesis. *Biochimicha et Biophysicha Acta*, **1576**: 1-14.

Schendel, S. L., Xie, Z., Montal, M.O., Matsuyama, S., Montal, M., and J.C. Reed. (1997) Channel formation by antiapoptotic protein Bcl-2. *Proceedings of the National Academy of Science of the USA*, **94**: 5113-5118.

Schlosser, I., Holzel, M., Murnseer, M., Burtscher, H., Weidle, U.H., and D. Eick. (2003) A role for c-Myc in the regulation of ribosomal RNA processing. *Nucleic Acids Research*, **21**: 6148-6156.

Schmidt, E.V. (1999) The role of c-myc in cellular growth control. *Oncogene*, **18**: 2988-2996.

Scott, R.C., Schuldiner, O., and T.P. Neufeld. (2004) Role and regulation of starvation-induced autophagy in the Drosophila fat body. *Developmental Cell*, **2**: 167-178.

Sears, R.C., Leone, G., DeGregori, J., and J.R. Nevins. (1999) Ras enhances Myc protein stability. *Molecular Cell*, **2**: 169-179.

Sears, R.C., and J.R. Nevins. (2002) Signaling networks that link cell proliferation and cell fate. *Journal of Biological Chemistry*, **277**: 11617-11620.

Shi, Y., Chen, J., Weng, C., Chen, R., Zheng, Y., Chen, Q., and H. Tang. (2003) Identification of the protein-protein contact site and interaction mode of human VDAC1 with Bcl-2 family proteins. *Biochemical and Biophysical Research Communications*, **305**: 989-996.

Shimizu, S., Narita, M., and Y. Tsujimoto. (1999) Bcl-2 family proteins regulate the release of apoptogenic cytochrome c by the mitochondrial channel VDAC. *Nature*, **399**: 483-487.

Sidoti-de Fraisse, C., Rincheval, V., Risler, Y., Mignotte, B., and J.L. Vayssiere. (1998) TNF- activates at least two apoptotic signaling cascades. *Oncogene*, **17**: 1639-1651.

Skurk, C., Izumiya, Y., Maatz, H., Razeghi, P., Shiojima, I., Sandri, M., Sato, K., Zeng, L., Schiekofer, S., Pimentel, D., Lecker, S., Taegtmeyer, H., Goldberg, A.L., and K. Walsh. (2005) The FOXO3a transcription factor regulates cardiac myocyte size downstream of AKT signaling. *Journal of Biological Chemistry*. **21**: 20814-20823.

Smirnova, E., Griparic, L., Shurland, D.L., and A.M. van der Bliek. (2001) Dynamin-related protein Drp1 is required for mitochondrial division in mammalian cells. *Molecular Biology of the Cell*, **12**: 2245-56.

Song, G., Ouyang, G., and S. Bao. (2005) The activation of Akt/PKB signaling pathway and cell survival. *Journal of Cell and Molecular Medicine*, **1**: 59-71.

Song, Q., Kuang, Y., Dixit, V.M. and C. Vincenz. (1999) Boo, a novel negative regulator of cell death, interacts with Apaf-1. *EMBO Journal*, **18:** 167-178.

Soucek, T., Rosner, M., Miloloza, A., Kubista, M., Cheadle, J., Sampson, J., and M. Hengstschlager. (2001) Tuberous sclerosis causing mutants of the TSC2 gene product affect proliferation and p27 expression. *Oncogene*, **20**: 4904-4909.

Stocker, H. and E. Hagen. (2000) Genetic control of cell size. Current Opinion in *Genetics and Development*, **10**: 529-535.

Strasser, A., Harris, A., Bath, M., and S. Cory. (1990) Novel primitive lymphoid tumours induced in transgenic mice by cooperation between myc and bcl-2. *Nature*, **348**: 331-333.

Suzuki, M., Youle, R.J., and N. Tjandra. (2000) Structure of Bax: coregulation of dimer formation and intracellular localization. *Cell,* **103**: 645.

Traven A, Wong JM, Xu D, Sopta M, Ingles CJ. (2001) Interorganellar communication. Altered nuclear gene expression profiles in a yeast mitochondrial dna mutant. *Journal of Biological Chemistry*, **276**:4020-4027.

Tsujimoto, Y., Finger, L., Yunis, J., Nowell, P. and Croce, C. (1984) Cloning of the chromosome breakpoint of neoplastic B cells with the t(14;18) chromosomal translocation. *Science*, **226:** 1097-1099.

Tsvetkov, L.M., Yeh, K.H., Lee, S.J., Sun, H., and H. Zhang. (1999) p27(Kip1) ubiquitination and degradation is regulated by the SCF(Skp2) complex through phosphorylated Thr187 in p27. *Current Biology*, **12**: 661-664.

Ungermannova, D., Gao, Y., and X. Liu. (2005) Ubiquitination of p27Kip1 Requires Physical Interaction with Cyclin E and Probable Phosphate Recognition by SKP2. *Journal of Biological Chemistry*, **34**: 30301-9.

Vail, M.E., Chaisson, M.L., Thompson, J., and N. Fausto. (2002) Bcl-2 expression delays hepatocyte cell cycle progression during liver regeneration. *Oncogene*, **21**: 1548-1555.

Vairo, G., Innes, K.M., and J.M. Adams. (1996) Bcl-2 has a cell cycle inhibitory function separable from its enhancement of cell survival. *Oncogene*, **13**: 1511-19.

Vairo, G., Soos, T.J., Upton, T.M., Zalvide, J., DeCaprio, J.A., Ewen, M.E., Koff, A.,

and J. M. Adams. (2000) Bcl-2 retards cell cycle entry through p27 (kip1), pRB relative p130, and altered E2F regulation. *Molecular and Cell Biology*, **20**: 4745-4753.

Vander Heiden, M.G., Chandel, N.S., Williamson, E.K., Schumacker, P.T., and C. B. Thompson. (1997) Bcl-x_L regulates the membrane potential and volume homeostasis of mitochondria. *Cell*, **91**: 627-637.

Vander Heiden, M.G., Chandel, N.S., Schumacker, P.T., and C. B. Thompson. (1999) Bcl-x_L prevents cell death following growth factor withdrawal by facilitating mitochondrial ATP/ADP exchange. *Molecular Cell*, **3**:159-167.

Vander Heiden, M.G. and C.B. Thompson. (1999) Bcl-2 proteins: regulators of apoptosis or of mitochondrial homeostasis? *Nature Cell Biology,* **1:** E209-E216.

Vander Heiden, M. G., Chandel, N., Li, X., Schumacker, P., Colombini, M., and C. B. Thompson. (2000) Outer mitochondrial membrane permeability can regulate coupled respiration and cell survival. *Proceedings of the National Academy of Science of the USA*, **97**: 4666-4671.

Vander Heiden, M.G., Li, X., Gottleib, E., Hill, B., C. Thompson and M. Colombini. (2001) Bcl-x_L promotes the open configuration of the voltage-dependent anion channel and metabolite passage through the outer mitochondrial membrane. The *Journal of Biological Chemistry*, **267**: 19414-19419.

Vaux, D.L., Cory, S. and J.M. Adams. (1988) Bcl-2 gene promotes haemopoietic cell survival and cooperates with c- myc to immortalize pre-B cells. *Nature*, **335:** 440-442.

Veis, D.J., Sorenson, C.M., Shutter, J.R. and S.J. Korsmeyer. (1993) Bcl-2-deficient mice demonstrate fulminant lymphoid apoptosis, polycystic kidneys, and hypopigmented hair. *Cell*, **75:** 229-240.

Verdu, J., Buratovich, M.A., Wilder, E.L., and M.J. Birnbaum. (1999) Cell-autonomous regulation of cell and organ growth in Drosophila by Akt/PKB. *Nature Cell Biology*, **8**: 500-506.

Wang, K., Yin, X.M., Chao, D.T., Milliman, C.I. and S.J. Korsmeyer. (1996) BID: A novel BH3 domain-only death agonist. *Genes and Development*, **10:** 2859-2869.

White, R.J. (2005) RNA polymerases I and III, growth control and cancer. *Nature Reviews Molecular Cell Biology*, **1**: 69-78.

Yang, E., J. Zha, J. Jockel, L. H. Boise, C. B. Thompson, and S. J. Korsemeyer. (1995) Bad, a heterodimeric partner for Bcl-xL and Bcl-2, displaces Bax and promotes cell death. *Cell*, **80**: 285-291.

Yang, W., Shen, J., Wu, M., Arsura, M., FitzGerald, M., Suldan, Z., Kim, D.W., Hofmann, C.S., Pianetti, S., Romieu-Mourez, R., Freedman, L.P., and G.E. Sonenshein. (2001) Repression of transcription of the p27 (Kip1) cyclin-dependent kinase inhibitor gene by c-Myc. *Oncogene*, **14**: 1688-1702.

Yunis, J., Oken, M., Kaplan, M., Ensrud, K., Howe, R. and A. Theologides. (1982) Distinctive chromosomal abnormalities in histologic subtypes of non-Hodgkin's lymphoma. *New England Journal of Medicine*, **307:** 1231-1236.

Zhu, W., Cowie, A., Wasfy, G.W., Penn, L.Z., Leber, B., and D.W. Andrews. (1996) Bcl-2 mutants with restricted subcellular location reveal spatially distinct pathways for apoptosis in different cell types. *The EMBO Journal*, **16**: 4130-4141.